

**Salinity Mitigation for Potash Mine Sites:  
Synergistic Cation and Anion Removal Using a Dual-Adsorbent**

A thesis submitted to the College of Graduate and Postdoctoral Studies in partial fulfillment of the requirements for the Master of Science Degree in the Department of Civil, Geological, and Environmental Engineering, University of Saskatchewan, Saskatoon, Saskatchewan

By

Nicholas Paul Gibb

# Permission to Use

In presenting this thesis/dissertation in partial fulfillment of the requirements for a Postgraduate degree from the University of Saskatchewan, I agree that the Libraries of this University may make it freely available for inspection. I further agree that permission for copying of this thesis/dissertation in any manner, in whole or in part, for scholarly purposes may be granted by the professor or professors who supervised my thesis/dissertation work or, in their absence, by the Head of the Department or the Dean of the College in which my thesis work was done. It is understood that any copying or publication or use of this thesis/dissertation or parts thereof for financial gain shall not be allowed without my written permission. It is also understood that due recognition shall be given to me and to the University of Saskatchewan in any scholarly use which may be made of any material in my thesis/dissertation.

Requests for permission to copy or to make other uses of materials in this thesis/dissertation in whole or part should be addressed to:

Head of the Department of Civil, Geological, and Environmental Engineering  
3B48 Engineering Building, 57 Campus Drive  
University of Saskatchewan  
Saskatoon, Saskatchewan, Canada  
S7N 5A9

OR

Dean of the College of Graduate and Postdoctoral Studies  
University of Saskatchewan  
107 Administration Place  
Saskatoon, Saskatchewan S7N 5A2  
Canada

# Abstract

Potash (KCl) mining generates large quantities of tailings and brine which can impact proximate aquifers, elevating the concentrations of  $\text{Na}^+$ ,  $\text{K}^+$ , and  $\text{Cl}^-$ . To desalinate brine-impacted groundwater near potash mines and other inland locations, two adsorbents were sequentially applied: (1) calcined layered double hydroxide (CLDH), to adsorb anions, divalent cations, and transiently raise the pH; and (2) acid-treated clinoptilolite zeolite, to adsorb monovalent cations and neutralize the effluent pH. To evaluate this dual-adsorbent process, equilibrium adsorption experiments were conducted and the adsorbents were characterized through X-ray diffraction, X-ray fluorescence, porosimetry, scanning electron microscopy, and synchrotron-based scanning transmission X-ray microscopy.

Using synthetic NaCl solution, the Langmuir maximum adsorption capacity for  $\text{Cl}^-$  onto CLDH and  $\text{Na}^+$  onto acid-treated zeolite was 116.3 and 28.4 mg/g, respectively. The  $\text{Na}^+$  uptake was greatly enhanced by solution pre-treatment (dechlorination) using CLDH, and also by zeolite acid treatment (with  $1\text{M} = 2\text{M} > 0.1\text{M} > \text{untreated}$ , irrespective of acid type). Pre-conditioning the zeolite with  $\text{Na}^+$  prior to acid treatment also improved the adsorption capacity and promoted crystallinity.

Desalination of potash brine-impacted groundwater was systematically investigated. Under the optimal conditions, the dual-adsorbent reduced the concentration of  $\text{Cl}^-$  by 95.8%,  $\text{Ca}^{2+}$  by 89.8%,  $\text{Mg}^{2+}$  by 92.3%,  $\text{Na}^+$  by 91.9%,  $\text{K}^+$  by 96.5%, preserved a neutral pH (7.72), and lowered the sodium adsorption ratio (36.5 to 12.5) and the hardness (574 to 56.3 mg/L as  $\text{CaCO}_3$ ). In contrast, natural zeolite alone only removed 51.2% of the  $\text{Na}^+$  and 79.6% of the  $\text{K}^+$ , and also generated extremely hard water (3620 mg/L as  $\text{CaCO}_3$ ) due to  $\text{Ca}^{2+}$  and  $\text{Mg}^{2+}$  exchange.

Finally, zeolite regeneration studies were conducted using 0.1 M HCl. The  $\text{Na}^+$  was efficiently desorbed, but  $\text{K}^+$  remained. Over four consecutive adsorption–desorption cycles, the net  $\text{K}^+$  loading increased from 4.8 to 21.2 mg/g. This K-form zeolite could potentially be applied as a slow-release fertilizer, thereby transforming a potash mining waste material into a valuable resource.

# Contribution of Authors

This thesis includes two journal manuscripts with author contributions as follows:

## Chapter Four

Nick Gibb, James J. Dynes, and Wonjae Chang. *Synergistic Desalination Using a Dual-Adsorbent*.

The adsorbents were developed and characterized by N. Gibb. Adsorption experiments were designed and conducted by N. Gibb. J. Dynes conducted the synchrotron study and associated analyses. The manuscript was written by N. Gibb and edited by J. Dynes and W. Chang. W. Chang supervised the research.

## Chapter Five

Nick Gibb and Wonjae Chang. *A Recyclable Adsorbent for Salinized Groundwater: Desalination and Potassium-Exchanged Zeolite Production*.

The adsorbents were developed and characterized by N. Gibb. Adsorption experiments and regeneration studies were designed and conducted by N. Gibb. The manuscript was written by N. Gibb. W. Chang provided research supervision and edited the manuscript.

# Acknowledgements

I would like to express my gratitude to the following individuals and institutions:

- To my supervisor, Dr. Wonjae Chang, for his guidance, inspiration, and support.
- To Dr. Lee Barbour and Dr. Jafar Soltan, for serving on my advisory committee and providing valuable feedback.
- To Helen Yin, for her assistance and pleasant company in the laboratory.
- To Dr. James Dynes, for conducting the synchrotron study.
- To Mitacs, the Natural Sciences and Engineering Research Council of Canada, the International Minerals Innovation Institute (IMII), PotashCorp, Agrium, and The Mosaic Company, for their funding and assistance.
- And to Sakeena and my family, for their love and support.

# Table of Contents

<b>Permission to Use .....</b>	<b>i</b>
<b>Abstract.....</b>	<b>ii</b>
<b>Contribution of Authors.....</b>	<b>iii</b>
<b>Acknowledgements .....</b>	<b>iv</b>
<b>Table of Contents .....</b>	<b>v</b>
<b>List of Tables .....</b>	<b>ix</b>
<b>List of Figures.....</b>	<b>x</b>
<b>Abbreviations and Symbols .....</b>	<b>xii</b>
<b>1. General Introduction .....</b>	<b>1</b>
1.1. Overview of Potash Mining in Saskatchewan .....	1
1.2. Salinity Mitigation at Potash Mine Sites .....	2
1.2.1. Research Needs .....	3
1.2.2. Potential Application of Adsorption .....	3
1.3. Manuscript-Style Thesis .....	4
<b>2. Literature Review .....</b>	<b>5</b>
2.1. Current Strategies for Salinity Mitigation .....	5
2.1.1. Natural Containment .....	5
2.1.2. Engineered Containment Systems .....	5
2.1.3. Deep-Well Injection.....	6
2.1.4. Performance Monitoring .....	6
2.2. Natural Zeolite .....	6
2.2.1. Modifications .....	8
2.2.2. Characterization Techniques.....	8
2.2.3. Na <sup>+</sup> Adsorption Studies Using Natural and Modified Zeolite .....	8
2.2.3.1. Natural zeolite.....	8
2.2.3.2. Modified zeolite .....	9
2.2.4. Zeolite Regeneration and Recycling.....	10
2.3. Layered Double Hydroxide .....	10
2.3.1. Anion Exchange.....	11

2.3.2. The Memory Effect.....	11
2.3.3. Cation Adsorption.....	12
2.3.4. Synthesis Techniques.....	12
2.3.4.1. Coprecipitation.....	12
2.3.4.2. Hydrothermal .....	13
2.3.4.3. Mechanochemical .....	13
2.3.4.4. Mechano–hydrothermal .....	14
2.3.5. Characterization Techniques.....	14
2.3.6. Factors Affecting $\text{Cl}^-$ Adsorption.....	15
2.3.6.1. Nature of the LDH .....	15
2.3.6.2. pH.....	15
2.3.6.3. Competitive ions .....	16
2.3.6.5. Adsorbent mass.....	16
2.3.6.6. Contact time.....	16
2.3.6.7. Temperature .....	16
2.4. Combined Application of Zeolite and Layered Double Hydroxide .....	17
<b>3. Research Framework.....</b>	<b>18</b>
3.1. Knowledge Gaps.....	18
3.2. Research Objectives.....	19
3.3. Main Approaches Applied .....	19
3.4. Research Scope .....	20
3.5. Research Contributions.....	20
<b>4. Synergistic Desalination Using a Dual-Adsorbent .....</b>	<b>22</b>
4.1. Abstract.....	23
4.2. Introduction.....	23
4.3. Materials and Methods.....	25
4.3.1. Adsorbents .....	25
4.3.2. Adsorbent Modification .....	26
4.3.3. Adsorption Experiments (Synthetic NaCl Solution).....	26
4.3.3.1. CLDH adsorption experiments ( $\text{Cl}^-$ removal).....	27
4.3.3.2. Zeolite adsorption experiments ( $\text{Na}^+$ removal).....	27
4.3.4. Adsorption Experiments (Potash Brine-Impacted Groundwater).....	28
4.3.4.1 Brine-impacted groundwater preparation .....	28

4.3.4.2 Dual-adsorbent desalination ( $\text{Na}^+$ and $\text{Cl}^-$ removal) .....	28
4.3.5. Statistical Analysis .....	29
4.3.6. Measurements and Instruments .....	29
4.4. Results and Discussion .....	30
4.4.1. Effect of CLDH Amount on $\text{Cl}^-$ Removal Efficiency .....	30
4.4.2. $\text{Cl}^-$ Adsorption Mechanism .....	31
4.4.3. Effect of Zeolite Treatment by Acids and Effect of Dechlorination .....	32
4.4.4. $\text{Na}^+$ Uptake Isotherms .....	37
4.4.5. $\text{Na}^+$ Adsorption Mechanisms .....	40
4.4.5.1. Effect of zeolite acid treatment .....	40
4.4.5.2. Effect of solution pre-treatment with CLDH .....	45
4.4.6. Distribution of $\text{Na}^+$ Adsorption Sites .....	45
4.4.7. Desalination of Simulated Potash Brine-Impacted Groundwater .....	46
4.5. Conclusion .....	49
4.6. Acknowledgements .....	49
<b>5. A Recyclable Adsorbent for Salinized Groundwater: Desalination and Potassium-Exchanged Zeolite Production .....</b>	<b>51</b>
5.1. Abstract .....	52
5.2. Introduction .....	52
5.3. Experimental (Materials and Methods) .....	54
5.3.1. Instruments .....	54
5.3.2. Adsorbent Development .....	55
5.3.3. Groundwater and Potash Brine .....	55
5.3.4. Adsorption Experiments .....	56
5.3.5. Regeneration Studies .....	57
5.4. Results and Discussion .....	58
5.4.1. Effect of CLDH Amount .....	58
5.4.2. $\text{Cl}^-$ Adsorption Isotherm .....	60
5.4.3. Effects of Zeolite Modification by $\text{Na}^+$ and $\text{H}^+$ .....	63
5.4.4. Desalination of Brine-Impacted Groundwater .....	67
5.4.5. Zeolite Regeneration .....	71
5.5. Conclusion .....	73
5.6. Acknowledgements .....	73
<b>6. Conclusions and Recommendations .....</b>	<b>74</b>



6.1. Conclusions.....	74
6.2. Recommendations.....	76
6.2.1. Dual-Adsorbent Implementation and Scale Up .....	76
6.2.2. Investigation of Other Zeolites and LDHs .....	76
6.2.3. Adsorbent Re-use .....	77
6.2.4. CLDH Regeneration .....	77
6.2.5. Economic Feasibility Study .....	77
<b>References .....</b>	<b>79</b>
<b>Appendix.....</b>	<b>91</b>

# List of Tables

<b>Table 1.1:</b> Nameplate production capacity (in millions of metric tons per year as KCl) and mining method for Saskatchewan potash mines (as of 2016).....	2
<b>Table 4.2.</b> Isotherm model parameters for Na <sup>+</sup> adsorption onto zeolite at 23 °C. ....	39
<b>Table 4.3:</b> Comparison of maximum Na <sup>+</sup> adsorption capacities of various zeolites. ....	40
<b>Table 4.4:</b> Chemical composition of natural zeolite and acid-treated zeolites, before and after reaction with NaCl or Na <sub>dc</sub> solution. ....	42
<b>Table 4.5:</b> Surface area ( $S_{BET}$ ), external surface area ( $S_{external}$ ), microporous surface area ( $S_{micro}$ ), and average pore width ( $D_{avg}$ ) for natural and H <sub>2</sub> SO <sub>4</sub> -treated zeolites (at 0.1 and 1 M). ....	43
<b>Table 4.6:</b> Desalination of potash brine-impacted groundwater with the dual-adsorbent (CLDH and AZ). Bonferroni collected probabilities (indicated by asterisks) compare each step with the previous. ....	48
<b>Table 5.1:</b> Chemistry of the groundwater and potash brine. ....	56
<b>Table 5.2:</b> Chemistry for the groundwater–brine initially (GB), after CLDH treatment (2.5 g/30 mL; GB <sub>dc</sub> ), and after CLDH and ANaZ treatment (2.5 and 7.5 g/30 mL, respectively). ....	60
<b>Table 5.3:</b> Isotherm model parameters for Cl <sup>-</sup> adsorption onto CLDH at 23 °C. ....	62
<b>Table 5.4:</b> Maximum effective adsorption capacity for reported Cl <sup>-</sup> sorbents at room-temperature. ....	62
<b>Table 5.5:</b> Chemical composition of the zeolite samples. NZ, natural zeolite; AZ, acid-treated zeolite; ANaZ, NaCl/HCl-treated zeolite; KZ, NaCl/HCl-treated zeolite after four consecutive adsorption–desorption cycles. ....	64
<b>Table 5.6:</b> Ion concentrations (mg/L) in the filtrate from the three zeolite modifications. ....	65
<b>Table 5.7:</b> Adsorbent mass, equilibrium pH, and desorption efficiencies over four consecutive adsorption–desorption cycles using ANaZ-GB <sub>dc</sub> . ....	71

# List of Figures

<b>Figure 1.1:</b> Conceptual illustration of using CLDH and acid-treated zeolite for desalination. ....	4
<b>Figure 2.1:</b> The microporous molecular structure of a zeolite. Reprinted from Zeolite, In Wikipedia, n.d., Retrieved December 24 2016, from <a href="https://en.wikipedia.org/wiki/Zeolite">https://en.wikipedia.org/wiki/Zeolite</a> . Copyright 2015 by Thomas Splettstoesser. <sup>43</sup> Reprinted with permission. ....	7
<b>Figure 2.2:</b> The selectivity sequence for clinoptilolite zeolite. Data compiled by Mumpton (1999). <sup>39</sup> .....	7
<b>Figure 2.3:</b> Illustration of the memory effect.....	12
<b>Figure 4.1:</b> Graphical abstract for Chapter Four.....	22
<b>Figure 4.2:</b> Cl <sup>-</sup> removal and equilibrium pH as a function of CLDH amount ( $V = 100$ mL, $[Cl^-]_i = 1542$ mg/L, $pH_i = 6.6$ ). .....	31
<b>Figure 4.3:</b> XRD patterns for MgAl-CO <sub>3</sub> LDH, CLDH, and MgAl-Cl LDH (after Cl <sup>-</sup> uptake)..	32
<b>Figure 4.4:</b> Na <sup>+</sup> percent removal for varying masses of natural and 0.1, 1.0, and 2.0 M H <sub>2</sub> SO <sub>4</sub> - treated zeolite ( $V = 25$ mL, $[Na^+] = 1000$ mg/L, $pH_i = 12.3$ ). .....	34
<b>Figure 4.5:</b> Equilibrium pH for varying masses of natural and 0.1, 1.0, and 2.0 M H <sub>2</sub> SO <sub>4</sub> -treated zeolite ( $V = 25$ mL, $[Na^+] = 1000$ mg/L, $pH_i = 12.3$ ). .....	34
<b>Figure 4.6:</b> Na <sup>+</sup> percent removal for different amounts of zeolite treated by different strong acids at 1 M concentration ( $V = 25$ mL, $[Na^+] = 1000$ mg/L, $pH_i = 12.3$ ). .....	35
<b>Figure 4.7:</b> Na <sup>+</sup> percent removal as a function of the mass of zeolite added ( $V = 25$ mL, $[Na^+]_i = 1000$ mg/L). .....	36
<b>Figure 4.8:</b> Equilibrium pH as a function of the mass of zeolite added ( $V = 25$ mL, $[Na^+]_i = 1000$ mg/L). .....	36
<b>Figure 4.9:</b> Linearized Langmuir isotherms. ....	38
<b>Figure 4.10:</b> Linearized Freundlich isotherms. ....	38
<b>Figure 4.11:</b> Na <sup>+</sup> adsorption isotherms. The solid and dashed lines indicate the Langmuir and Freundlich model fittings, respectively.....	39
<b>Figure 4.12:</b> Illustration of zeolite decationation induced by acid treatment. M <sup>I</sup> and M <sup>II</sup> represent monovalent and divalent cations, respectively. ....	41
<b>Figure 4.13:</b> Illustration of zeolite dealumination induced by acid treatment. ....	41
<b>Figure 4.14:</b> Scanning electron microscope images of (a) NZ and (b) AZ(1-HCl). .....	43
<b>Figure 4.15:</b> XRD patterns for NZ and AZ(1-HCl). .....	44
<b>Figure 4.16:</b> STXM images for (a) NZ-NaCl and (b) AZ(1-HCl)-Na <sub>dc</sub> . The 2 $\mu$ m scale bar applies to each system. The colour denotations are blue for Si, red for Al, and green for Na. The colours blend where ions co-occur (e.g., cyan where Na <sup>+</sup> maps onto Si). .....	46
<b>Figure 5.1:</b> Graphical abstract for Chapter Five. ....	51

<b>Figure 5.2:</b> $\text{Cl}^-$ percent removal and equilibrium pH as a function of CLDH amount ( $V = 30$ mL, $[\text{Cl}^-]_i = 4600$ mg/L, $\text{pH}_i = 8.23$ ). .....	59
<b>Figure 5.3:</b> Equilibrium isotherm for $\text{Cl}^-$ uptake onto CLDH at room-temperature. Experimental data are reported as points and models (Langmuir and Freundlich models) by curves. ....	61
<b>Figure 5.4:</b> Linearized Freundlich isotherm model. ....	61
<b>Figure 5.5:</b> Linearized Langmuir isotherm model. ....	62
<b>Figure 5.6:</b> XRD patterns from $4$ to $70^\circ$ two-theta for NZ, ANaZ, and AZ. ....	66
<b>Figure 5.7:</b> XRD patterns from $4$ to $16^\circ$ two-theta for the NZ, ANaZ, and AZ. ....	66
<b>Figure 5.8:</b> $\text{Na}^+$ removal efficiency for different amounts of NZ-GB, AZ-GB <sub>dc</sub> , and ANaZ-GB <sub>dc</sub> ( $V = 30$ mL).....	67
<b>Figure 5.9:</b> $\text{K}^+$ removal efficiency for different amounts of NZ-GB, AZ-GB <sub>dc</sub> , and ANaZ-GB <sub>dc</sub> ( $V = 30$ mL).....	68
<b>Figure 5.10:</b> $\text{Ca}^{2+}$ and $\text{Mg}^{2+}$ concentration remaining for varying masses of ANaZ-GB <sub>dc</sub> , AZ-GB <sub>dc</sub> , and NZ-GB ( $V = 30$ mL).....	69
<b>Figure 5.11:</b> Equilibrium pH for varying masses of AZ-GB <sub>dc</sub> , ANaZ-GB <sub>dc</sub> , and NZ-GB ( $V = 30$ mL).....	69
<b>Figure 5.12:</b> SAR values for varying masses of ANaZ-GB <sub>dc</sub> , AZ-GB <sub>dc</sub> , and NZ-GB ( $V = 30$ mL).....	70
<b>Figure 5.13:</b> $\text{Na}^+$ and $\text{K}^+$ removal efficiency over four consecutive cycles with ANaZ-GB <sub>dc</sub> .....	72
<b>Figure 5.14:</b> Net uptake of $\text{Na}^+$ and $\text{K}^+$ over four consecutive cycles with ANaZ-GB <sub>dc</sub> . ....	72
<b>Figure A1:</b> Image difference maps for (a) Al, (b) Na and (c) Si for the NZ- $\text{NaCl}$ system; (d) Al, (e) Na, and (f) Si for the AZ(1-HCl)- $\text{Na}_{dc}$ system. The gray scales indicate optical density. ....	91

# Abbreviations and Symbols

$\lambda$	Wavelength
$1/n$	Freundlich exponent (dimensionless)
ANaZ	Natural zeolite pre-conditioned with $\text{Na}^+$ , followed by acid treatment; optionally ANaZ- $z$ , where $z$ indicates the adsorbate solution
AZ	Acid-treated zeolite; optionally AZ( $x$ - $y$ )- $z$ , where natural zeolite is treated by acid $y$ of concentration $x$ and equilibrated with adsorbate solution $z$
$b$	Langmuir intensity of adsorption (L/g)
BRZ	Bear River zeolite
BET	Brunauer-Emmet-Teller
$C_0$	Initial concentration of solute in the aqueous-phase (mg/L)
$C_e$	Equilibrium concentration of solute in the aqueous-phase (mg/L)
CEC	Cation exchange capacity
CLDH	Calcined layered double hydroxide
CSG	Coal seam gas
$D_{avg}$	Average pore width (nm)
DI	Deionized
GB	Groundwater spiked with potash brine
GB <sub>dc</sub>	Groundwater spiked with potash brine after dechlorination (CLDH treatment)
$K_F$	Freundlich constant $[\text{mg/g})(\text{L/mg})^{1/n}]$
$K_L$	Langmuir constant (L/mg)
LDH	Layered double hydroxide. Optionally written in the form $\text{M}^{2+}\text{M}^{3+}\text{-A}^{n-}$ LDH, where $\text{M}^{2+}$ and $\text{M}^{3+}$ are the metal constituents and $\text{A}^{n-}$ is the interlayer anion
$m$	Adsorbent weight (g)
NaCl	$\text{Na}^+$ solution (1000 mg/L) prepared with NaCl in deionized water
Na <sub>dc</sub>	Na <sub>dc</sub> solution after CLDH treatment
NZ	Natural zeolite; optionally NZ- $z$ , where $z$ indicates the adsorbate solution
$q_e$	Solute concentration on adsorbent at equilibrium (mg/g)
$q_{max}$	Langmuir maximum adsorption capacity (mg/g)
rpm	Rotations per minute

$S_{\text{BET}}$	Brunauer, Emmett and Teller specific surface area ( $\text{m}^2/\text{g}$ )
SCZ	St. Cloud zeolite
$S_{\text{external}}$	External surface area ( $\text{m}^2/\text{g}$ )
SEM	Scanning electron microscope
$S_{\text{micro}}$	Microporous surface area ( $\text{m}^2/\text{g}$ )
STXM	Scanning transmission X-ray microscopy
TDS	Total dissolved solids
TMA	Tailings management area
$V$	Solution volume (L)
XRD	X-ray diffraction
XRF	X-ray fluorescence

# Chapter One

## General Introduction

### 1.1. Overview of Potash Mining in Saskatchewan

Potash (KCl) is an indispensable fertilizer input and is essential for global food security. Beginning in 1943, high-grade potash deposits were discovered in Saskatchewan.<sup>1</sup> These reserves, which formed from seawater evaporation in the middle Devonian period, amount to half of the world's total potash (an estimated 65 billion tonnes as K<sub>2</sub>O).<sup>2</sup> The deposits occur in flat-lying beds 1–2 km in depth. Potash ore, called sylvinite, is composed of halite (NaCl, 50–70%), sylvite (KCl, 30–40%), and water-insoluble impurities (e.g., clay, dolomite, quartz, 1–5%). The KCl and NaCl form discrete crystals which agglomerate in clusters. The insoluble minerals (such as clays) are located interstitially between KCl and NaCl crystals. The characteristic red colour of potash is imparted by trace iron impurities, occurring at the parts per million level.<sup>1</sup>

As of 2016, Saskatchewan has nine producing potash mines, with two more currently under construction (Table 1.1).<sup>3</sup> These potash operations employ thousands of local residents and greatly contribute to the provincial economy. In 2015, 18.7 million tonnes (as KCl) of potash was produced in Saskatchewan, representing approximately one-third of global production. Over 95% of this potash is typically sold for fertilizer applications.<sup>4, 5</sup>

There are two potash mining methods: conventional and solution. With the conventional technique, ore is first bored, conveyed to the shaft, and hoisted to the surface. The ore is then crushed, slurried with brine, and deslimed using cyclones. Next, flotation processes are used to remove the NaCl, and crystallization processes can be used to further improve the purity. Excess brine is removed through centrifugation, and the final product is dried and sized. The salt tailings are filtered, slurried with reclaim brine, and pumped to the tailings management area (TMA).<sup>6</sup>

Solution mining, which does not require the sinking of a shaft, is used by two of the nine Saskatchewan potash mines. This technique is advantageous for accessing deposits deeper than

1500 m. Patience Lake—one of Saskatchewan’s first potash mines—converted to a solution mine in 1991 following uncontrollable flooding, whereas Belle Plaine was constructed as a solution mine due the deposit depth (1600 m). With solution mining, hot brine (under-saturated with respect to KCl) is injected through boreholes into the potash ore zone to become saturated with KCl. The brine is pumped back to the surface (some distance away) and cooled in a pond and/or a series of crystallizers to produce potash. The milling processes in conventional and solution mining are identical.<sup>1</sup>

**Table 1.1:** Nameplate production capacity (in millions of metric tons per year as KCl) and mining method for Saskatchewan potash mines (as of 2016).

Producer	Location	Mining Method	Capacity
Agrium	Vanscoy	Conventional	3.0
Mosaic	Belle Plaine	Solution	2.5
	Colonsay	Conventional	1.5
	Esterhazy K1/K2	Conventional	3.9
PotashCorp	Allan	Conventional	4.0
	Cory	Conventional	3.0
	Lanigan	Conventional	3.8
	Patience Lake	Solution	0.3
	Rocanville	Conventional	3.0

Capacity values obtained from McEachern (2009)<sup>1</sup> and producer websites.

## 1.2. Salinity Mitigation at Potash Mine Sites

Potash mining generates considerable amounts of tailings and brine. For every kilogram of product refined, an estimated 1–2 L of brine and 2 kg of tailings are produced.<sup>1, 7, 8</sup> The coarse tailings are predominately composed of NaCl, with lesser quantities of KCl, whereas the fine tailings are composed of NaCl, KCl, and insolubles (e.g. clays). These tailings are formed into piles which can exceed 50 m in height and can grow to cover hundreds of hectares.<sup>7</sup> The brine, supersaturated in Na<sup>+</sup>, K<sup>+</sup>, and Cl<sup>-</sup> is held in ponds. Brine discharge into the natural environment is not permitted by provincial law.



The primary environmental concern for the potash industry is vertical or lateral brine migration from the mine site to proximal soils and groundwater systems.<sup>6</sup> In soils, elevated  $\text{Na}^+$  concentrations leads to soil structure degradation. The soil permeability, plasticity, water retention capacity, cation exchange capacity (CEC), and crop productivity are all adversely effected.<sup>9-11</sup>

Excess  $\text{Cl}^-$  is also problematic. High levels ( $>250$  mg/L) generate hypoosmotic conditions which can be toxic to life, cause corrosion of machinery and infrastructure (including water distribution pipes), impart a foul taste to water, and may render water unsuitable for drinking supplies.<sup>12-15</sup> These issues associated with excess salinity have been particularly well-researched in the context of road salt application.<sup>16</sup>

### **1.2.1. Research Needs**

Preventing brine migration, or remediating brine-impacted groundwater, is an important environmental objective for potash producers. However, current practices often show limited efficacy. With slurry walls, for example, cracks and preferential flow patterns can develop, and anions (i.e.,  $\text{Cl}^-$ ) are not effectively adsorbed. Desalination technologies, including reverse osmosis, membrane filtration, and evaporation, are costly. Thus, research is needed to efficiently remediate brine-impacted groundwater, or to better prevent its occurrence.

### **1.2.2. Potential Application of Adsorption**

Adsorption of salts onto engineered geomaterials is a potentially promising technique for salinity mitigation. Adsorption is defined as the adhesion of ions in the aqueous-phase to a surface.<sup>17</sup> One adsorption mechanism is ion-exchange: the exchange of an ion in the aqueous-phase with a similarly charged ion on a solid particle. For example, household water softening agents ion-exchange  $\text{Na}^+$  or  $\text{H}^+$  for  $\text{Ca}^{2+}$  and  $\text{Mg}^{2+}$ . The solid particle, termed the adsorbent, can either be synthetically produced or naturally occurring.

Many minerals, such as layered double hydroxide (LDH) and zeolite, are relatively inexpensive and possess excellent adsorption properties.<sup>18, 19</sup> The adsorption capacity can be further augmented through modifications, for example LDH calcination and zeolite acid treatment.<sup>20</sup> In this research, it was envisioned that calcined LDH (CLDH) and acid-treated zeolite could be used for synergistic cation and anion removal. Figure 1.1 is a conceptual

illustration of this “dual-adsorbent” desalination process. In the first step, CLDH removes anions, divalent cations, and transiently raises the pH. In the second step, acid-treated zeolite removes monovalent cations and neutralizes the pH. The potential for this dual-adsorbent process to treat brine-impacted groundwater is the main topic of this thesis.

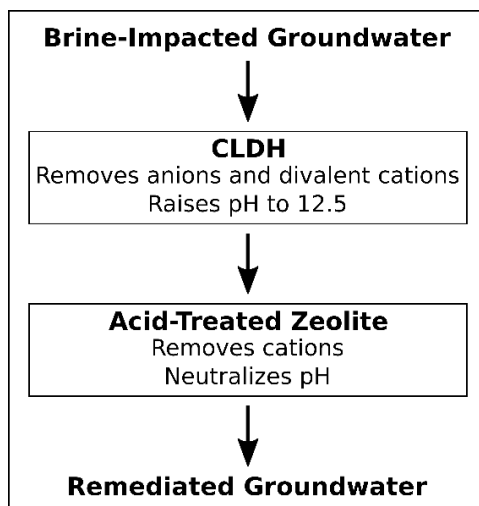


**Figure 1.1:** Conceptual illustration of using CLDH and acid-treated zeolite for desalination.

### 1.3. Manuscript-Style Thesis

This is a manuscript-style thesis consisting of six chapters. Chapter One provides an overview of potash mining in Saskatchewan and clarifies the need for salinity mitigation research. Chapter Two consists of a literature review which overviews current salinity mitigation strategies, zeolite, and LDH. Chapter Three details the research framework, including knowledge gaps, objectives, main approaches applied, scope, and research contributions. Chapters Four and Five contain standalone research manuscripts. A preface precedes each of the two manuscripts to provide context. Materials, methods, results, and discussion are detailed in each paper separately. In the first manuscript (Chapter Four), the dual-adsorbent was initially developed and evaluated through equilibrium adsorption experiments, primarily with synthetic NaCl solution. In the second manuscript (Chapter Five), equilibrium adsorption experiments were conducted with natural groundwater spiked with potash brine. The second paper (Chapter Five) also includes a superior zeolite modification technique, zeolite regeneration studies, and production of a K-form zeolite. Finally, Chapter Six offers overall conclusions and recommendations based on this research.

# **Chapter Two**

## **Literature Review**

This literature review is composed of four sections. Section 2.1 details the current strategies for salinity mitigation at potash mine sites. This is intended to provide greater context and insight into the problem of brine migration. The two subsequent sections describe zeolites (Section 2.2) and LDHs (Section 2.3), including their properties, modification techniques, characterization techniques, and adsorption studies. Finally, Section 2.4 reviews studies which have used zeolite and LDH in combination.

### **2.1. Current Strategies for Salinity Mitigation**

Various strategies are implemented at potash mine sites to minimize brine migration, as discussed in the following subsections.

#### **2.1.1. Natural Containment**

The location of the TMA at potash mines is selected based on site-specific geological and hydrogeological studies. Natural brine containment can be provided by geological formations with a low hydraulic conductivity ( $10^{-10}$  cm/s), such as clays.<sup>21, 22</sup>

#### **2.1.2. Engineered Containment Systems**

Potash brine ponds are underlain by clay liners. Synthetic liners are not widely used at potash mines due to their propensity to perforate under the load of the tailings pile.<sup>22</sup> Berms and dykes, constructed from low permeability clay, encircle the TMA and contain the tailings and decanted brine. Bentonite slurry walls (also called cut-off walls) also encircle the TMA, forming 15–40 m vertical barriers. With proper installation and maintenance, these slurry walls are

efficacious in the short-term at impeding brine seepage. Over time, however, cracks may develop, permitting brine migration.

### **2.1.3. Deep-Well Injection**

Excess brine is disposed of through injection into deep wells not drawn upon for drinking water. This reduces the hydraulic head acting on the base of the brine pond and the dykes, thereby reducing the potential for brine migration from the TMA.<sup>23</sup>

Injection wells must meet stringent regulatory standards. The well must be sufficiently deep to avoid freshwater contamination, but not too deep due to drilling costs. The well site must also be geologically stable and have an adequate injection capacity. In Saskatchewan, excess brine is injected into the Deadwood, Winnipeg, or Interlake Formations.<sup>24, 25</sup> These formations are 1100–1800 m deep, and the injection rates typically exceed 40 L/s. Low permeable geological units (shales) effectively isolate these deep reservoirs from overlying freshwater.<sup>26</sup> Deep-well injection of potash brine has been linked to seismic activity.<sup>27</sup>

### **2.1.4. Performance Monitoring**

Environmental performance is closely monitored while potash mines are in operation. This includes monitoring the groundwater quality within and outside the slurry walls. Diligent monitoring allows for adaptive management. For instance, if cracks develop in the slurry wall, patching or reconstruction can be implemented. If a brine plume is detected, it can be intercepted and pumped back to the mine site.

## **2.2. Natural Zeolite**

Zeolites are aluminosilicate minerals consisting of  $\text{SiO}_4$  and  $\text{AlO}_4^-$  tetrahedra joined by shared oxygens to form a porous, three-dimensional framework.<sup>28</sup> These porous channels, which can take numerous different configurations, expand the zeolite surface area and function as a molecular sieve.<sup>29, 30</sup> Isomorphous substitution of the  $\text{Al}^{3+}$  for  $\text{Si}^{4+}$  gives the zeolite lattice a negative charge which is balanced by exchangeable cations (some combination of  $\text{Ca}^{2+}$ ,  $\text{K}^+$ ,  $\text{Na}^+$ , and  $\text{Mg}^{2+}$ ).<sup>31-33</sup> These counterions are weakly held and can exchange with other cations in solution according to selectivity preferences.<sup>33</sup> Ion selectivity is influenced by the zeolite's mineralogy and native cations, as well as the solution temperature, pH, and ion concentrations.<sup>20</sup>

There are over forty different types of natural zeolites and hundreds of synthetic varieties.<sup>28, 32, 34</sup> The present research uses an abundant (i.e., millions of tons worldwide) and well-studied natural zeolite, clinoptilolite.<sup>35</sup> Clinoptilolite has a Si/Al molar ratio of approximately 5.7 and a chemical formula of  $(\text{Na}, \text{K}, \text{Ca}_{0.5})_{5.4}(\text{Al}_{5.4}\text{Si}_{30.6}\text{O}_{72}) \cdot 20\text{H}_2\text{O}$ .<sup>36</sup> It naturally occurs in altered volcanic tuffs and saline, alkaline-lake deposits in countries such as Canada, China, Greece, the UK, Italy, Mexico, USA, Iran, and Jordan.<sup>37</sup> It has the general formula  $(\text{Na}, \text{K}, \text{Ca}, \text{Mg})_6[\text{Al}_6\text{Si}_{30}\text{O}_{72}] \cdot n\text{H}_2\text{O}$ .<sup>38</sup> Its cation exchange selectivity, which is influenced by factors such as ion concentration, ionic radius, and valence, follows the general order given in Figure 2.2.<sup>39</sup> As  $\text{Na}^+$  is preferred over  $\text{Ca}^{2+}$ , Ca-type clinoptilolite has been used to lower the  $\text{Na}^+$  concentration of mine wastewater.<sup>32, 40-42</sup> The associated cation exchange reaction is

$$\text{Na}^+ + \frac{1}{2} \text{Ca-X} \rightarrow \text{Na-X} + \frac{1}{2} \text{Ca}^{2+} \quad (2.1)$$

where X is the clay surface.

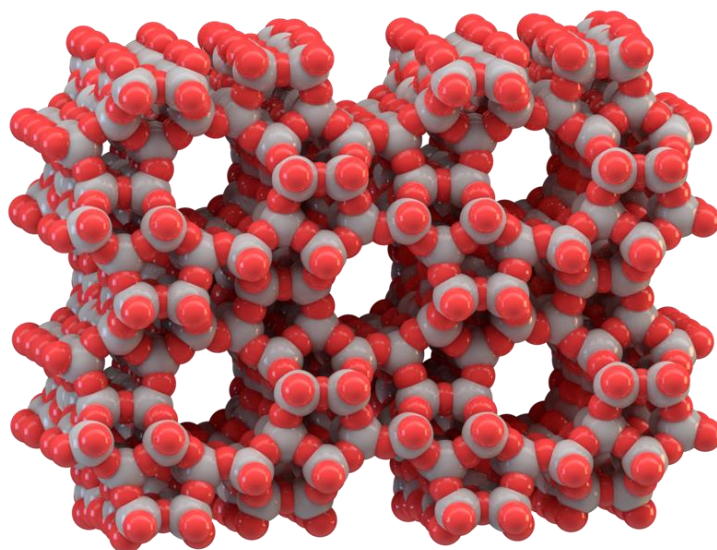


**Figure 2.1:** The microporous molecular structure of a zeolite. Reprinted from Zeolite, In *Wikipedia*, n.d., Retrieved December 24 2016, from <https://en.wikipedia.org/wiki/Zeolite>. Copyright 2015 by Thomas Splettstoesser.<sup>43</sup> Reprinted with permission.

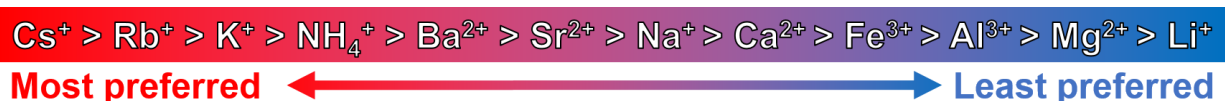


**Figure 2.2:** The selectivity sequence for clinoptilolite zeolite. Data compiled by Mumpton (1999).<sup>39</sup>

### 2.2.1. Modifications

To improve the  $\text{Na}^+$  removal efficiency, researchers have evaluated zeolites modified by acids<sup>20, 44, 45</sup> and inorganic salts.<sup>46</sup> These chemical modifications strip the zeolite of its native counterions, replacing them with the newly introduced cation species. The modified zeolite, in near-homoionic form, has a higher CEC because the new counterion is more easily exchangeable.<sup>47</sup> There are other factors, including the increase in reactive surface area observed in acid-treated zeolites (due to the removal of debris from the pore space and hydrolysis of Al-O-Si bonds).<sup>20</sup>

### 2.2.2. Characterization Techniques

Zeolite characterization is important for understanding and augmenting its adsorption capacity. X-ray diffraction (XRD) and X-ray fluorescence (XRF) are used to determine the mineral purity and chemical composition. The particle size, measured with a laser diffractor, can be important. Surface area can be quantified using a sorptometer. Scanning electron microscopy (SEM) can be used to determine the surface morphology.

### 2.2.3. $\text{Na}^+$ Adsorption Studies Using Natural and Modified Zeolite

Starting in the mid-2000s, natural zeolite began to attract attention for  $\text{Na}^+$  removal in coal seam gas (CSG) wastewater. The research has steadily grown since, with researchers increasingly making use of modified zeolites with enhanced adsorption properties.

#### 2.2.3.1. Natural zeolite

Huang and Natrajan (2006) conducted an early feasibility study for using St. Cloud zeolite (SCZ), a clinoptilolite from a New Mexico quarry, to treat CSG wastewater.<sup>40</sup> The estimated cost was \$3/barrel (159 L), compared with 0.75-\$4/barrel for deep well injection. The maximum adsorption capacity of the SCZ ( $q_{max}$ ) was determined to be 2.8 mg/g, far too low for the process to be economical. Other research groups using SCZ have found its maximum adsorption capacity for  $\text{Na}^+$  to be in the range of 4.76 to 9.7 mg/g.<sup>32, 41</sup> The discrepancy in the adsorption capacity is at least partly attributable to different  $\text{Na}^+$  concentrations used across studies.

In another study, three zeolite varieties were tested for Na<sup>+</sup> removal: SCZ, Bear River zeolite (BRZ, a clinoptilolite mined in Idaho), and a chabazite from Arizona.<sup>32</sup> The zeolites were evaluated based on their capacity to lower the sodium adsorption ratio (SAR), a measure of the preponderance of Na<sup>+</sup> relative to Ca<sup>2+</sup> and Mg<sup>2+</sup>:

$$SAR = \frac{[Na^+]}{\sqrt{\frac{[Ca^{2+}] + [Mg^{2+}]}{2}}} \quad (2.2)$$

Where the ion concentrations are expressed in meq/L. The saline–sodic CSG wastewater had an original SAR value of 30, far exceeding the allowable limit.<sup>48</sup> It was found that 1000 kg of the BRZ and SCZ could treat (i.e., reduce the SAR to the acceptable limit) 60,000 and 16,000 L of wastewater, respectively. The difference between the BRZ and SCZ was explained by differences in mineralogy and purity. Chabazite, with a higher selectivity for Ca<sup>2+</sup> than Na<sup>+</sup>, did not reduce the SAR to any significant degree; the tightly bound Ca<sup>2+</sup> precluded ion-exchange.

Another study aimed at reducing the SAR value in CSG water with a local Wyoming clinoptilolite zeolite.<sup>28</sup> This clinoptilolite, naturally rich in Na<sup>+</sup>, was pre-treated with Ca<sup>2+</sup> (as CaCl<sub>2</sub>). This removed Na<sup>+</sup> ions with from the adsorption sites, replaced by Ca<sup>2+</sup>. One metric tonne of this Ca-clinoptilolite was able to reduce the SAR to adequate levels for approximately 60,000 L of CSG water.

Finally, Millar and colleagues (2016) investigated an Australian natural zeolite for Na<sup>+</sup> removal (either NaCl or NaHCO<sub>3</sub> solution).<sup>42</sup> The maximum Na<sup>+</sup> adsorption capacity for the NaCl and NaHCO<sub>3</sub> solutions was 10.3 and 6.4 mg/g, respectively. The superior performance with the NaHCO<sub>3</sub> solution was attributed to greater Ca<sup>2+</sup>/Na<sup>+</sup> exchange due to CaCO<sub>3</sub> formation. In column studies, the performance of the zeolite declined, attributed to slow diffusion kinetics. The authors concluded that natural zeolite is unsuitable for CSG wastewater; modifications are necessary to enhance its adsorption capacity.

#### 2.2.3.2. *Modified zeolite*

There is a burgeoning interest in using zeolites for Na<sup>+</sup> removal and SAR reduction. Acid treatment is the most common modification, although other techniques have also been investigated. In one study, natural zeolite was treated by acetic acid (CH<sub>3</sub>COOH), HCl, and H<sub>2</sub>SO<sub>4</sub> at varying concentrations to lower the SAR value of CSG water.<sup>20</sup> The acetic acid

modification did not show a benefit over natural zeolite, whereas HCl and H<sub>2</sub>SO<sub>4</sub> treatment greatly improved the Na<sup>+</sup> removal efficiency. For instance, using 0.1 M H<sub>2</sub>SO<sub>4</sub> treatment, the Na<sup>+</sup> concentration (initially 563 mg/L) was reduced to 183 mg/L, compared with 365 mg/L for an equivalent mass of natural zeolite. The SAR was reduced from 70.3 to 18.5, and the pH decreased from 8.74 to 6.95. This pH drop (due to H<sup>+</sup> exchange) may be an issue in certain environmental contexts.

#### 2.2.4. Zeolite Regeneration and Recycling

To make ion-exchange more economical, it is worthwhile to regenerate or recycle the ion-exchanger. When used for contaminant removal (e.g., heavy metals), zeolites are often regenerated using a concentrated NaCl solution, but this is clearly not an option in the current research. Instead, a dilute acid can be used. It is expected that protons can easily ion-exchange with Na<sup>+</sup> on the zeolite, given its low affinity, but not K<sup>+</sup>, which has a high affinity. The acid concentration, reaction temperature, and contact time should not be overly severe. Ideally, the acid treatment can promote Na<sup>+</sup> exchange without affecting the zeolite framework mineralogy. Regeneration of zeolites used for Na<sup>+</sup> removal has not been studied, but there are comparable studies with heavy metal removal. For instance, 0.1 M HCl was used to regenerate a clinoptilolite used for Ni<sup>2+</sup> removal.<sup>49</sup> Over three cycles, the regeneration efficiency was 93, 88, and 80%.

### 2.3. Layered Double Hydroxide

Layered double hydroxides consist of positively charged brucite-like layers [Mg(OH)<sub>2</sub>], with some of the divalent cations substituted by a trivalent cation to give the layers a net positive charge. Anions (along with water) intercalate the interlayer region, providing charge neutrality.<sup>50, 51</sup> The crystal structure is well-defined, hexagonal, and plate-like. Depending on the LDH's composition, the layers are approximately 5 Å thick and the interlayer thickness is approximately 7-10 Å.<sup>52, 53</sup> LDHs have a large surface area—around 100 m<sup>2</sup>/g, depending on the composition and synthesis method.<sup>54</sup> The general formula for LDHs is [M<sup>2+</sup><sub>1-x</sub>M<sup>3+</sup><sub>x</sub>(OH)<sub>2</sub>]<sup>x+</sup>[A<sup>n-</sup>]<sub>x/n</sub> · mH<sub>2</sub>O, where M<sup>2+</sup> and M<sup>3+</sup> are divalent and trivalent cations, A<sup>n-</sup> is the interlayer charge compensation anion, and *x* is the M<sup>2+</sup>/M<sup>3+</sup> ratio.<sup>50, 51</sup> The most common LDH mineral is hydrotalcite,



$\text{Mg}_6\text{Al}_2\text{CO}_3(\text{OH})_{16}\cdot 4\text{H}_2\text{O}$ . There are many other varieties (sometimes called *hydrotalcite-like minerals*), such as meixnerite, iowaite, and hydrocalumite.

In this thesis, LDHs are denoted as  $\text{M}^{2+}\text{M}^{3+}\text{-A}^{n-}$  LDH. For instance, hydrotalcite is denoted  $\text{MgAl-CO}_3$  LDH. For simplicity, when the constituent metals are not relevant they may be omitted (e.g.,  $\text{CO}_3\text{-LDH}$ ).

### 2.3.1. Anion Exchange

Anion exchange reactions take place in the interlayer of LDHs according to its selectivity preference  $\text{CO}_3^{2-} > \text{Naphthol Yellow}^{2-} > \text{HPO}_4^{2-} > \text{HAsO}_4^{2-} > \text{CrO}_4^{2-} > \text{SO}_4^{2-} > \text{MoO}_4^{2-} > \text{OH}^- > \text{F}^- > \text{Cl}^- > \text{Br}^- > \text{NO}_3^- > \text{I}^-$ .<sup>55, 56</sup> As an example, based on this selectivity sequence (which is incomplete)  $\text{NO}_3\text{-LDHs}$  can be used to remove  $\text{Cl}^-$ .<sup>57</sup> For the potash industry, however, anion-exchange is illogical—equal-molar quantities of a secondary pollutant (e.g.,  $\text{NO}_3^-$ ) would be released into the system. Although anion-exchange is an attractive means of removing hazardous species from solution, it is not practical for  $\text{Cl}^-$  removal.

The selectivity sequence also presents the issue of competing ions. In the presence of anions such as  $\text{CO}_3^{2-}$  and  $\text{SO}_4^{2-}$ , uptake of  $\text{Cl}^-$  is diminished. In solutions with high carbonate alkalinity, lime softening prior to LDH application is valuable.<sup>58</sup>

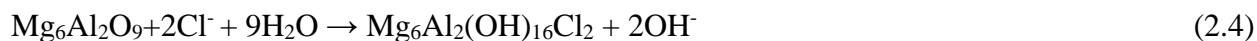
### 2.3.2. The Memory Effect

The most common LDH, and the simplest to synthesize, is  $\text{MgAl-CO}_3$  LDH. The interlayer  $\text{CO}_3^{2-}$  is difficult to displace from the LDH interlayer. That is,  $\text{MgAl-CO}_3$  LDH has a low anion exchange capacity.<sup>59</sup> However, if calcined, the interlayer  $\text{H}_2\text{O}$  and  $\text{CO}_3^{2-}$  is relinquished, leaving a mixed metal oxide (CLDH):



The optimal calcination temperature is typically 500–550 °C. At lower temperatures the destruction of the LDH is incomplete, and at higher temperatures (greater than 600 °C) spinel ( $\text{MgAl}_2\text{O}_4$ ) forms.

When CLDH is rehydrated in solution, the LDH original structure rapidly reforms, removing any anions in solution. For instance, putting CLDH in a  $\text{NaCl}$  solution will generate  $\text{Cl-LDH}$ :



This property of LDHs is termed *the memory effect* (Figure 2.3). It side-steps the aforementioned issue of secondary pollution generated through traditional ion-exchange. Calcination also increases the LDH's surface area and enhances its adsorption capacity.<sup>60</sup>

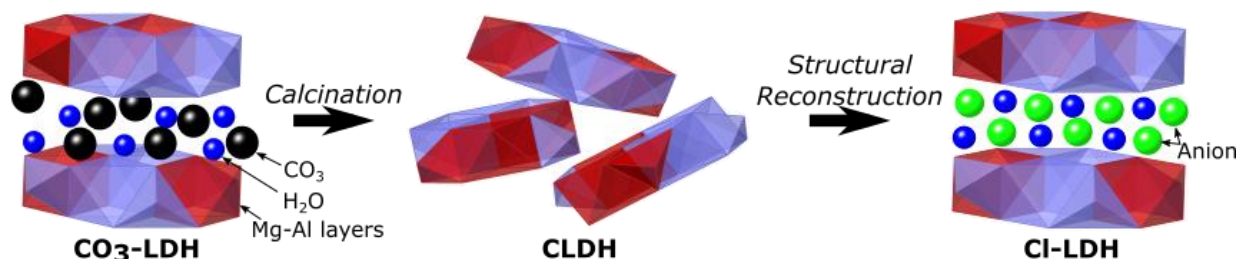


**Figure 2.3:** Illustration of the memory effect.

### 2.3.3. Cation Adsorption

In addition to anions, LDHs are excellent sorbents of divalent and trivalent cations. Often overlooked, this property of LDHs is as noteworthy as its anion exchange capacity. A comprehensive review of metal sorption by LDH outlined four mechanisms: precipitation, surface complexation, isomorphic substitution, and chelation with the interlayer anions.<sup>61</sup> It should be noted here that LDHs have no effect on monovalent ions (e.g., Na<sup>+</sup> and K<sup>+</sup>).

### 2.3.4. Synthesis Techniques

As LDHs are rare in nature, they must be synthesized to meet the purity levels and quantity demanded by industry.<sup>54</sup> A myriad of synthesis techniques have been developed, many of which are simple and economical. Coprecipitation, along with ancillary modifications, is by far the most common technique. Other techniques include hydrothermal, mechanochemical, and mechano-hydrothermal.

#### 2.3.4.1. Coprecipitation

With the coprecipitation method, a homogenous solution of divalent and trivalent cation salts (fixed ratio), is slowly titrated into a second solution. The second solution is either an alkaline solution containing the anion to be intercalated, or deionized water (in which case an alkaline solution is also titrated in, alongside the metallic salt solution). This is carried out under

vigorous stirring and often an N<sub>2</sub> atmosphere, unless CO<sub>3</sub><sup>2-</sup> is the desired interlayer anion. To favour crystallinity, the coprecipitation method is often supplemented by other treatments—aging, hydrothermal synthesis, microwave irradiation, ultrasound treatment, and urea hydrolysis.

Although the coprecipitation method is simple and effective, it generates a saline solution as waste (e.g., NaCl or NaNO<sub>3</sub>). There is one report of waste-free coprecipitation of MgAl-CO<sub>3</sub> LDH using MgO and Al(OH)<sub>3</sub> as precursor ingredients.<sup>62</sup>

#### 2.3.4.2. *Hydrothermal*

Hydrothermal synthesis can be used to generate LDH.<sup>63, 64</sup> It involves autoclaving the LDH precursor ingredients (i.e., MgO and Al<sub>2</sub>O<sub>3</sub> or Al(OH)<sub>3</sub>) under high pressure saturated steam (70 °C to 140 °C). The hot, high pressure conditions increase the solubility of ions, permitting their dissolution and diffusion into more favourable crystal configurations. This results in a LDH with enhanced crystallinity and a narrower particle size distribution.<sup>65</sup> This technique is attractive because it produces high-quality LDH with waste production. The drawback is that it requires high temperatures (in excess of 100 °C) for a long duration (typically several days).

#### 2.3.4.3. *Mechanochemical*

Layered double hydroxides can be synthesized using a mechanochemical technique,<sup>66-69</sup> as pioneered by Tongamp and colleagues.<sup>67</sup> In their original formulation, Mg and Al precursors (e.g., Mg(OH)<sub>2</sub> and Al(OH)<sub>3</sub> in a 3:1 ratio) were milled in a two-step process: first dry milling (~1 h), and then milling (~3 h) with a stoichiometric addition of water. Many subsequent researchers have made modifications to this method.<sup>68</sup>

The simplicity of the mechanochemical method is very attractive. It is rapid, scalable, environmentally friendly, and essentially waste-free. Unless a salt solution is used, the interlayer anion will be hydroxide,<sup>69</sup> which is desirable due to its high exchangeability and the lack of any secondary pollutant.

The mechanochemical approach has disadvantages. Namely, the resultant LDH samples may show relatively low crystallinity and poor dispersity. This may diminish its effectiveness as an adsorbent.<sup>67, 70, 71</sup>

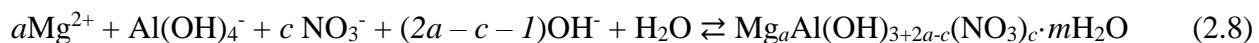
#### 2.3.4.4. Mechano–hydrothermal

Layered double hydroxides can be synthesized by combining the mechanochemical and hydrothermal techniques. This mechano–hydrothermal technique was only reported by Fengrong Zhang and his colleagues at Shandong University.<sup>70-72</sup> In many respects, this combined approach is superior to either technique in isolation.<sup>63, 67, 71</sup> LDHs synthesized this way have improved crystallinity and dispersion and are more regular in shape.<sup>71</sup> Furthermore, the pre-milling permits a lower hydrothermal reaction temperature and duration.

The general procedure is to first mill the precursors ingredients (MgO and Al<sub>2</sub>O<sub>3</sub>), thereby mixing the powders, decreasing their particle size, and increasing their reactivity. The resultant powder is then hydrothermally treated at 80 to 120 °C for 2 to 6 h. The MgO and Al<sub>2</sub>O<sub>3</sub>, activated from the ball milling, form reactive species:



The reaction of Mg<sup>2+</sup> and Al(OH)<sub>4</sub><sup>−</sup> produces LDH, as is written below. A nitrate salt is also added to provide the interlayer anion.



Where the values of *a* and *c* depend on the relative molar quantity of MgO, Al<sub>2</sub>O<sub>3</sub>, and NaNO<sub>3</sub>.

#### 2.3.5. Characterization Techniques

It is important to characterize the LDH to understand and augment its adsorption capacity. Routine techniques include XRD, FTIR, and thermogravimetric analysis (TGA). Other potentially useful techniques include SEM, transmission electron microscopy (TEM), particle size analysis, and surface area and porosimetry analysis.

X-ray diffraction is used to analyze crystal structure, atomic spacing, and phase purity. MgAl-CO<sub>3</sub> LDHs contain sharp and intense peaks at low two-theta values, characteristic of LDH compounds. Calcination at 500–600 °C destroys LDH's layered structure and produces a mixed metal oxide which is evident by XRD. Upon rehydration of the mixed metal oxide in solution, the LDH reconstructs and the d-spacing is almost identical to the original uncalcined MgAl-CO<sub>3</sub> LDH.<sup>60, 73</sup>

Fourier transform infrared spectroscopy can be used to identify the charge-balancing interlayer anions presence, orientation, and the type of bonds formed.<sup>60, 74</sup> For instance, FTIR can indicate the  $\text{CO}_3^{2-}$  and  $\text{H}_2\text{O}$  present in  $\text{MgAl-CO}_3$  LDH (and the absence of these molecules in CLDH).<sup>60, 73, 75</sup>

Thermogravimetric analysis measures changes in a sample's mass as it is heated. Because LDHs are routinely calcined, TGA is valuable tool for investigating thermal stability and chemical alterations at different temperature points. TGA is often complimented by mass spectrometry (MS) to determine the nature of the gaseous reaction products. There have been detailed TGA analyses conducted on  $\text{MgAl-Cl}$  LDH and  $\text{MgAl-CO}_3$  LDH.<sup>73, 75, 76</sup>

To visualize the sample morphology and particle size, SEM and TEM can be used. A laser scattering particle size analyzer can be used to determine the particle size distribution. Surface area and porosimetry measurements, including the Brunauer–Emmett–Teller (BET) surface area, can be obtained using an automated gas adsorption system.

### **2.3.6. Factors Affecting $\text{Cl}^-$ Adsorption**

The factors which influence  $\text{Cl}^-$  adsorption onto LDHs include the nature of the LDH, solution pH, competitive ions, mass of LDH, contact time, and temperature. These factors are discussed in the following subsections.

#### *2.3.6.1. Nature of the LDH*

Although a range of constituent metals are possible, for  $\text{Cl}^-$  removal most of the studies have employed calcined  $\text{MgAl-CO}_3$  LDH. The optimal calcination temperature is invariably in the range of 450-550 °C. The Mg/Al ratio is also important. LDH having a 4:1 Mg/Al molar ratio is superior to 3:1 and 2:1 ratios (149.5, 102.6, and 109.2 mg/g, respectively).<sup>75, 77</sup> LDHs intercalated with  $\text{NO}_3$  have also been evaluated for  $\text{Cl}^-$  removal (with  $\text{Zn}^{2+}$ ,  $\text{Mg}^{2+}$ , and  $\text{Ni}^{2+}$  as the divalent metal and  $\text{Al}^{3+}$  as the trivalent metal), with a maximum uptake of 108.3.<sup>57</sup>

#### *2.3.6.2. pH*

The effect of pH on adsorption is ambiguous in the literature. Most studies do not adjust the pH at any point, for doing so introduces foreign electrolytes which affect adsorption (e.g.,  $\text{NO}_3^-$  if  $\text{HNO}_3$  is used). Other studies configure the initial pH, then allow the system to

equilibrate. For these studies, the general observation is that, provided the initial pH is between 5 and 10, the percent removal of the targeted anion is largely constant, and the final pH will be approximately 11 to 12.5. The general conclusion is that adsorption is unaffected by pH provided it is not acidic (LDH deteriorates at  $\text{pH} < 5$ ) or basic (at  $\text{pH} > 10$  there is competition from  $\text{OH}^-$ ).<sup>78, 79</sup>

#### *2.3.6.3. Competitive ions*

For real-world implementation, it is important to consider the effect of competitive anions. Generally, the presence of higher valence anions will diminish the adsorption of lower valence anions (e.g.,  $\text{PO}_4^{3-} > \text{SO}_4^{2-} > \text{Cl}^-$ ). In addition to valence, steric effects are also important to consider—for instance, due to its smaller size,  $\text{Cl}^-$  is preferred over  $\text{NO}_3^-$ .<sup>57</sup>

#### *2.3.6.5. Adsorbent mass*

Increasing the amount of CLDH corresponds to more adsorption sites and a higher  $\text{Cl}^-$  removal efficiency. In one study, 3.0 g/L CLDH removed over 95 percent of the  $\text{Cl}^-$  within 6 hours ( $[\text{Cl}^-]_i = 100 \text{ mg/L}$ ), but with 2.0, 1.0, and 0.5 g/L, the removal percentage was lower—60, 40, and 30 percent, respectively.<sup>75</sup>

#### *2.3.6.6. Contact time*

The effect of contact time on  $\text{Cl}^-$  removal by  $\text{ZnAl-NO}_3$  LDH was studied by Lv and colleagues.<sup>57</sup> It was found that adsorption was maximized within 4 h; longer durations did not increase adsorption. Similarly, using calcined  $\text{MgAl-CO}_3$  LDH, the same research group found equilibrium was established within 3 hours.<sup>75</sup> Typically, in batch equilibrium tests a contact time of 24 h is typically used, which is more than adequate.

#### *2.3.6.7. Temperature*

The effect of temperature on the kinetics of uptake of  $\text{Cl}^-$  ion by CLDH was studied by Lv et al.<sup>75</sup> The removal efficiency and reaction kinetics increased with increasing temperature. This is replicable finding in adsorption studies.

## 2.4. Combined Application of Zeolite and Layered Double Hydroxide

Despite hundreds of studies on both LDH and zeolite, there are only a handful of studies which use both in conjunction. Just two research groups were identified in this literature review. The first is led by Takaaki Wajima at Chiba University (Chiba, Japan), and the second is a team of researchers at Sandia National Laboratories (Albuquerque, USA).

Wajima's group has published multiple papers on the combined use of zeolite and LDH.<sup>34, 80-83</sup> In the earliest of these studies,<sup>83</sup> natural zeolite and CLDH were used to desalinate seawater. The CLDH, applied first, greatly reduced the concentrations of anions ( $\text{Cl}^-$ ,  $\text{Br}^-$ , and  $\text{SO}_4^{2-}$ ), as well as  $\text{Ca}^{2+}$  and  $\text{Mg}^{2+}$ . Additionally, because  $\text{OH}^-$  groups are relinquished from the CLDH, the pH increase to 12.7. Next, natural zeolite was added and stirred. At equilibrium, the solution was filtered and zeolite was again added. Repeated ten times altogether, zeolite treatment greatly lowered the  $\text{Na}^+$  and  $\text{K}^+$  concentrations. Concentrations of  $\text{Ca}^{2+}$  and  $\text{Mg}^{2+}$  increased, as these ions were exchanged from the natural zeolite with  $\text{K}^+$  and  $\text{Na}^+$  in solution. This final pH was neutral, likely attributable to  $\text{H}^+$  desorption and  $\text{Ca}(\text{OH})_2$  and  $\text{Mg}(\text{OH})_2$  precipitation. Thus, the seawater was essentially purified through this two-step adsorption process. As a further step, radish sprouts were cultivated for 10 days using either the untreated seawater or the treated seawater. The radish sprouts did not grow with the seawater, but grew healthily with the treated water.

A research team at Sandia National Laboratories also used a combination of zeolite and LDH to desalinate brackish inland waters.<sup>58</sup> The brackish water was first run through a CLDH-packed column, then through by a column filled with synthetic zeolite. This synthetic zeolite (permutite) had  $\text{H}^+$  as the charge-balancing cation, which avoids secondary pollution and allows for pH neutralization. In the first experiment, using synthetic brackish water, total dissolved solids (TDS) decreased from 2222 mg/L to less than 500 mg/L. In the second experiment, using actual brackish water, TDS decreased from 11,000 mg/L to 600 mg/L, and the pH was neutralized. Of note, a lime pre-treatment was also implemented to eliminate  $\text{CO}_3^{2-}$  competition. This pre-treatment is only necessary if the  $\text{CO}_3^{2-}$  alkalinity is very high

# Chapter Three

## Research Framework

This chapter outlines the general framework which guided this research. This includes the knowledge gaps, research objectives, main approaches applied, research scope, and research contributions.

### 3.1. Knowledge Gaps

From the literature review (Chapter Two), four major knowledge gaps were identified:

1. In the case of acid-treated zeolite, the optimal acid treatment has not been clearly established in the literature. Systematic studies are required to determine the effect of different treatments on the zeolite's physiochemical properties and adsorption capacity. Critical parameters include acid contact time, reaction temperature, acid strength, and acid type.
2. The combined application of CLDH and acid-treated zeolite has been understudied. Synergistic effects between the two adsorbents have never been established. A comprehensive study on CLDH and acid-treated zeolite is justified based on the work of Pless et al. (2006).<sup>58</sup>
3. Adsorbents (including acid-treated zeolite and CLDH) have never been evaluated as a remediation option for potash brine-impacted groundwater, which has a unique chemistry (i.e., high concentrations of not only  $\text{Na}^+$  and  $\text{Cl}^-$ , but also  $\text{K}^+$ ).
4. Zeolite's regeneration capacity following  $\text{Na}^+$  and  $\text{K}^+$  uptake has never been assessed. It is unknown whether cyclical  $\text{Na}^+$  and  $\text{K}^+$  adsorption–desorption is achievable. If  $\text{Na}^+$  desorbs, but  $\text{K}^+$  does not, it may be feasible to generate a zeolite with a high K-loading, which theoretically could be applied as a slow-release fertilizer.

These knowledge gaps led to the research objectives.



### 3.2. Research Objectives

The overall objective of this research was to develop and evaluate adsorbent materials for salinity mitigation at potash mine sites. Specifically, CLDH and acid-treated zeolite were combined as a dual-adsorbent to remove cations and anions. This dual-adsorbent was evaluated with both synthetic NaCl solution and groundwater spiked with potash brine. The specific objectives of this research were to:

1. Evaluate different variations of zeolite acid treatment (i.e., adjusting parameters such as acid strength, acid type, and  $\text{Na}^+$  preconditioning) in terms of the zeolite's physiochemical properties and adsorption capacity.
2. Investigate potential synergies between CLDH and acid-treated zeolite, namely pH neutralization and the zeolite's cation adsorption capacity.
3. Evaluate the feasibility of using CLDH and acid-treated clinoptilolite zeolite with brine-impacted water. Specifically targeted are significant reductions in the concentrations of  $\text{Na}^+$ ,  $\text{K}^+$ , and  $\text{Cl}^-$ , but without generating any secondary pollution or perturbing the pH.
4. Selectively extract residual  $\text{K}^+$  from waste potash brine to obtain a K-form zeolite (for potential use as a slow-release fertilizer). Confirm through various techniques.
5. Evaluate the zeolite's regeneration potential (weak acid regeneration).
6. Investigate the adsorption mechanisms and characterize the adsorbents (e.g., their crystallinity, composition, and surface area).

### 3.3. Main Approaches Applied

To fulfill the research objectives, various approaches were applied. Acid and thermal treatments were used to modify and regenerate the adsorbents. Equilibrium adsorption studies were conducted to evaluate the adsorption capacity of the adsorbents. In these experiments, a measured mass of the adsorbent was agitated for 24 hours with synthetic NaCl solution or natural groundwater spiked with potash brine. Adsorption isotherms and removal efficiency plots were generated.

The  $\text{Ca}^{2+}$ ,  $\text{Mg}^{2+}$ ,  $\text{K}^+$ , and  $\text{Al}^{3+}$  concentrations were measured using atomic absorption spectroscopy. The  $\text{Na}^+$  and  $\text{Cl}^-$  concentrations were measured using ion-selective electrodes probes. The pH was measured using a pH probe.

The characterization techniques included particle size analyses, X-ray fluorescence, X-ray diffraction, porosimetry, scanning electron microscopy, and synchrotron-based scanning transmission X-ray microscopy.

### **3.4. Research Scope**

The overarching aim of this research was to develop the dual-adsorbent desalination process and determine its fundamental properties. Experiments were conducted at the laboratory-scale only. This research scope is clearly delineated in the research objectives (Section 3.2). The following items were excluded from the research scope: investigation into other LDHs and zeolites; LDH synthesis; improving hydraulic conductivity; adsorbent re-use; CLDH regeneration; technology scale-up (i.e., pilot or industrial units); and an economic feasibility study. These topics are given as recommendations for future research (Section 6.2).

### **3.5. Research Contributions**

This thesis offers a new potential option for salinity mitigation at potash mine sites. The research findings could be implemented at potash mine sites to better prevent brine migration or to remediate salinized water. This thesis also offers a method for extracting residual  $K^+$  from potash brine. With this method,  $K^+$  is selectively adsorbed onto natural zeolite, which can be then potentially applied as a slow-release  $K^+$  fertilizer. Overall, this research is important and relevant for the potash industry, which continuously seeks to reduce its environmental impact and enhance product recovery.

This research has broad applicability outside of the potash industry. Although salt removal was the focus of this research, toxic metals can also be efficiently removed by CLDH and acid-treated zeolite. Because of this capacity, the dual-adsorbent could potentially be used (or re-used via ion-exchange) to treat wastewater in other mining contexts, as well as in the oil and gas industry. For instance, selenium can be removed from coal mining wastewater, and uranium compounds from uranium mining wastewater.

Aside from its practical value to industry, this research has intrinsic scientific value. Foundational knowledge is contributed to the fields of environmental engineering, clay science, water treatment, and desalination. Novel intellectual contributions include (1) establishing the synergies between CLDH and acid-treated zeolite (i.e., pH neutralization and enhanced

adsorption), (2) elucidating the benefits of pre-treating the zeolite with  $\text{Na}^+$  prior to acid treatment, and (3) zeolite regeneration and conversion to its K-form (by selectively extracting  $\text{K}^+$  from waste potash brine). These are important scientific advancements which could pave the way for future discoveries and innovations.

# Chapter Four

## Synergistic Desalination Using a Dual-Adsorbent

**Preface:** This chapter lays the foundations of the dual-adsorbent process, which is designed for salinity mitigation at potash mine sites. It is presented as a standalone scientific paper: (4.1) Abstract; (4.2) Introduction; (4.3) Experimental; (4.4) Results and Discussion; (4.5) Conclusion; and (4.6) Acknowledgements. This paper is contextualized and related to the research project as a whole in Chapter Six of this thesis.

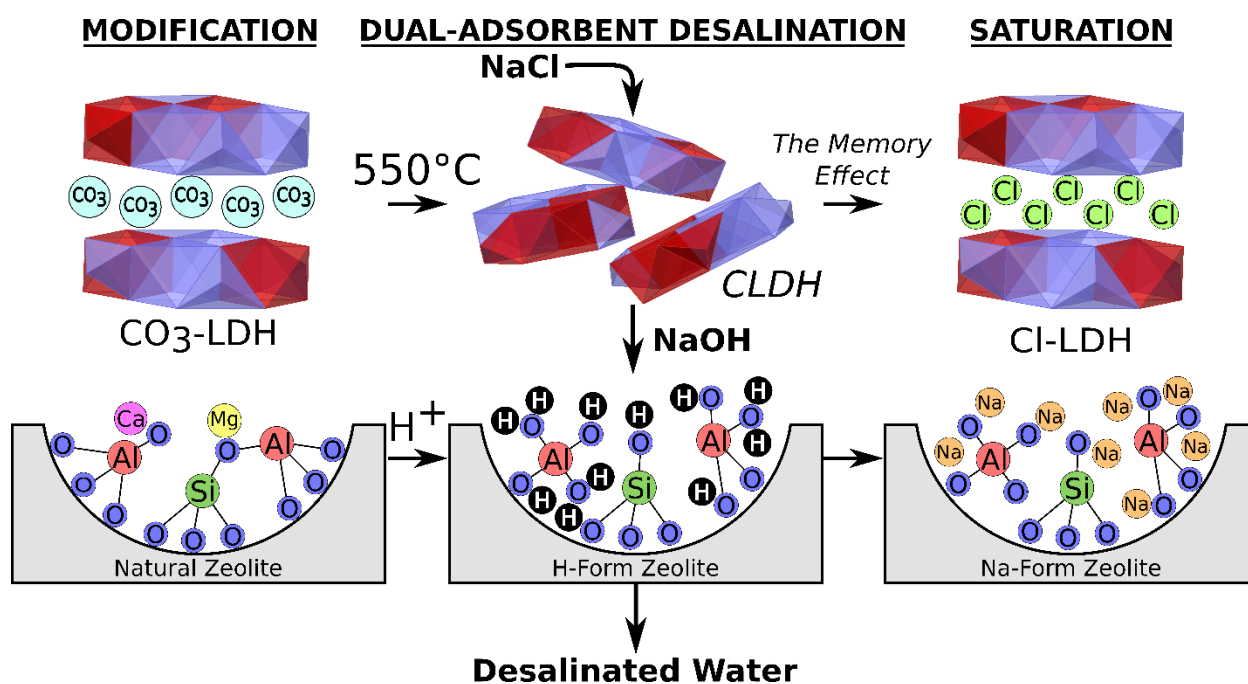


**Figure 4.1:** Graphical abstract for Chapter Four.

## 4.1. Abstract

A dual-adsorbent treatment based on the sequential application of calcined layered double hydroxide (CLDH) and acid-treated zeolite was developed and assessed for the desalination of potash brine-impacted groundwater. A series of batch adsorption experiments revealed that the  $\text{Na}^+$  removal efficiency of zeolite was synergistically increased when preceded by dechlorination using CLDH, and further improved by zeolite acid treatment. The Langmuir adsorption capacity achieved for  $\text{Na}^+$  was 28.4 mg/g, a significant improvement over conventional approaches. Using brine-impacted groundwater, the dual adsorbent decreased the concentrations of  $\text{Na}^+$ ,  $\text{K}^+$ , and  $\text{Cl}^-$  by 87, 97, and 87%, respectively, to below drinking water standards. It also exhibited the additional advantages of neutralizing the effluent pH and decreasing the hardness, sodium adsorption ratio, and  $\text{SO}_4^{2-}$  concentrations. Removal mechanisms including the memory effect, dealumination, and cation exchange were addressed. Synchrotron-based scanning transmission X-ray microscopy (STXM) analyses provided visual evidence of enhanced sodium adsorption by the acid-treated zeolites.

## 4.2. Introduction

Recent studies have consistently reported that amplified industrial activities have greatly increased the concentration of salts in receiving freshwater bodies in various regions of the world.<sup>84, 85</sup> The elevated salinity of water bodies has led to growing concerns over water security, particularly in developed regions.<sup>85, 86</sup> Inputs include road deicing salts, sewage and water softeners, accelerated geological weathering, as well as tailings and saline industrial effluents (e.g., brine) from mining, oil, and gas operations.<sup>84, 87, 88</sup> Improper containment or uncontrolled discharges of salts and brines, including chronic and accidental releases, can salinize proximate soils and shallow aquifers.<sup>7</sup> High sodium ( $\text{Na}^+$ ) concentrations may degrade soils, disturb biogeochemical cycling, and mobilize contaminants.<sup>9-11, 89</sup> Chloride ( $\text{Cl}^-$ ) is toxic to plants and freshwater species at high concentrations<sup>12, 13</sup>, and  $\text{Cl}^-$ -induced infrastructure corrosion (e.g., water distribution pipes) can have serious health, economic, and engineering repercussions<sup>90</sup>. High salinity can ultimately render groundwater unsuitable for beneficial uses, including drinking water, irrigation, and feedlot watering.<sup>9, 84, 86</sup>

Widespread attention has focused on the saline water originating from mining and oil and gas production.<sup>20, 32, 40-42, 44-46, 91-93</sup> For example, due to intensified coal seam gas (CSG) gas

extraction in North Dakota (USA), the reported number of saline effluent spills has greatly increased over the last two decades.<sup>88</sup> In Australia, the burgeoning CSG industry produces large quantities of saline–sodic water with total dissolved solids (TDS) concentrations generally ranging from 200 to 10,000 mg/L.<sup>94</sup> Similarly, in Saskatchewan (Canada), potash (KCl) mining generates large quantities of hypersaline tailings and brine.<sup>7</sup> Preventing brine migration from the mine site to proximate soils and aquifers is a continual challenge for the potash industry.<sup>6</sup> Overall, there is a strong and growing demand within the mining and oil and gas industries for effective technologies to remediate salt-impacted sites (e.g., abandoned mines, spill sites, and waste disposal sites) or to contain or treat saline produced water.<sup>93</sup>

Mineral adsorbents show great potential for salinity mitigation. Layered double hydroxide (LDH) minerals, such as hydrotalcite, consist of positively charged brucite-like sheets with anions occupying the interlayers and can be used to remove anions and divalent cations. For example, through calcination and reconstruction (i.e., *the memory effect*) LDHs have been used to remove a range of anions (e.g.,  $\text{Cl}^-$ ,  $\text{SO}_4^{2-}$ ,  $\text{NO}_3^-$ ,  $\text{PO}_4^{3-}$ ) from solution.<sup>18, 75</sup>

Zeolite minerals can be used to remove a wide range of cations, including monovalent cations (e.g.  $\text{Na}^+$  and  $\text{K}^+$ ). Zeolites consist of  $\text{SiO}_4$  and  $\text{AlO}_4^-$  tetrahedra joined by shared oxygen atoms to form a cage-like, three-dimensional framework.<sup>28</sup> The  $\text{AlO}_4^-$  bears a negative charge, which is neutralized by weakly held, exchangeable cations (varying amounts of  $\text{Ca}^{2+}$ ,  $\text{K}^+$ ,  $\text{Na}^+$ , and  $\text{Mg}^{2+}$ ).<sup>31–33</sup> Zeolites can be modified using heat and/or chemical treatments (alkali, acids, surfactants, or salts of alkali and alkaline earth metals) to augment their adsorption capacity. Acid treatment is particularly useful; it removes pore-blocking impurities, increases the surface area and porosity, and strips away sorbed cations by replacing them with  $\text{H}^+$  ions (conversion to a near-homoionic H-form zeolite).<sup>95, 96</sup> Acid-treated zeolites have recently garnered attention for  $\text{Na}^+$  removal from saline industrial produced water.<sup>20 46</sup>

By using CLDH and acid-treated zeolite in combination, both anions and cations can be removed while achieving a neutral effluent pH.<sup>58</sup> Yet, this combined application of acid-treated zeolite and CLDH has not been extensively investigated despite numerous studies on their independent uses.<sup>19, 60, 97, 98</sup> In a lone study by Pless and co-workers, permutite (a synthetic, weak acid-treated zeolite) was combined with CLDH to desalinate CSG produced water, which is dominated by  $\text{Na}^+$ ,  $\text{Cl}^-$ , and  $\text{HCO}_3^-$ .<sup>58</sup> After this dual-adsorbent treatment, the TDS content decreased from 11,000 to 600 ppm and the effluent pH was 5.0.

The objectives of this study are to develop, evaluate, and characterize a dual adsorbent as a potential remedial agent that sequentially combines CLDH and acid-treated zeolites for the purpose of mitigating the salinity of groundwater impacted by potash brine (both  $\text{Na}^+$  and  $\text{Cl}^-$ ). This dual-adsorbent treatment, initially developed by Pless et al.<sup>58</sup>, is applied in the present study with several distinctive elements. First, natural clinoptilolite zeolite is used and converted to its H-form by strong acid (up to 2 M) treatment. The application of CLDH and acid-treated clinoptilolite zeolite in combination, and the associated effects and mechanisms for salinity mitigation, have not been extensively addressed in previous studies. Second, the potential synergies that result from the combination of CLDH and the acid-treated zeolite treatments are investigated. Dechlorination (i.e., solution pre-treatment using CLDH) is hypothesized to synergistically improve subsequent  $\text{Na}^+$  removal using acid-treated zeolite due to its basicity, while at the same time ensuring that the treated water is of neutral pH. Therefore, the proposed dual-adsorbent treatment to remove both  $\text{Na}^+$  and  $\text{Cl}^-$  may overcome problems associated with the typically very low pH of adsorption effluents generated by conventional salinity mitigation treatments using acid-treated zeolites. Third, natural groundwater spiked with potash brine is used as the adsorbate solution, providing multiple competitive ions for adsorption sites and mimicking real-world problems. potash brine has high concentrations of not only  $\text{Na}^+$  (roughly 90,000 mg/L) and  $\text{Cl}^-$  (220,000 mg/L), but also  $\text{K}^+$  (50,000 mg/L). Given clinoptilolite's selectivity sequence ( $\text{Cs} > \text{Rb} > \text{K} > \text{NH}_4 > \text{Ba} > \text{Sr} > \text{Na} > \text{Ca} > \text{Fe} > \text{Al} > \text{Mg} > \text{Li}$ ), the presence of  $\text{K}^+$  is expected to reduce the  $\text{Na}^+$  adsorption.<sup>39</sup> To determine the effects of  $\text{K}^+$  and other co-existing competitive ions, the complete solution chemistry is characterized at each step of the dual-adsorbent treatment using natural groundwater by spiking actual potash brine.

The developed adsorbents are characterized through porosimetry, X-ray diffraction (XRD), X-ray fluorescence (XRF), and synchrotron-based scanning transmission X-ray microscopy (STXM). In particular, the STXM analyses provide elemental maps to visualize sodium adsorption sites in the natural and acid-treated zeolites.

### **4.3. Materials and Methods**

#### **4.3.1. Adsorbents**

The zeolite sample was obtained from Bear River zeolite (Preston, Idaho). Using quantitative XRD, the sample was determined to be approximately 85% clinoptilolite. Its cation

exchange capacity, obtained using the ammonium acetate method<sup>99</sup>, was 1.67 meq/g. The sample was rich in K<sup>+</sup> and Ca<sup>2+</sup> (as exchangeable cations) and the Si/Al molar ratio was determined through XRF to be 5.95. The received sample was ground to a powder (Bico UA disk pulveriser) to an average particle size of 80 µm (measured using a Malvern Mastersizer S laser diffractor). Kyowa Chemical Industry (Sakaide, Japan) provided Mg<sub>6</sub>Al<sub>2</sub>(OH)<sub>16</sub>CO<sub>3</sub> (MgAl-CO<sub>3</sub> LDH). According the manufacturer, this MgAl-CO<sub>3</sub> LDH sample had a Mg/Al molar ratio of 3.0 and an average particle size of approximately 30 µm. XRD analysis confirmed that impurities of the MgAl-CO<sub>3</sub> LDH were negligible (i.e., synthetically produced).

#### 4.3.2. Adsorbent Modification

The MgAl-CO<sub>3</sub> LDH was calcined using a muffle furnace at 550 °C for 6 h (subsequently referred to as CLDH). This calcination temperature and duration has been widely used in previous studies.<sup>18, 97</sup> For the zeolite acid treatment, H<sub>2</sub>SO<sub>4</sub> (0.1, 1.0, and 2.0 M), HNO<sub>3</sub> (1.0 M), and HCl (1.0 M) solutions were prepared (all acids were obtained from Fisher Scientific Canada). The natural zeolite was contacted with the selected acid solutions (1:10 weight ratio) in a 1 L polyethylene container which was agitated at room temperature (23 °C) using an orbital shaker (200 rpm). After 30 min contact time, the acid-treated zeolite was separated through vacuum filtration (Whatman 42), washed with DI water until no substantial difference was observed in the pH of two sequential washing steps, and oven-dried overnight at 103 °C. The acid-treated zeolites were denoted AZ with the acid strength and type in parentheses. For instance, zeolite treated with 1 M HCl was denoted AZ(1-HCl).

#### 4.3.3. Adsorption Experiments (Synthetic NaCl Solution)

Batch equilibrium experiments were used to study the uptake of Cl<sup>-</sup> and Na<sup>+</sup> onto the CLDH and zeolite samples, respectively. The adsorption experiments were conducted by mixing specified masses of the adsorbent with one of two adsorbate solutions at 200 rpm and at room temperature. After 24 h (equilibrium condition), the aqueous phase was separated from the solid phase by centrifugation. For CLDH, the pH and Cl<sup>-</sup> concentration were measured; for the zeolite samples, the pH and the Na<sup>+</sup> concentration were measured. The removal efficiency (RE, %) was determined as

$$RE = [(C_0 - C_e)/C_0] \times 100\% \quad (4.1)$$



where  $C_0$  (mg/L) is the solute initial concentration in solution and  $C_e$  (mg/L) is its equilibrium concentration. The target ion uptake ( $q_e$ , mg/g) was calculated as

$$q_e = (V/m)(C_0 - C_e) \quad (4.2)$$

where  $m$  (g) is the adsorbent mass and  $V$  (L) is the volume of solution.

#### 4.3.3.1. CLDH adsorption experiments ( $Cl^-$ removal)

The first adsorbate solution, denoted  $NaCl$ , was prepared using deionized (DI) water and analytical grade  $NaCl$  (Fisher Scientific Canada). It had a  $NaCl$  concentration of 0.043 M ( $Na^+$  concentration of 1,000 mg/L and  $Cl^-$  concentration of 1542 mg/L), which exceeds the Health Canada and World Health Organization (WHO) criteria for  $Na^+$  and  $Cl^-$  in drinking water of 200 and 250 mg/L, respectively.<sup>14, 15</sup> These concentrations of  $Na^+$  and  $Cl^-$  are representative of saline, brine-impacted groundwater.<sup>100, 101</sup> This salinity level is too low for the implementation of large-scale active water treatment systems, but high enough to adversely affect living organisms, plants, and soils, as similarly stated in Li et al. (2008).<sup>102</sup>

Varying masses of CLDH (0.75–2.24 g) were placed in 250 mL polyethylene bottles and mixed with 100 mL of the  $NaCl$  solution for 24 h. Based on preliminary studies, this contact time was sufficient for equilibrium to be reached. The CLDH mass that reduced the  $Cl^-$  concentration to less than 250 mg/L (the regulatory drinking water limit)<sup>14, 15</sup> was used to dechlorinate a 2 L volume of an identical solution ( $NaCl$ ). After 24 h contact time the aqueous phase was separated from the solid phase using vacuum filtration. The resultant solution (CLDH pre-treated) was the second adsorbate solution and is hereafter denoted  $Na_{dc}$ , where the “dc” subscript indicates that the solution is dechlorinated.

#### 4.3.3.2. Zeolite adsorption experiments ( $Na^+$ removal)

In the zeolite adsorption experiments, both  $NaCl$  ( $[Na^+]_i = 1000$  mg/L) and  $Na_{dc}$  ( $[Na^+]_i = 1050$  mg/L) solutions were used. The solution used is indicated after the name of the adsorbent. For instance, NZ- $Na_{dc}$  indicates natural zeolite (NZ) equilibrated with  $Na_{dc}$  (dechlorinated) solution, and AZ(1-HCl)- $NaCl$  indicates 1 M HCl-treated zeolite equilibrated with  $NaCl$  solution (without dechlorination). The  $Na^+$  removal efficiency was calculated for all experiments.

The optimal acid strength was first evaluated by mixing varying masses (0–3.75 g) of NZ, AZ(0.1- $H_2SO_4$ ), AZ(1- $H_2SO_4$ ), and AZ(2- $H_2SO_4$ ) with 25 mL of  $Na_{dc}$  solution in capped 50

mL centrifuge tubes. Upon determining the optimal acid strength for the H<sub>2</sub>SO<sub>4</sub> systems, the effect of different acid types (HNO<sub>3</sub>, HCl, and H<sub>2</sub>SO<sub>4</sub>) was similarly evaluated, again with Na<sub>dc</sub> solution.

Next, adsorption isotherms were generated for natural zeolite and the best-performing acid-treated zeolite (i.e., having the highest removal efficiency) using both NaCl and Na<sub>dc</sub> solutions. The constant solution normality isotherm method was used. Varying masses (0–7.5 g) of zeolite were placed in capped 50 mL centrifuge tubes and agitated for 24 h with 25 mL of either NaCl or Na<sub>dc</sub> solution. The Na<sup>+</sup> uptake was calculated and the Langmuir and Freundlich isotherm models applied.<sup>103, 104</sup> The Langmuir model can be written as

$$q_e = (q_{max}K_L C_e)/(1 + K_L C_e) \quad (4.3)$$

where  $q_{max}$  is the maximum uptake (mg/g) and  $K_L$  (L/mg) is the Langmuir constant. The Freundlich model can be written as

$$q_e = K_F C_e^{1/n} \quad (4.4)$$

where  $K_F$  [(mg/g)(L/mg)<sup>1/n</sup>] is the Freundlich constant and  $n$  is the Freundlich exponent (dimensionless).

#### 4.3.4. Adsorption Experiments (Potash Brine-Impacted Groundwater)

##### 4.3.4.1 Brine-impacted groundwater preparation

Potash brine was obtained from the tailings pond at a Saskatchewan potash mine. The brine was very high in Na<sup>+</sup> (87,400 mg/L), K<sup>+</sup> (52,900 mg/L), and Cl<sup>-</sup> (220,000 mg/L), and the pH was 7.19. Pristine groundwater was also obtained from a well near the town of Patience Lake, Saskatchewan. This groundwater sample was low in Na<sup>+</sup> (76 mg/L), K<sup>+</sup> (7.7 mg/L), and Cl<sup>-</sup> (42 mg/L) and had a pH of 8.1. To simulate an actual brine impact, the groundwater was spiked with brine (0.07% potash brine by volume). After spiking, the pH was 8.15, the ionic strength was 0.073 mol/L, and the ion concentrations were 673 ± 6 mg/L Na<sup>+</sup>, 1657 ± 25 mg/L Cl<sup>-</sup>, and 440 mg/L K<sup>+</sup>. This groundwater–brine solution (denoted GB) can be classified as saline.<sup>100, 101</sup>

##### 4.3.4.2 Dual-adsorbent desalination (Na<sup>+</sup> and Cl<sup>-</sup> removal)

This groundwater–brine solution (GB) was treated by first adding 4 g of CLDH to 150 mL of GB solution in a 250 mL polyethylene bottle. After agitating for 24 h using an orbital

shaker, the CLDH was separated through vacuum filtration (which minimized volume loss). Next, 18.25 g of acid-treated zeolite was added to the resultant solution (i.e., the dechlorinated solution) in a 250 mL polyethylene bottle. After agitating for 24 h using an orbital shaker, the zeolite was then separated through vacuum filtration. A groundwater chemistry analysis was performed at each stage: before the treatment, after the CLDH treatment, and after the sequential treatment using CLDH and acid-treated zeolite (the adsorbents were not mixed). This chemical analysis consisted of the major ions, pH, sodium absorption ratio (SAR), ionic strength, sum of ions, and hardness.

#### **4.3.5. Statistical Analysis**

All adsorption experiments were conducted in triplicate and the mean value is presented with error bars (where visible) indicating the standard deviation. Where shown, values correspond to means  $\pm$  standard deviation. GraphPad Prism V5 software was used to perform the statistical analysis of the groundwater chemistry data obtained from the dual-adsorbent experiments for potash brine-impacted groundwater (two-way analysis of variance with Bonferroni post-test).

#### **4.3.6. Measurements and Instruments**

Aqueous concentrations of  $\text{Na}^+$  and  $\text{Cl}^-$  were measured using ROSS ion-selective electrode probes attached to an Orion Star A214 benchtop meter (Thermo Fisher Scientific Canada). The ion-sensitive electrode probes were calibrated daily prior to use using manufacturer-provided standard solutions. Groundwater chemistry analyses were conducted by the Environmental Analytical Laboratories at the Saskatchewan Research Council (SRC) in Saskatoon, Canada, using standard test methods.<sup>105</sup> The major ions ( $\text{Ca}^{2+}$ ,  $\text{Mg}^{2+}$ ,  $\text{Na}^+$ ,  $\text{K}^+$ , and  $\text{SO}_4^{2-}$ ) were determined by inductively coupled plasma optical emission spectrometry (ICP-OES). The concentration of  $\text{OH}^-$ ,  $\text{HCO}_3^-$ , and  $\text{CO}_3^{2-}$  were simultaneously determined using a Mantech automatic titration system. The  $\text{Cl}^-$  concentration was determined by the mercuric thiocyanate colorimetric method on an AquaKem 200 Discrete analyzer.

XRD patterns of the samples were obtained using a diffractometer (Bruker D4 Endeavor) operating at 40 kV and 40 mA with  $\text{Cu K}\alpha$  radiation ( $\lambda = 0.154056$  nm). Phase identification was conducted using the Match! software package (Crystal Impact, Bonn, Germany). The whole

sample chemical composition was determined by XRF (Bruker S8 Tiger). The natural and modified zeolite samples were imaged using scanning electron microscopy (SEM, Hitachi S-3000N equipped with an energy dispersive spectrometer). The surface areas and particle porosity of the zeolites were determined by N<sub>2</sub> adsorption–desorption isotherms at 77 K and a relative pressure of 0.05–0.3 on a Micromeritics ASAP 2000 instrument. Prior to the N<sub>2</sub> isotherm analysis the samples were degassed at 150 °C for 2 h under vacuum.

X-ray imaging and spectromicroscopy were conducted on the STXM endstation on the spectromicroscopy beamline (10ID-1) at the Canadian Light Source (Saskatoon, Canada). The samples examined were the NZ-NaCl and AZ(1-HCl)-Na<sub>dc</sub> from the adsorption experiments. Air-dried samples were slurried in water, then 1–2 µL deposited onto silicon nitride windows and air-dried for 5 to 10 min. The Na, Al, and Si distributions in the samples were mapped by collecting on- and off-resonance transmission images with a 50-nm pixel size using the Na, Al, and Si K-edges, respectively. The measured transmission images were converted to absorbance images (i.e., optical density) using an area on the window without any particles. The image difference maps were derived by subtracting the optical density off-resonance image from the on-resonance image.<sup>106</sup> The processing was done using aXis2000 software.<sup>107</sup> Correlation analysis of the Na, Al, and Si image difference maps was conducted using ImageJ correlation plugin.<sup>108</sup>

## 4.4. Results and Discussion

### 4.4.1. Effect of CLDH Amount on Cl<sup>-</sup> Removal Efficiency

Cl<sup>-</sup> removal efficiency increased with the mass of CLDH added (Figure 4.2). At the highest CLDH amount (2.24 g/100 mL solution), the Cl<sup>-</sup> concentration was reduced by 85.3 ± 0.7% to 227 ± 11 mg/L, which is beneath the regulatory drinking water limit of 250 mg/L.<sup>14, 15</sup> Based on this result, a 2 L volume of NaCl solution was treated using this CLDH amount (i.e., 2.24 g of CLDH/100 mL). The resultant solution (dechlorinated water), denoted Na<sub>dc</sub>, had a Cl<sup>-</sup> concentration of 190 mg/L, a Na<sup>+</sup> concentration of 1,045 mg/L, and a pH of 12.3. The high pH is attributed to OH<sup>-</sup> release. This 2 L of pre-treated Na<sub>dc</sub> solution was used for subsequent Na<sup>+</sup> adsorption experiments.

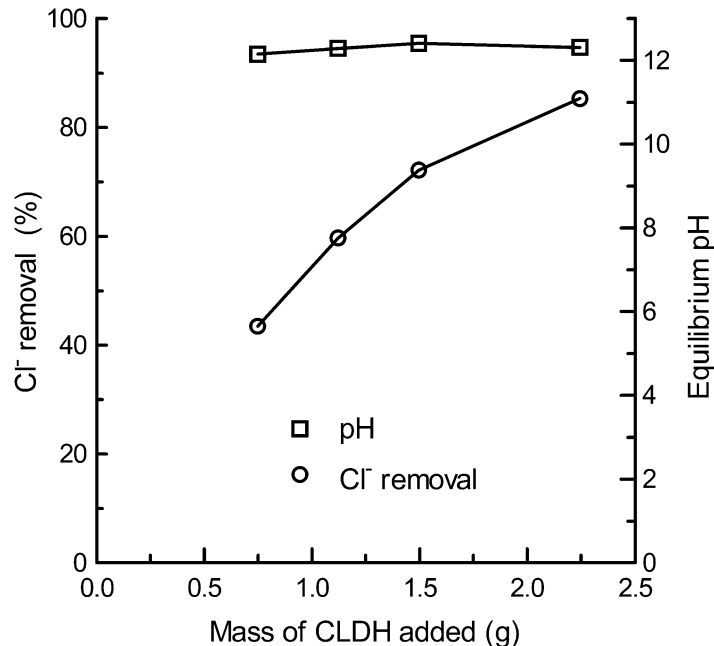
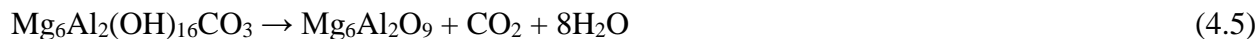


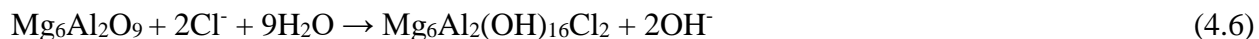
**Figure 4.2:** Cl<sup>-</sup> removal and equilibrium pH as a function of CLDH amount ( $V = 100$  mL,  $[\text{Cl}^-]_i = 1542$  mg/L,  $\text{pH}_i = 6.6$ ).

#### 4.4.2. Cl<sup>-</sup> Adsorption Mechanism

The XRD diffractograms (Figure 4.3) for the three different states of the LDH adsorbent (before calcination, after calcination, and after Cl<sup>-</sup> adsorption) indicated a structural reconstruction (termed *the memory effect*). The MgAl-CO<sub>3</sub> LDH (before calcination) had narrow and sharp XRD peaks at low  $2\theta$  values, which are characteristic of LDH compounds and indicate high crystallinity.<sup>53, 109, 110</sup> Upon calcination the MgAl-CO<sub>3</sub> LDH structure was destroyed and a mixed Mg-Al oxide (Mg<sub>6</sub>Al<sub>2</sub>O<sub>9</sub>, CLDH) formed. The corresponding chemical reaction is expressed by



When the CLDH was rehydrated in NaCl solution, the LDH structure reconstructed as MgAl-Cl LDH. To accommodate the larger Cl<sup>-</sup> ion, the  $d_{003}$  basal spacing of the MgAl-Cl LDH (0.791 nm) was marginally larger than in the MgAl-CO<sub>3</sub> LDH (0.789 nm). The structural reconstruction of LDH is expressed by



The Mg/Al molar ratio was nearly identical in the MgAl-CO<sub>3</sub> LDH and the MgAl-Cl LDH, reflecting that the predominant Mg-Al layered structures are stable.

This observed mechanism for  $\text{Cl}^-$  removal is in agreement with previous studies. Lv and co-workers (2006) and Zhao and co-workers (2011) also observed the memory effect when using calcined  $\text{MgAl-CO}_3$  LDH (various  $\text{Mg/Al}$  molar ratios and  $500^\circ\text{C}$  calcination) for  $\text{Cl}^-$  removal from a  $\text{NaCl}$ -water solution.<sup>73, 75</sup>

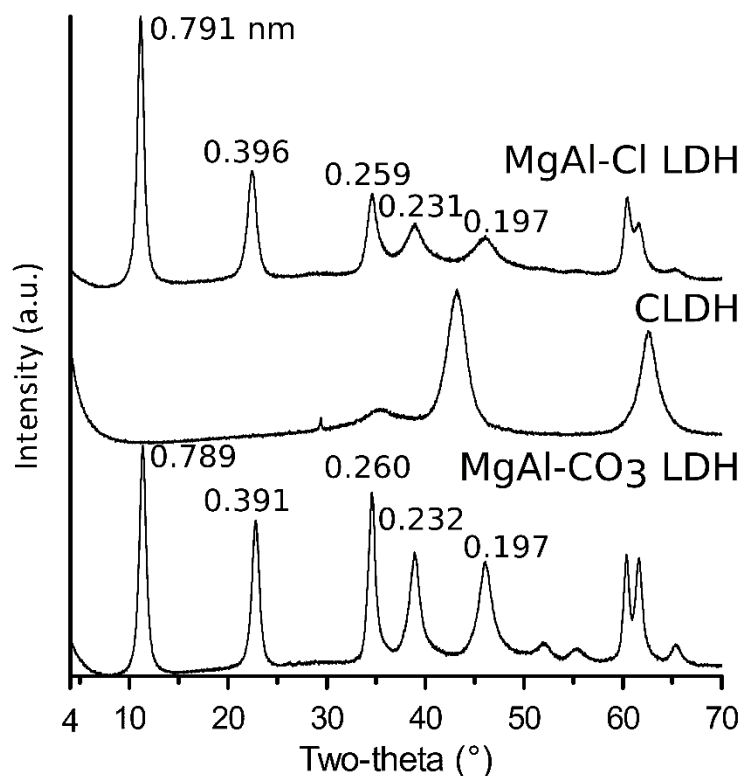


**Figure 4.3:** XRD patterns for  $\text{MgAl-CO}_3$  LDH, CLDH, and  $\text{MgAl-Cl}$  LDH (after  $\text{Cl}^-$  uptake).

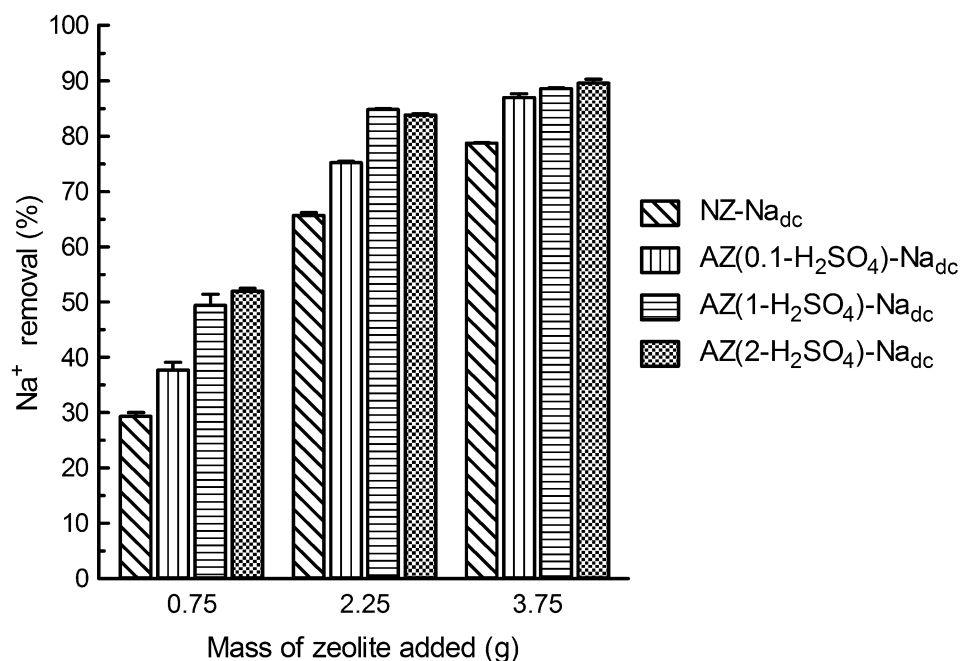
#### 4.4.3. Effect of Zeolite Treatment by Acids and Effect of Dechlorination

Using  $\text{Na}_{\text{dc}}$  solution, all acid-treated zeolites (0.1, 1, and 2 M  $\text{H}_2\text{SO}_4$ ) had a higher  $\text{Na}^+$  removal efficiency than natural zeolite, particularly at the lower masses of 0.75 and 2.25 g (Figure 4.4). The 1 and 2 M  $\text{H}_2\text{SO}_4$ -treated zeolites had similar  $\text{Na}^+$  removal efficiencies at any amount (up to 89.6%), and both outperformed the natural zeolite (9.9–22.6% higher  $\text{Na}^+$  removal, depending on the amount). The 0.1 M  $\text{H}_2\text{SO}_4$ -treated zeolite also outperformed the natural zeolite (1.6–14.3% higher  $\text{Na}^+$  removal, depending on the amount). At an adsorbent mass of 2.25 g, the  $\text{Na}^+$  removal was  $65.7 \pm 0.5$ ,  $75.2 \pm 0.3$ ,  $84.8 \pm 0.1$ , and  $83.8 \pm 0.2\%$  for natural and 0.1 M, 1.0 M, and 2.0 M  $\text{H}_2\text{SO}_4$ -treated zeolite, respectively. At the highest adsorbent mass

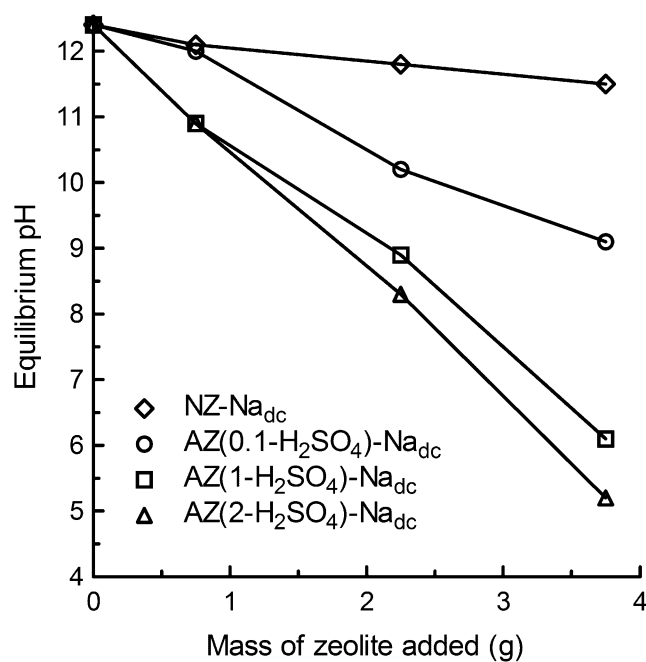
(3.75 g), the  $\text{Na}^+$  removal efficiencies approached 90% for all three acid-treated zeolites (Figure 4.4).

Uptake of  $\text{Na}^+$  onto zeolite was greatly influenced by the solution pH, which was initially 12.3 for the  $\text{Na}_{\text{dc}}$  solution (Figure 4.5). Due to  $\text{H}^+$  exchange, the pH decreased with increasing mass of acid-treated zeolite and with increasing degree of acid modification (i.e., 0.1, 1, or 2 M  $\text{H}_2\text{SO}_4$ ). At the highest adsorbent amount (3.75 g), the equilibrium pH values were 9.1, 6.1, and 5.2 for 0.1 M, 1 M, and 2 M  $\text{H}_2\text{SO}_4$ -treated zeolite, respectively. Thus, acid-treated zeolite simultaneously decreased the  $\text{Na}^+$  concentration and neutralized the pH of the adsorption effluent.

The  $\text{Na}^+$  removal efficiency was nearly identical for all strong acid types evaluated at a concentration of 1.0 M (Figure 4.6). With an acid-treated zeolite mass of 2.25 g or higher, the  $\text{Na}^+$  concentration was reduced to an acceptable value (i.e., below the regulatory drinking water limit of 200 mg/L). At the highest adsorbent amount (3.75 g), the removal efficiencies (and equilibrium  $\text{Na}^+$  concentration in parentheses) were 91.3% (91 mg/L), 90.4% (101 mg/L), and 88.6% (121 mg/L) for  $\text{AZ}(1\text{-HNO}_3)\text{-Na}_{\text{dc}}$ ,  $\text{AZ}(1\text{-HCl})\text{-Na}_{\text{dc}}$ , and  $\text{AZ}(1\text{-H}_2\text{SO}_4)\text{-Na}_{\text{dc}}$ , respectively. Given this parity, two previous findings were considered to select an acid type for further investigation: (1) concentrated HCl can be sourced from regenerating Cl-intercalated LDHs<sup>111, 112</sup>; and (2) HCl-treated zeolite shows less dealumination than  $\text{H}_2\text{SO}_4$ -treated zeolite<sup>113</sup>. Therefore,  $\text{AZ}(1\text{-HCl})$  was selected for further experiments with both  $\text{NaCl}$  and  $\text{Na}_{\text{dc}}$  solution.

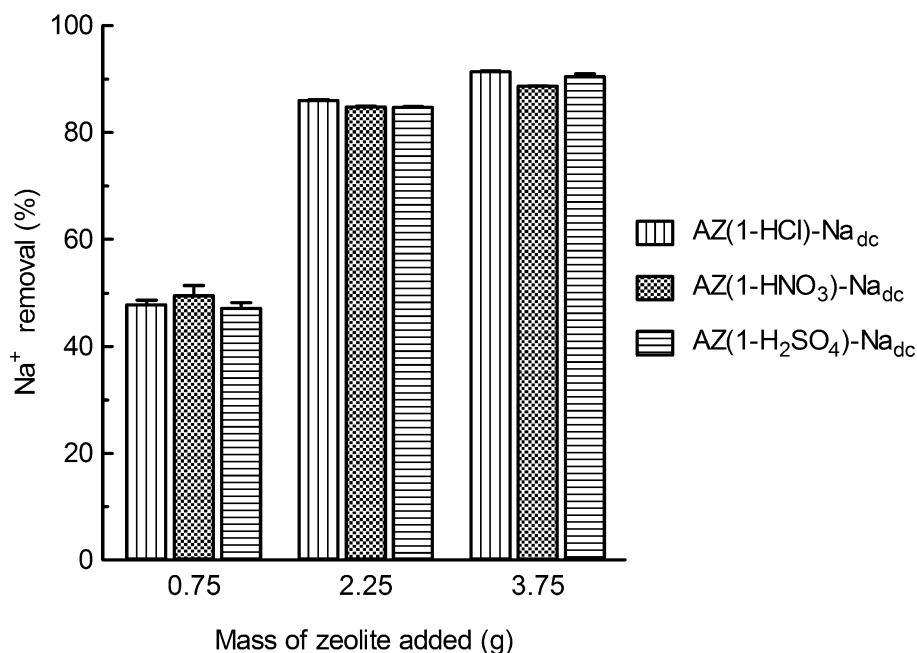


**Figure 4.4:** Na<sup>+</sup> percent removal for varying masses of natural and 0.1, 1.0, and 2.0 M H<sub>2</sub>SO<sub>4</sub>-treated zeolite ( $V = 25$  mL,  $[\text{Na}^+] = 1000$  mg/L,  $\text{pH}_i = 12.3$ ).



**Figure 4.5:** Equilibrium pH for varying masses of natural and 0.1, 1.0, and 2.0 M H<sub>2</sub>SO<sub>4</sub>-treated zeolite ( $V = 25$  mL,  $[\text{Na}^+] = 1000$  mg/L,  $\text{pH}_i = 12.3$ ).

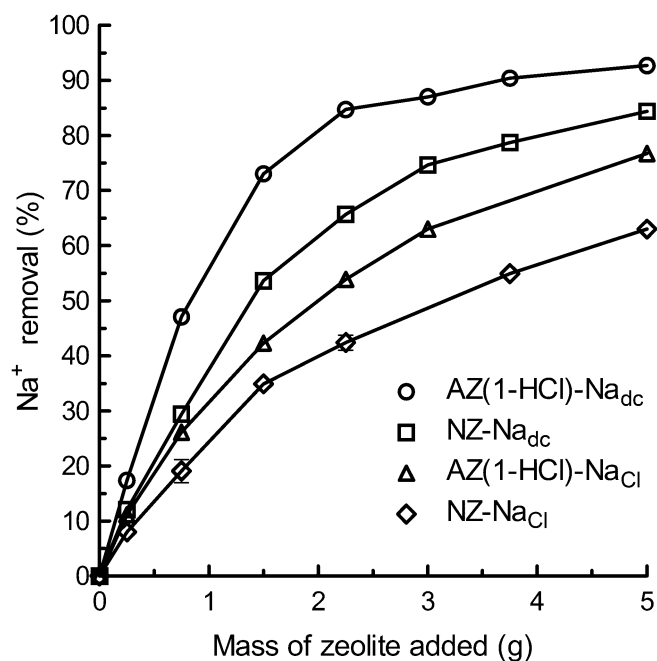




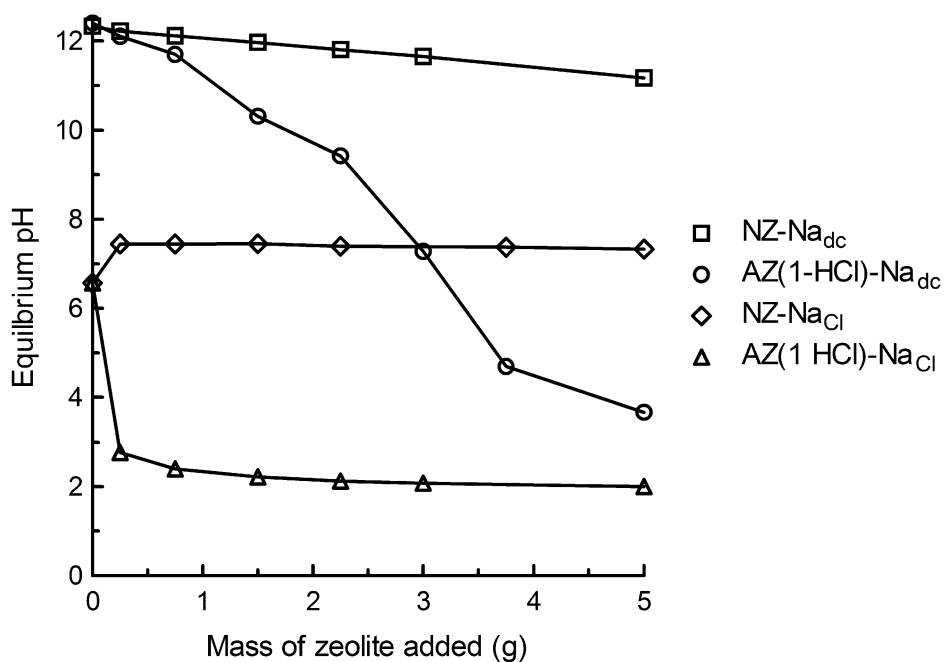
**Figure 4.6:** Na<sup>+</sup> percent removal for different amounts of zeolite treated by different strong acids at 1 M concentration ( $V = 25$  mL,  $[\text{Na}^+] = 1000$  mg/L,  $\text{pH}_i = 12.3$ ).

Figure 4.7 shows the Na<sup>+</sup> removal efficiency as a function of the mass of NZ and AZ(1-HCl) added, using either the NaCl or Na<sub>dc</sub> solution, indicating a significant dechlorination effect for both treatments for Na<sup>+</sup> removal. The Na<sup>+</sup> removal efficiency of AZ(1-HCl)-Na<sub>dc</sub> was up to 2.5 times higher than that of NZ-NaCl, depending on the adsorbent type and quantity. For instance, at a mass of 0.75 g, 19.1% of the Na<sup>+</sup> was removed using NZ-NaCl compared to 47.1% using AZ(1-HCl)-Na<sub>dc</sub>.

As discussed, the pH of the Na<sub>dc</sub> solution (12.3) was reduced by acid-treated zeolite (Figure 4.8). Using AZ(1-HCl)-Na<sub>dc</sub> at a mass of 3 g, the pH came to neutral (7.28) with 87% Na<sup>+</sup> removal. In contrast, NZ-Na<sub>dc</sub> exchanged Ca<sup>2+</sup> for Na<sup>+</sup> and only slightly lowered the pH. This small pH reduction may be through exchange of H<sup>+</sup> from Si-O-H or Al-O-H groups in the lattice.



**Figure 4.7:** Na<sup>+</sup> percent removal as a function of the mass of zeolite added ( $V = 25$  mL,  $[\text{Na}^+]_i = 1000$  mg/L).



**Figure 4.8:** Equilibrium pH as a function of the mass of zeolite added ( $V = 25$  mL,  $[\text{Na}^+]_i = 1000$  mg/L).

The NaCl solution, prepared with DI water, initially had a near-neutral pH (6.57). With NZ-NaCl, the pH slightly increased (pH 7.37 with an adsorbent mass of 5.0 g) due to surface protonation, a trend that has been reported in previous studies.<sup>42</sup> With AZ(1-HCl)-NaCl, the pH sharply dropped to 2.0. This acidity renders acid-treated zeolite unsuitable for many environmental remediation applications. However, if acid-treated zeolite is used with CLDH, which is highly basic, a neutral final pH is achievable and cation uptake is synergistically enhanced. The treatment sequence is important—CLDH should be used first, followed by acid-treated zeolite. This is because CLDH partially or fully dissolves under acidic conditions (as generated by the acid-treated zeolite), causing a large decrease in its adsorption capacity.<sup>114</sup> Under basic conditions (as generated by the CLDH), acid-treated clinoptilolite zeolite is stable and its adsorption capacity is greatly improved.<sup>115, 116</sup>

#### 4.4.4. Na<sup>+</sup> Uptake Isotherms

Na<sup>+</sup> adsorption isotherms were modelled using the Langmuir and Freundlich isotherm models.<sup>103, 104</sup> The plotted linearized isotherms and associated model parameters are given in Figure 4.9, Figure 4.10, and Table 4.2. Based on the coefficient of determination ( $R^2$ ), the Langmuir model ( $R^2 = 0.986\text{--}0.995$ ) fit the data marginally better than the Freundlich model ( $R^2 = 0.946\text{--}0.994$ ). Many previous studies have found that Na<sup>+</sup> uptake onto zeolite can be acceptably modelled using the Langmuir equation, which assumes monolayer adsorption on homogeneous surfaces.<sup>32, 41, 42</sup> The one exception in this study was the NZ-NaCl, in which the Na<sup>+</sup> uptake increased linearly ( $n = 1.01$ ) and was poorly fitted by the Langmuir model; this was also observed by Huang (2005).<sup>40</sup> The Freundlich model, which assumes multilayer adsorption on heterogeneous adsorption sites, however, provided a good fit for NZ-NaCl. Figure 4.11 shows the isotherm plots (Langmuir or Freundlich) for each zeolite adsorbent.

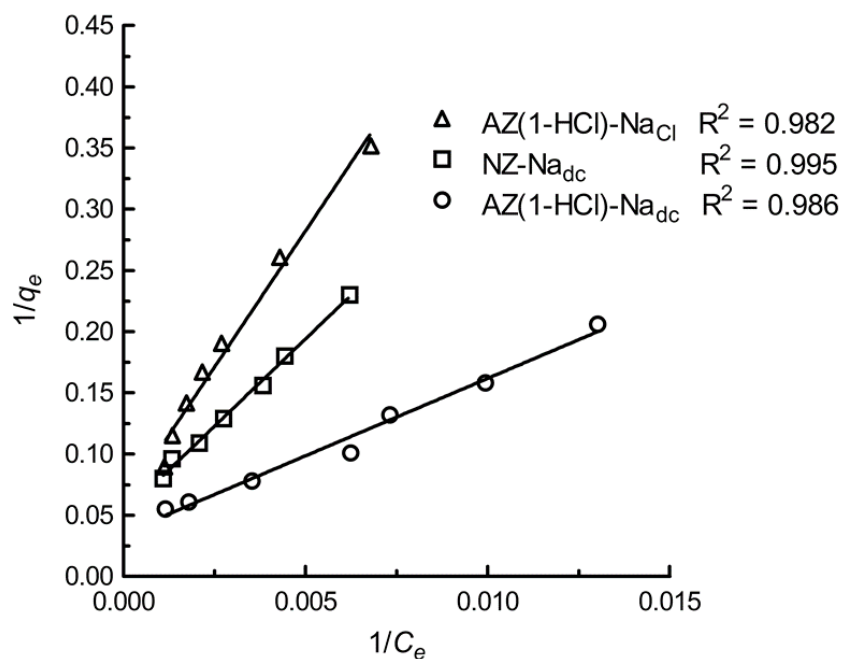


**Figure 4.9:** Linearized Langmuir isotherms.

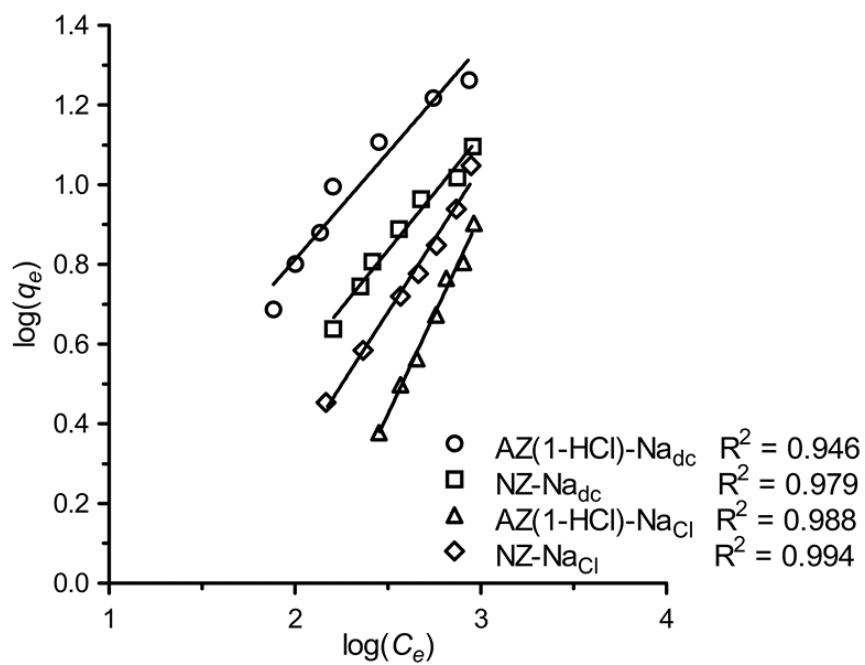


**Figure 4.10:** Linearized Freundlich isotherms.

**Table 4.2.** Isotherm model parameters for Na<sup>+</sup> adsorption onto zeolite at 23 °C.

Sample	Freundlich Model			Langmuir Model		
	$K_F$ [mg/g)(L/mg) <sup>1/n</sup> ]	1/n	R <sup>2</sup>	$q_{max}$ (mg/g)	$K_L$ (L/mg)	R <sup>2</sup>
NZ-NaCl	0.0081	1.0069	0.994	—	—	—
NZ-Na <sub>dc</sub>	0.2469	0.5767	0.979	19.5	0.00179	0.995
AZ(1-HCl)-NaCl	0.0722	0.7284	0.988	16.7	0.00134	0.982
AZ(1-HCl)-Na <sub>dc</sub>	0.5450	0.5374	0.946	28.4	0.00276	0.986

– For NZ-NaCl, the Langmuir model did not apply.

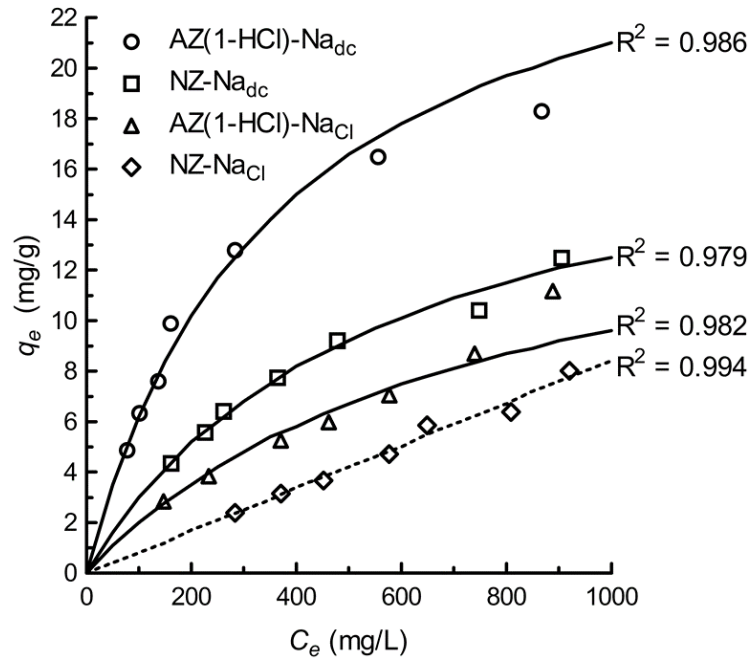


**Figure 4.11:** Na<sup>+</sup> adsorption isotherms. The solid and dashed lines indicate the Langmuir and Freundlich model fittings, respectively.

The Langmuir adsorption capacity ( $q_{max}$ ) varies in the order AZ(1-HCl)-Na<sub>dc</sub> (28.4 mg/g) > NZ-Na<sub>dc</sub> (19.5 mg/g) > AZ(1-HCl)-NaCl (16.7 mg/g) > NZ-NaCl. The NZ-NaCl isotherm result is comparable to a similar study by Zhao and co-workers (2008), who determined the Langmuir Na<sup>+</sup> adsorption capacity for natural Bear River zeolite to be 12.3 mg/g.<sup>32</sup> The difference (8.0 and 12.3 mg/g) is likely attributable to the different initial Na<sup>+</sup> concentrations in the two studies. In most Na<sup>+</sup> adsorption studies, including those by Zhao (2008) and several others given in Table 4.3, the Na<sup>+</sup> concentration used for the isotherm generation is upwards of 5,000 mg/L as opposed

to 1,000 mg/L used in this study. Notwithstanding the low initial  $\text{Na}^+$  concentration in this study, the maximum  $\text{Na}^+$  adsorption capacity for AZ(1-HCl)- $\text{Na}_{\text{dc}}$  (28.4 mg/g) was much higher than previously reported values for natural and modified zeolites (Table 4.3). The mechanisms explaining this exceptionally high uptake are discussed in the following section.

**Table 4.3:** Comparison of maximum  $\text{Na}^+$  adsorption capacities of various zeolites.

Zeolite	Solution	$q_{\text{max}}$ (mg/g)	Reference
St. Cloud zeolite	Synthetic CSG water	2.8	Huang et al. (2006) <sup>40</sup>
St. Cloud zeolite	$\text{NaHCO}_3$	4.76–8.39	Ganjegunte et al. (2011) <sup>41</sup>
Natural zeolite	$\text{NaCl}$	4.8	Santiago et al. (2016) <sup>46</sup>
Acid-treated zeolite	$\text{NaCl}$	6.07	Santiago et al. (2016) <sup>46</sup>
Castle Mountain zeolite	$\text{NaCl}$	6.4	Millar et al. (2016) <sup>42</sup>
$\text{K}^+$ -modified zeolite	$\text{NaCl}$	8.0	Santiago et al. (2016) <sup>46</sup>
$\text{NH}_4^+$ -modified zeolite	$\text{NaCl}$	9.4	Santiago et al. (2016) <sup>46</sup>
St. Cloud zeolite	$\text{NaCl}$ and $\text{NaHCO}_3$	9.6	Zhao et al. (2008) <sup>32</sup>
Castle Mountain zeolite	$\text{NaHCO}_3$	10.3	Millar et al. (2016) <sup>42</sup>
Bear River zeolite	$\text{NaCl}$ and $\text{NaHCO}_3$	12.3	Zhao et al. (2008) <sup>32</sup>
Acid-treated zeolite	$\text{Na}_{\text{dc}}$	28.4	This study

#### 4.4.5. $\text{Na}^+$ Adsorption Mechanisms

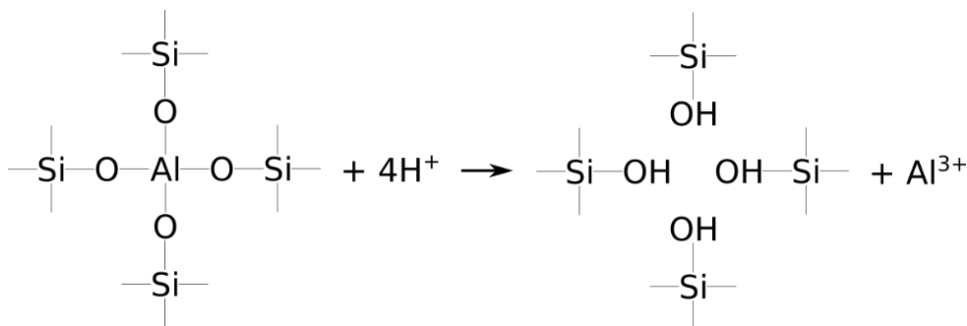
Two factors that additively increased the  $\text{Na}^+$  uptake onto zeolite were (1) zeolite acid treatment; and (2) solution pre-treatment (dechlorination) using CLDH. Several techniques were used to investigate these factors, including XRD, XRF, surface area and porosimetry, and STXM.

##### 4.4.5.1. Effect of zeolite acid treatment

The acid treatment produced a number of effects. First, the native exchangeable cations were replaced by protons, as evidenced by the chemical composition of the NZ and AZ(1-HCl) samples (Table 4.4). Both the  $\text{K}_2\text{O}$  and the  $\text{CaO}$  content were greatly reduced in the acid-treated zeolite, indicating proton exchange with the sorbed cations and the transition of the zeolite to its near-homoionic H-form (this process is illustrated Figure 4.12). After reaction of AZ(1-HCl)

$$\begin{array}{c}
 \text{---Si---} \\
 | \\
 \text{O} \quad M'' \quad \text{O} \quad \text{O} \quad \text{O} \\
 | \quad \quad | \quad | \quad | \\
 \text{---Si---O---Al---O---Si---O---Si---O---Al---} \\
 | \quad \quad | \quad \quad \quad | \\
 \text{O} \quad \quad \text{O} \quad \quad \quad \text{O} \\
 | \\
 \text{---Si---}
 \end{array}
 \xrightarrow{H^+}
 \begin{array}{c}
 \text{---Si---} \\
 | \\
 \text{O} \\
 | \\
 \text{---Si---O---Al} \quad \text{HO---Si---O---Si---O---Al} \quad H^+ \\
 | \quad \quad | \quad | \quad | \quad | \\
 \text{O} \quad \quad \text{O} \quad \text{O} \quad \text{O} \quad \text{O} \\
 | \\
 \text{---Si---}
 \end{array}$$

In addition to zeolite decationation, the acid treatment caused Si-O-Al hydrolysis (illustrated in Figure 4.13). This generated polarized silanol groups with protons that participate in ion-exchange reactions. The acid treatment also caused dealumination (Al-O bond hydrolysis), as evidenced by the Si/Al molar ratio increasing to 6.82 in the acid-treated sample compared to 5.95 in the natural precursor (Table 4.4).



41

**Table 4.4:** Chemical composition of natural zeolite and acid-treated zeolites, before and after reaction with NaCl or Na<sub>dc</sub> solution.

Constituent (Wt. %)	<u>Unreacted</u>		<u>Reacted</u>	
	NZ	AZ(1-HCl)	AZ(1-HCl)-NaCl	AZ(1-HCl)-Na <sub>dc</sub>
Na <sub>2</sub> O	0.04	<0.01	0.70	1.52
MgO	0.59	0.58	0.52	0.58
Al <sub>2</sub> O <sub>3</sub>	10.13	9.68	8.95	9.15
SiO <sub>2</sub>	71.00	74.73	71.97	71.96
P <sub>2</sub> O <sub>5</sub>	0.08	0.06	0.05	0.07
K <sub>2</sub> O	4.14	3.21	3.08	3.14
CaO	2.98	1.75	1.49	2.29
TiO <sub>2</sub>	0.32	0.35	0.31	0.30
MnO	0.04	0.03	0.02	0.03
Fe <sub>2</sub> O <sub>3</sub>	2.10	2.33	2.13	1.97
S	<0.01	<0.01	<0.01	<0.01
Si/Al Ratio	5.95	6.82	7.10	6.95

Acid treatment caused a large expansion in the surface area of the zeolite (Table 4.5). The Brunauer–Emmett–Teller surface area ( $S_{BET}$ ; representing pore sizes  $>0.4$  nm)<sup>117</sup> was 39.6 m<sup>2</sup>/g for the NZ compared to 63.5 m<sup>2</sup>/g for the AZ(1-H<sub>2</sub>SO<sub>4</sub>). The microporous surface area ( $S_{micro}$ ; representing pore sizes  $<0.4$  nm) was 4.5 m<sup>2</sup>/g for the NZ compared to 13.9 m<sup>2</sup>/g for the AZ(0.1-H<sub>2</sub>SO<sub>4</sub>) and 25.0 m<sup>2</sup>/g for the AZ(1-H<sub>2</sub>SO<sub>4</sub>). The acid-treated samples also had a lower average pore diameter ( $D_{avg}$ ). The higher surface area was apparent in the SEM images, with the acid-treated zeolite showing less aggregation and a more spherical texture (Figure 4.14).

The expanded surface was attributed to acid-induced Si-O-Al and Al-O bond hydrolysis and the clearing of pore-blocking impurities. The higher surface area can partially account for the improvement in Na<sup>+</sup> adsorption observed in the acid-treated zeolites (greater number of ion-exchange sites). Indeed, the AZ(1-H<sub>2</sub>SO<sub>4</sub>) sample showed the highest Na<sup>+</sup> uptake and the largest surface area.



**Table 4.5:** Surface area ( $S_{BET}$ ), external surface area ( $S_{external}$ ), microporous surface area ( $S_{micro}$ ), and average pore width ( $D_{avg}$ ) for natural and  $H_2SO_4$ -treated zeolites (at 0.1 and 1 M).

Adsorbent	NZ	AZ(0.1- $H_2SO_4$ )	AZ(1- $H_2SO_4$ )
$S_{BET}$ ( $m^2/g$ )	39.6	51.4	63.5
$S_{external}$ ( $m^2/g$ )	35.1	37.5	38.5
$S_{micro}$ ( $m^2/g$ ) <sup>a</sup>	4.5	13.9	25.0
$D_{avg}$ (nm)	12.3	9.6	7.92

$$^a S_{micro} = S_{BET} - S_{external}$$

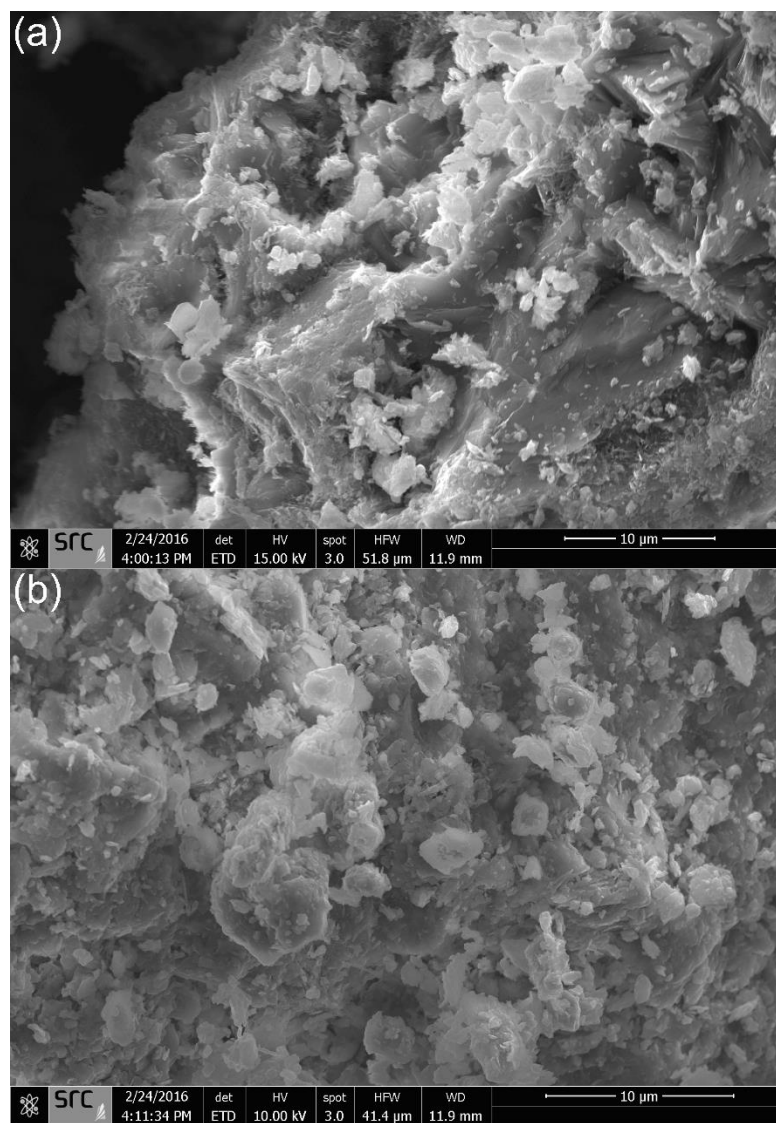


**Figure 4.14:** Scanning electron microscope images of (a) NZ and (b) AZ(1-HCl).

XRD was used to investigate potential mineralogical alterations induced by the acid treatment (Figure 4.15). The NZ showed high crystallinity with peaks characteristic of clinoptilolite.<sup>118</sup> Following acid treatment, there was a slight reduction in the basal spacing and the peak intensity, as well as a small shift towards higher two-theta values. This indicates that the acid treatment affected the crystalline nature of the zeolite, which can be attributed to ion leaching, particularly  $\text{Al}^{3+}$ . However, due to the zeolite's high Si/Al ratio (5.95 in this study), the acid treatment was relatively well tolerated. The  $\text{SiO}_4$  tetrahedra are the predominant framework structure and have good stability under acidic conditions, unlike  $\text{AlO}_4^-$ .<sup>20, 95, 116, 119</sup>

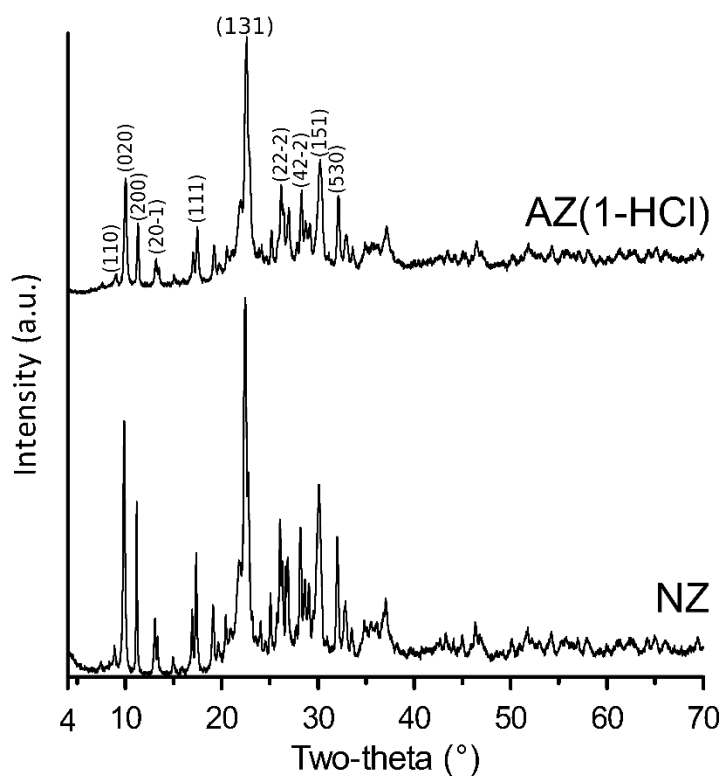


**Figure 4.15:** XRD patterns for NZ and AZ(1-HCl).

The XRD patterns for the natural and acid-treated zeolite were consistent with previous research. Li and co-workers (2007) found that clinoptilolite treated at pH 1–5 for 144 h had slightly diminished XRD peak intensities, but the crystallinity was not significantly affected.<sup>102</sup> Wang et al. (2016) noted profound structural collapse for a Na-Y zeolite subjected to 0.1–5 M  $\text{H}_2\text{SO}_4$  treatment, but the contact time was very long (70 h).<sup>95</sup> In this study, the acid

concentration was high (1.0 M), but lattice decomposition was mitigated by the brief contact time (30 min).

#### 4.4.5.2. Effect of solution pre-treatment with CLDH

In addition to zeolite acid treatment, the second factor that (additively) increased the Na<sup>+</sup> uptake was the CLDH solution pre-treatment (i.e., the Na<sub>dc</sub> solution—dechlorinated). Note that the composition of the Na<sub>dc</sub> solution was basically NaOH (pH 12.3), with small amounts of residual Cl<sup>-</sup>. The protons adsorbed on acid-treated zeolite (in near-homoionic H-form) will readily ion-exchange with Na<sup>+</sup> in solution, then react with the abundant OH<sup>-</sup> groups to produce water and neutralize the pH:



The Na<sup>+</sup> uptake was exceptionally high due to the high pH and the absence of H<sup>+</sup> competition, as observed in similar previous studies.<sup>120, 121</sup> The Si/Al molar ratio of the AZ(1-HCl)-Na<sub>dc</sub> was roughly equal to that of the AZ(1-HCl)-NaCl (6.95 and 7.10, respectively). Under basic conditions, as in the Na<sub>dc</sub> solution, zeolite has good stability (moderate desilication, but minimal dealumination).<sup>116, 119, 122</sup> It is beneficial to retain crystallinity and a low Si/Al ratio.

#### 4.4.6. Distribution of Na<sup>+</sup> Adsorption Sites

To further understand the Na<sup>+</sup> adsorption mechanisms, the distributions of Al, Na, and Si within NZ-NaCl and AZ(1-HCl)-Na<sub>dc</sub> samples were visualized using synchrotron-based STXM. The Al, Na, and Si image difference maps of the various systems are shown in Figure A1 and their color overlays are shown in Figure 4.16.

Si and Al blend together in the NZ-NaCl (pink regions). However, Si and Al were more distinct and segregated in the acid-treated zeolite (Figure 4.16b), suggesting that Al dissolution occurred. In Fig. A1 (Appendix), the optical density of Al in the elemental map of the acid-treated zeolites was lower than that of the natural zeolites, consistently supporting the occurrence of dealumination in the acid-treated zeolites. The optical density of Si in the AZ(1-HCl)-Na<sub>dc</sub> (after dechlorination) was also lower than in the natural zeolite before dechlorination, reflecting that the loss of Si (desilication) may occur due to the high effluent pH after the CLDH treatment.

$\text{Na}^+$  adsorption sites were not homogenous and broadly scattered throughout the natural zeolites (Figure 4.16a). However, in the acid-treated zeolites,  $\text{Na}^+$  adsorption appeared to be more concentrated on certain particles (Figure 4.14b). Overlapping Si and Na was distinctly observable in the AZ(1-HCl)- $\text{Na}_{\text{dc}}$  samples (cyan regions in Figure 4.16b), but not in the NZ- $\text{NaCl}$ . This was attributed to the acid-induced hydrolysis of Si-O-Al bonds and ion exchanges between  $\text{Na}^+$  and protons on opened silanol groups, as expressed by eq. 4.7. The  $\text{Na}^+$  adsorption sites (Si-O-Na) visualized by the STXM analyses provides evidence that enhanced sodium adsorption is supported by dealumination and the associated formation of  $\text{Na}^+$  adsorption sites in the acid-treated zeolites.

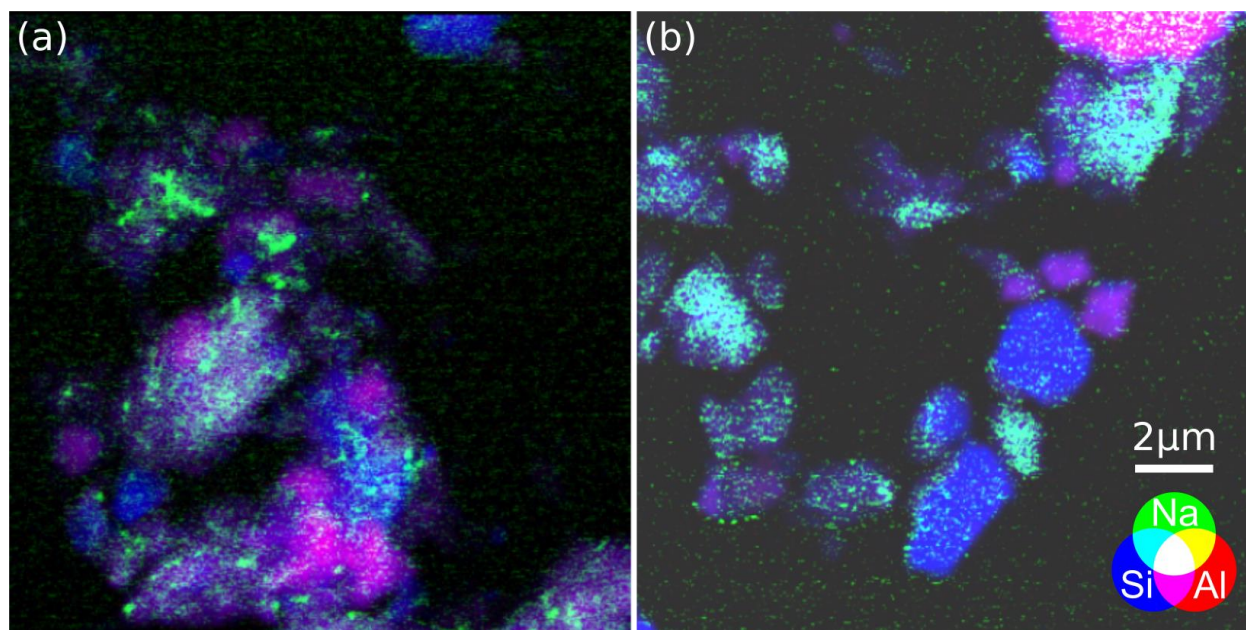


**Figure 4.16:** STXM images for (a) NZ- $\text{NaCl}$  and (b) AZ(1-HCl)- $\text{Na}_{\text{dc}}$ . The 2  $\mu\text{m}$  scale bar applies to each system. The colour denotations are blue for Si, red for Al, and green for Na. The colours blend where ions co-occur (e.g., cyan where  $\text{Na}^+$  maps onto Si).

#### 4.4.7. Desalination of Simulated Potash Brine-Impacted Groundwater

Desalination was demonstrated using groundwater spiked with potash brine (i.e., saline groundwater). Because this saline groundwater contained a large suite of ions at significant concentrations (namely  $\text{Na}^+$ ,  $\text{K}^+$ ,  $\text{Cl}^-$ ,  $\text{HCO}_3^-$ , and  $\text{SO}_4^{2-}$ ), a complete ion analysis was conducted at each stage of the treatment process (Table 4.6). The water chemistry datasets in Table 4.6

were statistically evaluated (two-way analysis of variance with Bonferroni post-test), which showed that the effect of the dual-adsorbent treatment on improving multiple water quality parameters is statistically significant.

The CLDH treatment transiently raised the pH (12.38) and greatly reduced the concentrations of anions (i.e.,  $\text{HCO}_3^-$ ,  $\text{Cl}^-$ ,  $\text{SO}_4^{2-}$ ) as well as divalent cations. After CLDH treatment, the  $\text{SO}_4^{2-}$  concentration (initially 400 mg/L) was reduced to  $4.0 \pm 1.53$  mg/L, the  $\text{HCO}_3^-$  concentration (initially 194 mg/L) was undetectable, and the  $\text{Cl}^-$  concentration (initially  $1,656 \pm 25$  mg/L) was  $203 \pm 18$  mg/L. CLDH clearly showed a higher affinity for  $\text{SO}_4^{2-}$  and  $\text{HCO}_3^-$  (given their near complete removal), likely due to their high charge density. The mechanisms for divalent cation sorption on CLDH include isomorphic substitution, adsorption, and precipitation, as reviewed by Liang (2013).<sup>123</sup>

The monovalent cations ( $\text{K}^+$  and  $\text{Na}^+$ ) were unaffected by CLDH but efficiently removed through the AZ(1-HCl) treatment. Consistent with previous studies,  $\text{K}^+$  was preferred over  $\text{Na}^+$  (respective removal efficiencies of  $97.3 \pm 0.1$  and  $81.4 \pm 0.6\%$ ).<sup>39</sup> Importantly, the AZ(1-HCl) neutralized the pH (7.31).

**Table 4.6:** Desalination of potash brine-impacted groundwater with the dual-adsorbent (CLDH and AZ). Bonferroni collected probabilities (indicated by asterisks) compare each step with the previous.

	Groundwater–brine	After CLDH	After CLDH and AZ(1-HCl)
HCO <sub>3</sub> (mg/L)	194 ± 3.2	<1 <sup>***</sup>	27 <sup>**</sup>
Cl (mg/L)	1657 ± 25	203 ± 18 <sup>***</sup>	219 ± 9
pH	8.15 ± 0.01	12.38 ± 0.03 <sup>***</sup>	7.31 ± 1.1 <sup>***</sup>
Sum of ions (mg/L)	3506 ± 23	2233 ± 38 <sup>***</sup>	382 ± 12 <sup>***</sup>
Total hardness (mg/L as CaCO <sub>3</sub> )	481 ± 2.1	6.3 ± 5.1 <sup>***</sup>	90.7 ± 2.5 <sup>***</sup>
Ca (mg/L)	65 ± 0.6	3 ± 2.1 <sup>***</sup>	20 ± 1
Mg (mg/L)	78 ± 0.6	<1 <sup>***</sup>	10
K (mg/L)	440	460 ± 10	13 ± 6 <sup>***</sup>
Na (mg/L)	673 ± 6	750 ± 10 <sup>***</sup>	86 ± 3 <sup>***</sup>
SO <sub>4</sub> (mg/L)	400	4 ± 1.53 <sup>***</sup>	6 ± 0.58
SAR	13.3 ± 0.1	121 ± 35.3 <sup>***</sup>	3.9 ± 0.1 <sup>***</sup>
Ionic strength (mol/L)	0.063	0.025	0.007

<sup>\*\*</sup> Statistical significance at  $p < 0.01$ .

<sup>\*\*\*</sup> Statistical significance at  $p < 0.001$ .

The water hardness was originally  $480.7 \pm 2.3$  mg CaCO<sub>3</sub>/L, which is exceptionally hard and can cause corrosion and encrustation issues.<sup>14</sup> By removing Ca<sup>2+</sup> and Mg<sup>2+</sup>, CLDH reduced the hardness to  $6.3 \pm 5.1$  mg CaCO<sub>3</sub>/L. With the acid-treated zeolite, H<sup>+</sup>/Na<sup>+</sup> exchange was dominant (as evidenced by the pH drop), but some Ca<sup>2+</sup>/Na<sup>+</sup> and Mg<sup>2+</sup>/Na<sup>+</sup> exchange still occurred. Accordingly, after AZ(1-HCl) application the hardness increased to  $90.7 \pm 2.5$  mg CaCO<sub>3</sub>/L, which is still within regulatory limits for drinking water.<sup>14, 15</sup> Moreover, the simultaneous removal of Na<sup>+</sup> (81.4% reduction) and slight release of Ca<sup>2+</sup> and Mg<sup>2+</sup> following AZ(1-HCl) application improved the SAR, defined as

$$\text{SAR} = \frac{[\text{Na}^+]}{\sqrt{\frac{[\text{Ca}^{2+}] + [\text{Mg}^{2+}]}{2}}} \quad (4.9)$$

where the ion concentrations are expressed in meq/L. The SAR was initially 13.3 and decreased

to  $3.9 \pm 0.1$  after treatment with the dual adsorbent. A SAR less than 4, as achieved in this experiment, indicates that the water is suitable for agricultural irrigation (i.e., ensures proper soil permeability).<sup>48</sup>

In addition to the hardness and SAR, the dual adsorbent was able to dramatically decrease the sum of ions, which is defined as the sum of the concentrations of  $\text{Ca}^{2+}$ ,  $\text{Mg}^{2+}$ ,  $\text{Na}^+$ ,  $\text{K}^+$ ,  $\text{CO}_3^{2-}$ ,  $\text{HCO}_3^-$ ,  $\text{SO}_4^{2-}$ ,  $\text{Cl}^-$ , and  $\text{NO}_3^-$  (similar to TDS). Initially, the sum of ions the groundwater–brine solution was  $3,506 \pm 23$  mg/L, much higher than the aesthetic threshold of 500 mg/L.<sup>14, 15</sup> This value decreased to  $2,233 \pm 38$  mg/L after CLDH treatment and to  $382 \pm 12$  mg/L following AZ(1-HCl) application.

## 4.5. Conclusion

This study achieved desalination by synergistically combining two adsorbents: CLDH and acid-treated zeolite. Their properties and adsorption capacities were investigated through analytical techniques and batch equilibrium experiments. The AZ(1-HCl)- $\text{Na}_{\text{dc}}$  had a strikingly high  $\text{Na}^+$  adsorption capacity (increased by a factor of 2-3, relative to NZ). The mechanisms for this augmented  $\text{Na}^+$  adsorption, including Si-O-Na and Al-O-Na bonding, were explained and evidenced through STXM analyses. Anions (mainly  $\text{Cl}^-$ , but also  $\text{NO}_3^-$  and  $\text{SO}_4^{2-}$ ) were concurrently removed by the CLDH and the final pH brought to near neutral. As proof of concept, desalination was also demonstrated with natural groundwater spiked with potash brine, suggesting potential real-world applicability for the CLDH-AZ dual adsorbent. In addition, the dual adsorbent improved groundwater quality parameters (hardness, SAR, and sum of ions). Possible applications for this process include the mining industry, particularly potash, as well as the oil and gas industry. These results provide a fundamental basis for the development of an improved desalination and water treatment technology.

## 4.6. Acknowledgements

We acknowledge technical advice and assistance provided by Jeff Meadows, Kathlene Jacobson, Richard Weighaupt, and Al Shpyth through the International Minerals Innovation Institute (IMII). Thanks also to Blain Paul for assistance with XRD analysis and Kyowa Chemical Industry for providing the LDH sample. This research was funded by PotashCorp, Agrium, The Mosaic Company, the IMII, a Mathematics of Information Technology and

Complex Systems (Mitacs) Accelerate Cluster Grant (IT04529), and the Natural Sciences and Engineering Research Council of Canada (CRDPJ 487008-15). The STXM analyses described in this study was performed at the Canadian Light Source, which is supported by the Natural Sciences and Engineering Research Council of Canada, the National Research Council Canada, the Canadian Institutes of Health Research, the Province of Saskatchewan, Western Economic Diversification Canada, and the University of Saskatchewan.



# Chapter Five

## A Recyclable Adsorbent for Salinized Groundwater: Desalination and Potassium-Exchanged Zeolite Production

**Preface:** In the previous chapter, the dual-adsorbent was evaluated primarily using synthetic NaCl solution. In this chapter, groundwater spiked with potash brine is exclusively used. The modified zeolite is also enhanced, and a K-form zeolite is produced. This chapter is presented as a standalone scientific paper: (5.1) Abstract; (5.2) Introduction; (5.3) Experimental; (5.4) Results and Discussion; and (5.5) Acknowledgements. This paper is contextualized and related to the research project as a whole in Chapter Six of this thesis.

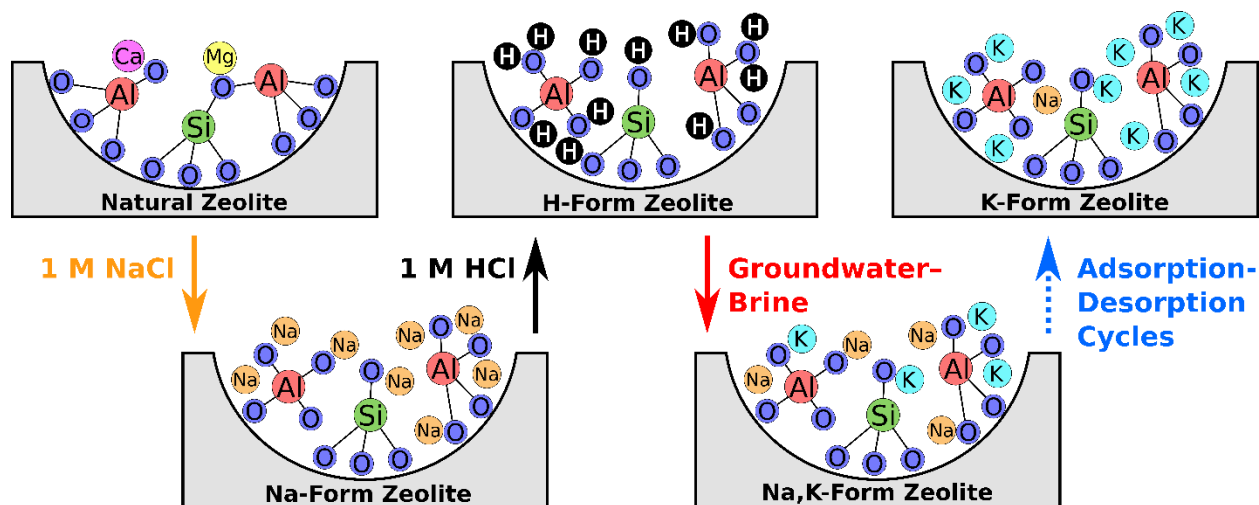


**Figure 5.1:** Graphical abstract for Chapter Five.

## 5.1. Abstract

The combination of calcined layered double hydroxide (CLDH) and zeolite adsorbents is effective for the removal of chloride ( $\text{Cl}^-$ ) and sodium ( $\text{Na}^+$ ) ions from saline industrial effluents. Yet, development of the dual-adsorbent desalination technique has not been pursued and the feasibility of regenerating the spent, acid-treated zeolite adsorbents in conjunction with the desalination treatment has not been extensively examined. This study focuses on (1) desalination, (2) regeneration of the acid-treated zeolites, and (3) production of K-rich zeolites from the dual-adsorbent treatment of groundwater spiked with potash brine, which contains large amounts of  $\text{Na}^+$ ,  $\text{K}^+$ , and  $\text{Cl}^-$ .  $\text{Na}^+$  pre-conditioning prior to acid treatment maintained the framework and crystallinity of the zeolite and augmented its adsorption capacity. Under the optimal adsorbent amounts, CLDH first reduced the concentration of  $\text{Cl}^-$  by 95.8%,  $\text{Ca}^{2+}$  by 89.8%, and  $\text{Mg}^{2+}$  by 92.3% and transiently raised the pH to 12.80. Then,  $\text{NaCl}/\text{HCl}$  modified zeolite removed 91.9% of the  $\text{Na}^+$  and 96.5% of the  $\text{K}^+$ , neutralized the pH (7.72), and lowered the sodium adsorption ratio (SAR; 36.5 to 12.5) and the hardness (574 to 56.3 mg/L as  $\text{CaCO}_3$ ). In comparison, an equivalent amount of natural zeolite removed amount only 51.2 and 79.6% of the  $\text{Na}^+$  and  $\text{K}^+$ , respectively, and also generated extremely hard water (3620 mg/L as  $\text{CaCO}_3$ ) due to  $\text{Ca}^{2+}$  and  $\text{Mg}^{2+}$  release. In zeolite regeneration studies (using 0.1 M  $\text{HCl}$ ), the  $\text{Na}^+$  efficiently desorbed but  $\text{K}^+$  remained. Over four consecutive adsorption–desorption cycles, the net  $\text{K}^+$  loading increased from 4.8 (cycle one) to 21.2 mg/g (cycle four). This K-form of zeolite could potentially be applied as a slow-release fertilizer or soil amendment, thereby transforming a potash mine waste material into a valuable resource.

## 5.2. Introduction

Increased freshwater salinization is now recognized as a global environmental concern.<sup>86</sup> If current trends continue unabated, many surface waters are projected to become uninhabitable by aquatic life and not potable for humans.<sup>84</sup> Excess  $\text{Cl}^-$  is toxic to plants and freshwater species, and also causes infrastructure corrosion.<sup>12, 13</sup> Excess  $\text{Na}^+$  degrades soils, perturbs biogeochemical cycling, and decreases plant growth.<sup>124</sup>

Human inputs such as road de-icers and mining, oil, and gas operations contribute to this freshwater salinization. In particular, potash ( $\text{KCl}$ ) mining produces large quantities of saline effluent (tailings and brine predominated by  $\text{NaCl}$ ).<sup>1</sup> Potash tailings are formed into piles

approximately 50 m in height and covering hundreds of hectares. The brine is held in ponds and continuously recycled for potash processing or disposed of through deep well injection.<sup>7</sup> Notwithstanding natural and engineered containment systems, brine migration from potash mine sites is an ongoing environmental concern.<sup>6, 7</sup>

To remediate brine-impacted water, or to better prevent its occurrence, versatile and sustainable adsorbents have been considered.<sup>20, 32, 40-42, 44-46, 91, 92</sup> Specifically, two mineral adsorbents show promise: natural zeolite and layered double hydroxide (LDH). Natural zeolite is an aluminosilicate mineral consisting of  $\text{AlO}_4^-$  and  $\text{SiO}_4$  tetrahedra bridged together by shared O atoms.<sup>19, 125</sup> Its negative lattice charge is neutralized by exchangeable cations, typically some combination of  $\text{Ca}^{2+}$ ,  $\text{Mg}^{2+}$ ,  $\text{Na}^+$ , and  $\text{K}^+$ . Owing to its three-dimensional, porous structure and exceptionally high surface area, zeolites have a high cation exchange capacity. There are many different types of zeolite (both synthetic and natural), each varying with respect to the Si/Al molar ratio, framework configuration, and exchangeable ions. Clinoptilolite zeolite has been particularly well studied as a remedial agent, such as for  $\text{Na}^+$  removal from saline produced water.<sup>40, 41, 126</sup>

Researchers have modified clinoptilolite by acid to augment its  $\text{Na}^+$  adsorption capacity.<sup>20, 44, 45</sup> With acid treatment, zeolite's pre-existing native cations are replaced by protons (transitions to an H-form zeolite). Pre-conditioning the zeolite with  $\text{Na}^+$  prior to acid treatment has been shown to further enhance the conversion to a homoionic H-form.<sup>96, 127</sup> When an H-form zeolite is agitated with a saline solution,  $\text{Na}^+$ ,  $\text{K}^+$ , and other salt cations are adsorbed through ion exchange. Because  $\text{H}^+$  is ion exchanged, the pH may be significantly reduced.<sup>128</sup>

Layered double hydroxide is an anionic clay family representable by the formula  $[\text{M}^{2+}_1 \cdot x\text{M}^{3+}_x(\text{OH})_2]^{x+}[\text{A}^{n-}]_{x/n} \cdot m\text{H}_2\text{O}$ , where  $\text{M}^{2+}$  and  $\text{M}^{3+}$  are divalent and trivalent cations, respectively,  $\text{A}^{n-}$  is the interlayer charge compensation anion, and  $x$  is the  $\text{M}^{2+}/\text{M}^{3+}$  ratio.<sup>18, 54, 97, 129</sup> Calcined LDHs (CLDHs) have been used to remove a range of anions from solution, including  $\text{Cl}^-$ .<sup>73, 75</sup>

There is great potential in sequentially combining CLDH and acid-treated (H-form) zeolite for desalination and water treatment. CLDH can be first used to remove anions and divalent cations and to raise the pH, and then acid-treated zeolite can be applied to remove monovalent cations and neutralize the pH. Pless et al. (2006) used CLDH and permutite (a synthetic zeolite) to treat coalbed methane produced water, which is high in total dissolved solids

(11,000 ppm TDS, primarily as NaCl). After treatment, the TDS was reduced to 600 ppm and the effluent pH was 5.0.<sup>58</sup>

Unlike the coalbed methane produced water, potash brine is high in not only Na<sup>+</sup> and Cl<sup>-</sup>, but also K<sup>+</sup>. After adsorption of both Na<sup>+</sup> and K<sup>+</sup>, it is hypothesized that acid regeneration of the zeolite will selectively desorb Na<sup>+</sup> ions without significantly affecting the K<sup>+</sup> content (due to clinoptilolite's high affinity for K<sup>+</sup>).<sup>39</sup> If the zeolite is used over several adsorption–desorption cycles, the K<sup>+</sup> loading is expected to increase. The resultant K-form zeolite could be applied as a fertilizer (e.g., for golf greens, house plants, and agricultural crops). Zeolites can deliver and retain soil nutrients,<sup>130-134</sup> particularly if combined with potash.<sup>135</sup> Augmenting zeolite's K content may enhance the efficacy of zeolite soil amendment, which is of great potential value due to demands for increased fertilizer use efficiency and environmental protection. Therefore, the present study aims to i) assess the feasibility of using combined zeolite and CLHD adsorption to desalinate potash-brine-spiked groundwater, ii) investigate the potential for regenerating the adsorbents, and iii) explore the simultaneous production of K-form zeolites. This study also investigates the effects of Na<sup>+</sup> pre-conditioning prior to zeolite acid treatment. A natural clinoptilolite zeolite was treated by a strong acid and evaluated through batch adsorption experiments. The effect of Na<sup>+</sup> pre-conditioning prior to acid treatment—intended to preserve zeolite crystallinity and enhance its conversion to a homoionic H-form—was also evaluated. The solution chemistry (i.e., pH, Cl<sup>-</sup>, Na<sup>+</sup>, K<sup>+</sup>, Ca<sup>2+</sup>, and Mg<sup>2+</sup>) was characterized at each treatment step. Finally, several adsorption–desorption cycles were attempted to obtain a K-form zeolite, which can potentially be used as a slow-release fertilizer.

## 5.3. Experimental (Materials and Methods)

### 5.3.1. Instruments

X-ray diffraction (XRD) patterns of the adsorbents were obtained using a diffractometer (Bruker D4 Endeavor) operating at 40 kV and 40 mA with Cu K $\alpha$  radiation ( $\lambda = 1.54056 \text{ \AA}$ ). Phase identification was conducted using the Match! software package (Crystal Impact, Bonn, Germany). The whole sample chemical composition was determined using a Bruker S8 Tiger X-ray fluorescence (XRF) spectrometer. Particle size analysis was conducted using a Malvern Mastersizer S laser diffractor. The Na<sup>+</sup> and Cl<sup>-</sup> ion concentrations were determined using ROSS ion-selective electrode (ISE) probes attached to an Orion Star A214 benchtop meter (Thermo

Fisher Scientific Orion). The ISE probes were calibrated daily prior to use using manufacturer-provided standard solutions. The  $\text{Ca}^{2+}$ ,  $\text{Mg}^{2+}$ ,  $\text{K}^{+}$ , and  $\text{Al}^{3+}$  concentrations were measured using an atomic absorption spectrometer (Thermo Fisher Scientific iCE 3300). The pH was measured using a Hach HQ40D pH meter which was calibrated prior to use using Hach buffer solutions (pH 4.01 and 7.00).

### 5.3.2. Adsorbent Development

Natural zeolite (NZ) was obtained from Bear River Zeolite (Preston, Idaho) and LDH was obtained from Kyowa Chemical Industry (Sakaide, Japan). The zeolite sample was determined (using quantitative XRD and XRF) to be approximately 85% clinoptilolite with predominately  $\text{Ca}^{2+}$  and  $\text{K}^{+}$  as exchangeable ions. The LDH sample had  $\text{Mg}^{2+}$  and  $\text{Al}^{3+}$  as constituent cations (3.0 Mg/Al molar ratio according to the manufacturer),  $\text{CO}_3^{2-}$  as the interlayer anion, and was representable by the formula  $\text{Mg}_6\text{Al}_2(\text{OH})_{16}\text{CO}_3$ . The average particle size of the LDH and ground zeolite were 30  $\mu\text{m}$  (manufacturer provided data) and 80  $\mu\text{m}$ , respectively.

The LDH sample was calcined at 500 °C for 6 h to produce Mg-Al oxide (CLDH). The zeolite sample was converted to its Na-form (NaZ) by contacting it with 1 M NaCl solution (1:5 weight ratio). After 24 h of agitation (200 rpm), the NaZ was separated by vacuum filtration, rinsed with deionized (DI) water until the  $\text{Cl}^{-}$  concentration of the filtrate was less than 10 mg/L, and then oven dried at 103 °C overnight. Next, both NZ and NaZ were acid treated with 1.0 M HCl (1:5 weight ratio). After 30 min of agitation (200 rpm), the zeolite was separated by vacuum filtration, rinsed with DI water until no significant difference was observed in the pH of two sequential washing steps, and oven dried at 103 °C overnight. Acid-treated NZ is denoted AZ, and acid-treated NaZ is denoted ANaZ.

### 5.3.3. Groundwater and Potash Brine

Potash brine was obtained from a Saskatchewan potash mine and pristine groundwater was obtained from near Patience Lake, Saskatchewan. The brine was very high in  $\text{Na}^{+}$  (87,400 mg/L),  $\text{K}^{+}$  (52,900 mg/L), and  $\text{Cl}^{-}$  (220,000 mg/L), and the pH was 7.19. The groundwater was low in  $\text{Na}^{+}$  (78 mg/L),  $\text{K}^{+}$  (6.8 mg/L), and  $\text{Cl}^{-}$  (44 mg/L) and had a pH of 8.03 and a hardness of 381 mg/L as  $\text{CaCO}_3$ . Complete chemical analyses for the groundwater and brine are given in Table 5.1.

**Table 5.1:** Chemistry of the groundwater and potash brine.

	Groundwater	Potash brine
HCO <sub>3</sub> <sup>-</sup> (mg/L)	177	60
CO <sub>3</sub> <sup>2-</sup> (mg/L)	<1	<1
Cl <sup>-</sup> (mg/L)	41	220000
pH	8.03	7.19
NO <sub>3</sub> <sup>-</sup> (mg/L)	<0.04	<0.04
Ca <sup>2+</sup> (mg/L)	44	1800
Mg <sup>2+</sup> (mg/L)	66	1600
K <sup>+</sup> (mg/L)	6.8	52900
Na <sup>+</sup> (mg/L)	78	87400
Al <sup>3+</sup> (mg/L)	0.012	<0.5
Fe <sup>2+</sup> /Fe <sup>3+</sup> (mg/L)	0.026	<0.1
Mn <sup>2+</sup> (mg/L)	0.0019	2.8
SO <sub>4</sub> <sup>2-</sup> (mg/L)	360	2200
Specific conductivity (μS/cm)	1100	203000
Sum of ions <sup>a</sup> (mg/L)	773	379000
Total hardness (mg/L as CaCO <sub>3</sub> )	381	12400

<sup>a</sup>Sum of ions is defined as the sum of the concentrations of Ca<sup>2+</sup>, Mg<sup>2+</sup>, Na<sup>+</sup>, K<sup>+</sup>, CO<sub>3</sub><sup>2-</sup>, HCO<sub>3</sub><sup>-</sup>, SO<sub>4</sub><sup>2-</sup>, Cl<sup>-</sup>, and NO<sub>3</sub><sup>-</sup> (similar to TDS).

#### 5.3.4. Adsorption Experiments

Adsorption experiments were conducted in duplicate or triplicate using CLDH, NZ, AZ, and ANaZ. Experiments were conducted by placing a specified mass of the adsorbent in a 50 mL screw-cap centrifuge tube with 30 mL of solution. The mixtures were agitated at 200 rpm using an orbital shaker at 23 °C. After 24 h contact time, the aqueous phase was separated from the solid phase by centrifugation and the pH and relevant ion concentrations determined. For CLDH, the pH and Cl<sup>-</sup> concentration were measured; for the zeolite samples, the pH and concentrations of Na<sup>+</sup>, K<sup>+</sup>, Mg<sup>2+</sup>, and Ca<sup>2+</sup> were measured. The removal efficiency (*RE*, %) was determined as

$$RE = [(C_0 - C_e)/C_0] \times 100\% \quad (5.1)$$

where *C*<sub>0</sub> (mg/L) is the solute initial concentration in solution and *C<sub>e</sub>* (mg/L) is its equilibrium

concentration. The ion uptake ( $q_e$ , mg/g) was calculated as

$$q_e = (V/m)(C_0 - C_e) \quad (5.2)$$

where  $m$  (g) is the adsorbent mass and  $V$  (L) is the volume of solution.

An equilibrium isotherm for  $\text{Cl}^-$  uptake onto CLDH was generated and fitted using the Langmuir and Freundlich models.<sup>103, 104</sup> The Langmuir model can be written as

$$q_e = (q_{\max} K_L C_e) / (1 + K_L C_e) \quad (5.3)$$

where  $q_{\max}$  is the maximum uptake (mg/g) and  $K_L$  is the Langmuir constant (L/mg). The Freundlich model can be written as

$$q_e = K_F C_e^{1/n} \quad (5.4)$$

where  $K_F$  [mg/g)(L/mg)<sup>1/n</sup>] is the Freundlich constant and  $n$  is the Freundlich exponent (dimensionless).

Two solutions were used. The first, denoted GB, was prepared using natural groundwater spiked with potash brine (2% by volume). This solution had an ionic strength of 0.134 mol/L, which is classified as saline.<sup>100, 101</sup> Varying amounts of CLDH (0–3 g in 0.5 g increments) and NZ (0–10 g in 2.5 g increments) were equilibrated with 30 mL of GB solution.

The CLDH amount that reduced the  $\text{Cl}^-$  concentration to beneath 250 mg/L (the World Health Organization and Canadian drinking water standard)<sup>14, 15</sup> was determined and used to dechlorinate 2 L of GB solution. After 24 h contact time, the CLDH was separated from solution using vacuum filtration, and the filtrate recovered. This resultant solution was denoted GB<sub>dc</sub>, with the “dc” subscript indicating that it is dechlorinated groundwater–brine. Varying masses of AZ and ANaZ (0–10 g in 2.5 g increments) were equilibrated with 30 mL of GB<sub>dc</sub> solution.

The solution with which the zeolite sample was equilibrated is indicated after the name of the zeolite sample. For instance, NZ-GB indicates natural zeolite equilibrated with groundwater–brine, and ANaZ-GB<sub>dc</sub> indicates NaCl/HCl modified zeolite equilibrated with dechlorinated groundwater–brine (CLDH pre-treatment).

### 5.3.5. Regeneration Studies

The ANaZ sample was regenerated using 0.1 M HCl. To saturate the ANaZ, 7.5 g was agitated for 24 h with 30 mL of GB<sub>dc</sub> solution. The adsorbent was then separated from the solution using vacuum filtration and oven dried at 103 °C overnight. The pH and  $\text{Na}^+$  and  $\text{K}^+$

concentrations of the filtrate were measured. The Na<sup>+</sup> and K<sup>+</sup> removal efficiencies were also determined.

Next, the adsorbent was regenerated by agitating with 0.1 M HCl (1:5 weight ratio) at 200 rpm and room temperature. After 1 h contact time, the adsorbent was separated using vacuum filtration, rinsed with 500 mL DI water, and then oven dried at 103 °C overnight. The concentrations of Na<sup>+</sup> and K<sup>+</sup> in the regeneration filtrate were determined and used to calculate the net ion uptake ( $q_{net}$ ), which considers the cumulative amount of K<sup>+</sup> and Na<sup>+</sup> adsorbed and desorbed:

$$q_{net} = [\sum(C_0 - C_e)V_a - \sum(C_d V_d)]/m \quad (5.5)$$

where  $C_0$  (mg/L) is the solute initial concentration in solution,  $C_e$  (mg/L) is the solute equilibrium concentration,  $V_a$  (L) is the volume of the adsorption experiment,  $C_d$  (mg/L) is the concentration of the solute in the desorption effluent,  $V_d$  (L) is the volume of the desorption effluent, and  $m$  (g) is the mass of zeolite used in the adsorption experiment. These adsorption–desorption experiments were repeated in triplicate for a total of four cycles.

## 5.4. Results and Discussion

### 5.4.1. Effect of CLDH Amount

The Cl<sup>−</sup> removal efficiency increased with increasing masses of CLDH added (Figure 5.). With a CLDH mass of 2.5 g, 94.9% Cl<sup>−</sup> removal was achieved (equilibrium concentration of 230 mg/L). The mechanism for this Cl<sup>−</sup> removal, termed *the memory effect*, has been well established in the literature. Briefly, calcination of the LDH relinquished the interlayer CO<sub>3</sub><sup>2−</sup> and generated Mg–Al oxide (CLDH). Next, upon rehydration of the CLDH in saline solution, the LDH reformed with anions (i.e., Cl<sup>−</sup>) occupying the interlayer<sup>73, 75</sup> and, due to the coincident OH<sup>−</sup> release, the equilibrium pH was highly basic (>12) across all CLDH dosages (Figure 5.).



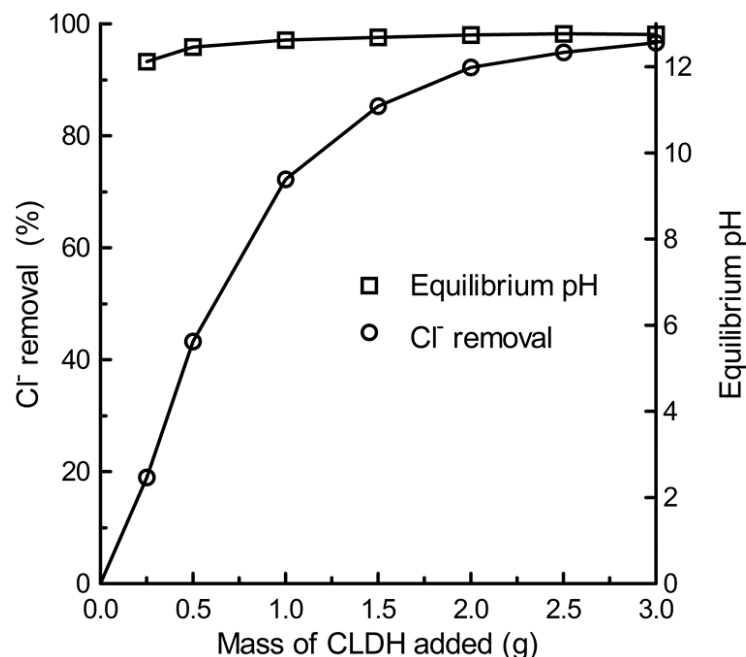


**Figure 5.2:**  $\text{Cl}^-$  percent removal and equilibrium pH as a function of CLDH amount ( $V = 30 \text{ mL}$ ,  $[\text{Cl}^-]_i = 4600 \text{ mg/L}$ ,  $\text{pH}_i = 8.23$ ).

Based on this result, 2 L of GB solution were treated with CLDH at a dose of 2.5 g/30 mL solution. The results of this CLDH treatment are given in Table 5.2. The  $\text{Cl}^-$  concentration was reduced by 95.8% (to 193 mg/L), and the  $\text{Ca}^{2+}$  and  $\text{Mg}^{2+}$  concentrations were reduced by 89.7% (to 6.9 mg/L) and 92.3% (to 7.6 mg/L), respectively. Accordingly, the water hardness decreased from 574 to 48.4 mg/L as  $\text{CaCO}_3$ . The mechanisms for divalent cation sorption on CLDH include isomorphic substitution, adsorption, and precipitation, as reviewed by Liang et al. (2013).<sup>123</sup> Because the equilibrium pH was 12.80 and the  $\text{Na}^+$  and  $\text{K}^+$  concentrations remained elevated, a second treatment step involving acid-treated zeolite was necessary.

**Table 5.2:** Chemistry for the groundwater–brine initially (GB), after CLDH treatment (2.5 g/30 mL; GB<sub>dc</sub>), and after CLDH and ANaZ treatment (2.5 and 7.5 g/30 mL, respectively).

Feed	GB	After CLDH (GB <sub>dc</sub> )	After CLDH and ANaZ
Na <sup>+</sup> (mg/L)	2010	2190 ± 85	180.0 ± 18.5
K <sup>+</sup> (mg/L)	1119.4	1267 ± 180	41.3 ± 20.3
Ca <sup>2+</sup> (mg/L)	67.1	6.9 ± 8.9	4.9 ± 2.5
Mg <sup>2+</sup> (mg/L)	98.8	7.6 ± 1.5	10.7 ± 7.5
Cl <sup>-</sup> (mg/L)	4600	193 ± 22	262 ± 6.5
Hardness (mg/L as CaCO <sub>3</sub> )	574	48.4 ± 16.2	56.3 ± 37
Ionic strength (mol/L)	0.134	0.068	0.009
SAR	36.5	139.6 ± 18.3	12.5 ± 5.4
pH	8.23	12.80 ± 0.03	7.72 ± 0.14

#### 5.4.2. Cl<sup>-</sup> Adsorption Isotherm

Adsorption isotherms, which show how molecules distribute between the aqueous phase and solid phase at equilibrium, are of fundamental importance when analyzing adsorption systems. Figure 5.3 plots the adsorption isotherm data for Cl<sup>-</sup> uptake onto CLDH. Two common isotherm models were applied to this data: the Langmuir model (Langmuir, 1918) and the Freundlich model.<sup>103, 104</sup> The linearized isotherms are given in Figure 5.4 and Figure 5.5, and the model parameters are given in in Table 5.3. Based on the coefficients of determination, the Langmuir model fit the data better than the Freundlich model ( $R^2$  values of 0.978 and 0.934, respectively). The maximum Cl<sup>-</sup> uptake capacity was 116.3 mg/g, close to the reported values in previous studies on CLDHs (103–149.5 mg/g), as listed in Table 5.4.

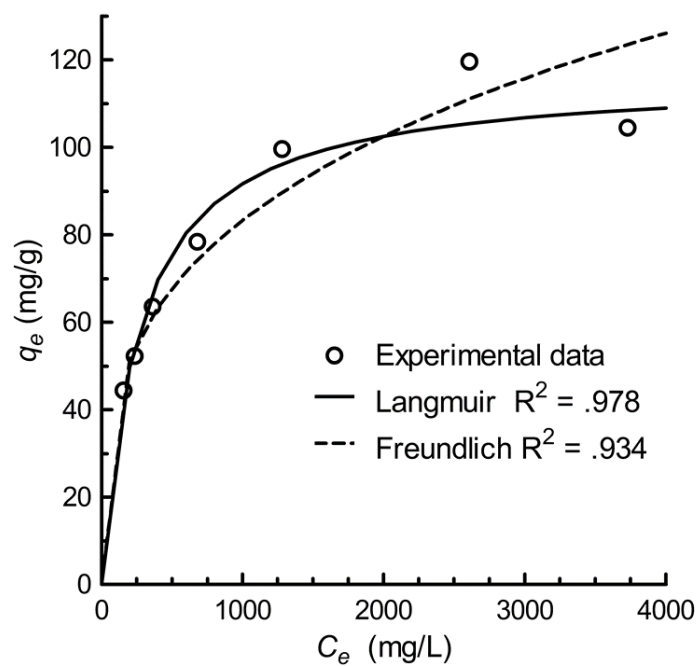


**Figure 5.3:** Equilibrium isotherm for  $\text{Cl}^-$  uptake onto CLDH at room-temperature. Experimental data are reported as points and models (Langmuir and Freundlich models) by curves.

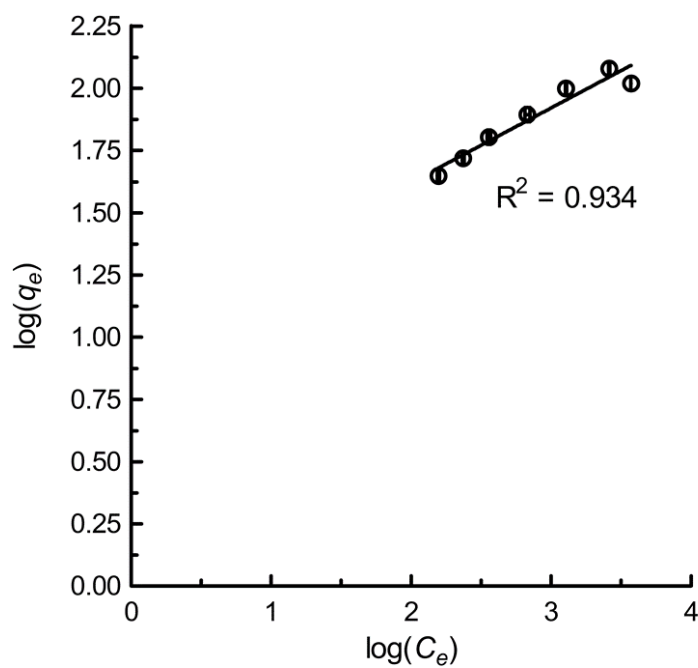


**Figure 5.4:** Linearized Freundlich isotherm model.

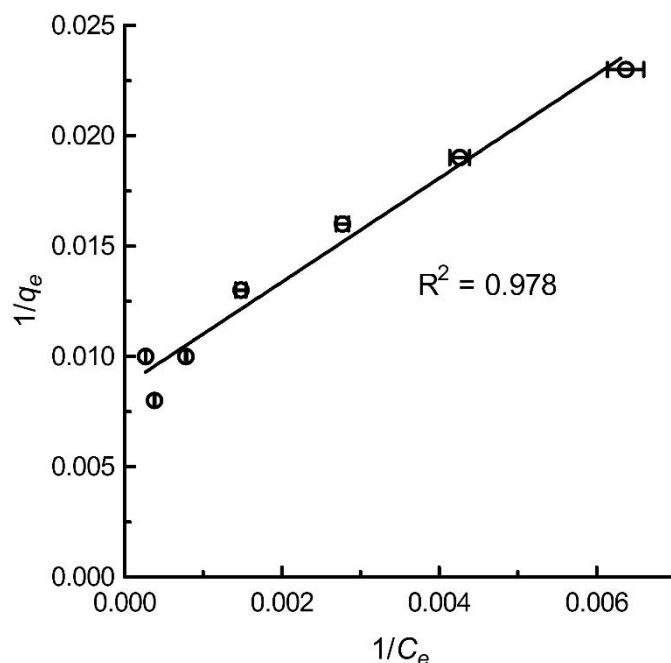


**Figure 5.5:** Linearized Langmuir isotherm model.

**Table 5.3:** Isotherm model parameters for  $\text{Cl}^-$  adsorption onto CLDH at 23 °C.

Freundlich Model			Langmuir Model		
$K_F [\text{mg/g})(\text{L/mg})^{1/n}]$	$1/n$	$R^2$	$q_{max} (\text{mg/g})$	$K_L (\text{L/mg})$	$R^2$
10.51	0.300	0.934	116.3	0.0037	0.978

**Table 5.4:** Maximum effective adsorption capacity for reported  $\text{Cl}^-$  sorbents at room-temperature.

Sorbent	$q_{max} (\text{mg/g})$	Reference
Double hydroxide ( $\text{Fe}_2\text{O}_3 \cdot \text{Al}_2\text{O}_3 \cdot x\text{H}_2\text{O}$ )	70	Chubar et al. (2005) <sup>136</sup>
Weakly acidic and weakly basic ion-exchange resins	85.2	Koul and Gupta (2004) <sup>137</sup>
Mg-Al oxide (Mg/Al molar ratio of 3.5)	103	Kameda et al. (2002) <sup>77</sup>
Mg-Al oxide (Mg/Al molar ratio of 2.0)	109	Kameda et al. (2002) <sup>77</sup>
ZnAl- $\text{NO}_3$ LDH (Zn/Al molar ratio of 2.0)	108.3	Lv et al. (2009) <sup>57</sup>
Mg-Al oxide (Mg/Al molar ratio of 3.0)	116.3	This study
Mg-Al oxide (Mg/Al molar ratio of 4.0)	149.5	Lv et al. (2006) <sup>75</sup>

### 5.4.3. Effects of Zeolite Modification by $\text{Na}^+$ and $\text{H}^+$

To better understand (and therefore augment) their adsorption properties, the zeolite samples were further characterized by XRD, XRF, and measuring the ion content of the filtrate from the zeolite modifications. Specifically, the effects of the  $\text{Na}^+$  pre-conditioning and acid treatment were determined. Zeolite acid treatment is known to cause physiochemical effects that generally occur stepwise according to the severity of the treatment (i.e., the acid concentration, acid type, contact time, temperature, and the exchangeable cations of the zeolite).<sup>95, 96, 127</sup> Mild acid treatment produces decationation, moderate acid treatment results in dealumination (without major structural changes),<sup>20</sup> and severe acid treatment destroys the zeolite lattice.<sup>95</sup> Excess dealumination and lattice disintegration are not conducive to adsorption, as the cation exchange capacity of the zeolite arises from framework substitution of  $\text{Al}^{3+}$  for  $\text{Si}^{4+}$  (exchangeable cations provide charge neutrality).

The ANaZ sample was obtained by modifying natural zeolite in two sequential steps: first with 1.0 M NaCl and then with 1.0 M HCl. In these pre-conditioning steps, the natural zeolite, which has predominantly  $\text{Ca}^{2+}$  and  $\text{K}^+$  as exchangeable ions, was converted to Na-form (NaZ). This  $\text{Na}^+$  pre-conditioning was intended to improve the response of the zeolite to subsequent acid treatment. Acid treatment of NaZ resulted in release of  $\text{Na}^+$  (and some residual  $\text{Ca}^{2+}$ ,  $\text{Mg}^{2+}$ , and  $\text{K}^+$ ) and the zeolite transitioning to its homoionic H-form (ANaZ). These ion-exchange reactions were evidenced by the chemical composition data (Table 5.5) as well as the ions released during the two modification steps (Table 5.6).

The AZ sample was obtained by mixing 1.0 M HCl solution with natural zeolite. With this modification, the native cations in the zeolite were directly substituted by protons. However, in the absence of the  $\text{Na}^+$  pre-conditioning, the conversion of the zeolite to its H-form was demonstrably less complete. The AZ sample had more  $\text{Ca}^{2+}$ ,  $\text{Mg}^{2+}$ , and  $\text{K}^+$  adsorbed than ANaZ, although both had much less of these cations than the natural zeolite (Table 5.5). This is also consistent with data from Table 5.6 that show the concentrations of  $\text{Ca}^{2+}$ ,  $\text{Mg}^{2+}$ , and  $\text{K}^+$  leached from the NZ acid treatment (to produce AZ) were substantially lower than from the NaZ acid treatment.

**Table 5.5:** Chemical composition of the zeolite samples. NZ, natural zeolite; AZ, acid-treated zeolite; ANaZ, NaCl/HCl-treated zeolite; KZ, NaCl/HCl-treated zeolite after four consecutive adsorption–desorption cycles.

Constituent (Wt. %)	NZ	AZ	ANaZ	KZ
Na <sub>2</sub> O	0.04	0.00	0.20	0.79
MgO	0.53	0.46	0.36	0.25
Al <sub>2</sub> O <sub>3</sub>	9.54	8.82	8.79	9.25
SiO <sub>2</sub>	69.23	70.6	71.88	74.66
P <sub>2</sub> O <sub>5</sub>	0.08	0.06	0.05	0.03
K <sub>2</sub> O	4.09	3.48	3.38	5.34
CaO	2.99	1.75	0.86	0.45
TiO <sub>2</sub>	0.31	0.3	0.28	0.24
MnO	0.03	0.03	0.03	0.02
Fe <sub>2</sub> O <sub>3</sub>	2.06	1.96	1.76	1.61
S	<0.01	<0.01	<0.01	0.00
∑ CaO + MgO + Na <sub>2</sub> O+K <sub>2</sub> O	7.65	5.69	4.80	6.83

Zeolite acid treatment resulted in dealumination, but to a lesser degree with Na<sup>+</sup> pre-conditioning. The Al<sup>3+</sup> concentration in the filtrate from the NaZ acid treatment was 795 mg/L, which is 15% less than the NZ acid treatment (930 mg/L; Table 5.6). This finding is in agreement with Rožić et al. (2005), who showed that proton exchange (using 0.1 M HCl) was easiest with a Na-form clinoptilolite zeolite, followed by Mg- and Ca-form zeolite, and worst with K-form zeolite (i.e., Na<sup>+</sup> > Mg<sup>2+</sup> > Ca<sup>2+</sup> > K<sup>+</sup>); due to the relative ease of proton exchange in Na-form zeolite, the aluminosilicate lattice was effectively spared from damage.<sup>127</sup> However, with Ca-, Mg-, and particularly K-form zeolites, protons exchange less efficiently, leaving the aluminosilicate lattice (Al-O bonds) vulnerable to proton attack. Because natural zeolites are abundant in Ca<sup>2+</sup>, Mg<sup>2+</sup>, and K<sup>+</sup>, it is beneficial to first remove these ions through Na<sup>+</sup> pre-conditioning prior to acid treatment.

**Table 5.6:** Ion concentrations (mg/L) in the filtrate from the three zeolite modifications.

Ion content (mg/L)	Al <sup>3+</sup>	Ca <sup>2+</sup>	K <sup>+</sup>	Mg <sup>2+</sup>	Na <sup>+</sup>
1.0 M NaCl mixed with NZ	2.8	1816	821	38	ND
1.0 M HCl mixed with NaZ	795	860	625	148	2260
Sum <sup>a</sup>	797	2676	1446	186	2260
1.0 M HCl solution mixed with NZ <sup>b</sup>	930	1520	1269	86	281

<sup>a</sup>Sum from the NaCl and HCl filtrates; produces ANaZ.

<sup>b</sup>Produces AZ.

Figure 5.6 shows the XRD pattern for ANaZ from 4 to 70° 2 $\theta$ . The XRD patterns for AZ and NZ (unpublished results) are also shown as a reference comparison. The NZ sample showed high crystallinity with peaks characteristic of clinoptilolite.<sup>118</sup> The ANaZ pattern closely resembled the NZ precursor. The AZ sample, however, showed a decrease in the intensity of the clinoptilolite peaks, a peak shifting towards higher angles, and a reduced basal spacing. This is most evident in Figure 5.7, which shows the XRD patterns from 4-16° 2 $\theta$ . For example, the (020) peak was at 9.89° (8.968 nm) for the NZ, 9.93° (8.933 nm) for the ANaZ, and 10.01° (8.862 nm) for the AZ. This change in mineral structure observed in the AZ, but not in the ANaZ, provides further support for the protective effect of Na<sup>+</sup> pre-conditioning. Rivera et al. (2013) also found Na-form zeolite to be more resistant than natural zeolite to HCl treatment (i.e., greater crystallinity and less dealumination).<sup>96</sup>

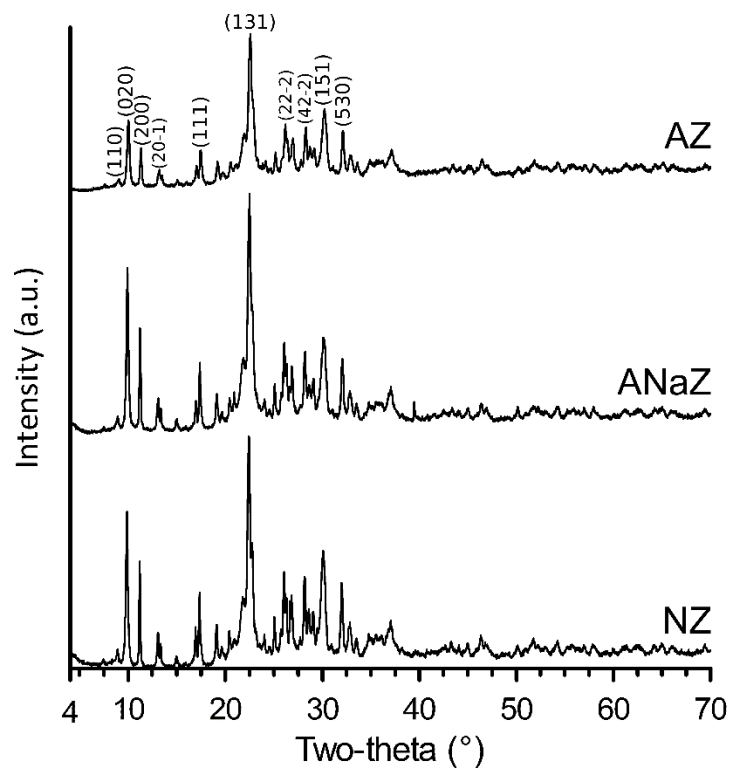


**Figure 5.6:** XRD patterns from 4 to 70° two-theta for NZ, ANaZ, and AZ.

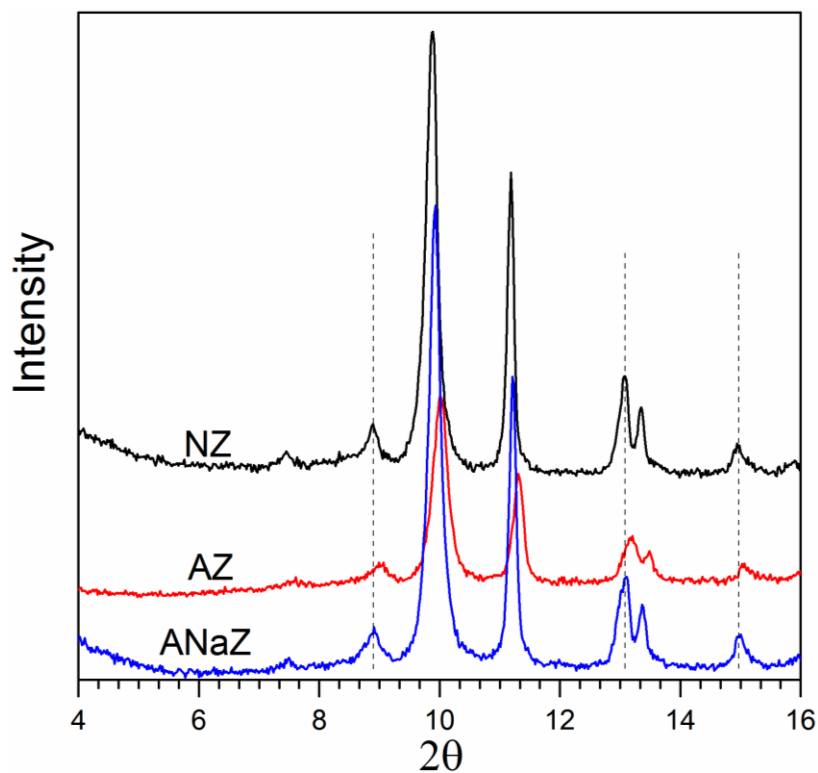


**Figure 5.7:** XRD patterns from 4 to 16° two-theta for the NZ, ANaZ, and AZ.



#### 5.4.4. Desalination of Brine-Impacted Groundwater

Three zeolites were evaluated for the treatment of saline groundwater. Natural zeolite, which does not substantially affect the pH, was used with the GB solution ( $\text{pH}_i = 8.23$ ). The two acid-treated zeolites, AZ and ANaZ, have a pH-lowering effect and thus were used with the basic  $\text{GB}_{\text{dc}}$  solution ( $\text{pH}_i = 12.78$ ). The chemistry of the feed solutions (GB and  $\text{GB}_{\text{dc}}$ ) is given in Table 5.2.

In terms of the  $\text{Na}^+$  and  $\text{K}^+$  removal efficiencies (Figures 5.7 and 5.8), both modified zeolites (AZ and ANaZ) were superior to the natural precursor (NZ) when non-dechlorinated groundwater (GB) was used. Depending on the adsorbent mass, the  $\text{Na}^+$  removal efficiency was 23 to 48% higher using the modified samples (Figure 5.8). For example, at an adsorbent mass of 10 g, the  $\text{Na}^+$  removal efficiencies were 60, 93, and 93% using NZ, AZ, and ANaZ, respectively. Similarly, the removal efficiency for  $\text{K}^+$  was 5 to 25% higher using the modified zeolites (Figure 5.9). For example, at an adsorbent mass of 5 g, 75, 92, and 97%  $\text{K}^+$  removals were achieved using NZ, AZ, and ANaZ, respectively. Zeolite clearly had a higher affinity for  $\text{K}^+$  ions over  $\text{Na}^+$  ions. For example, at a mass of 2.5 g ANaZ, 89% of the  $\text{K}^+$  was removed compared to 46% of the  $\text{Na}^+$ .

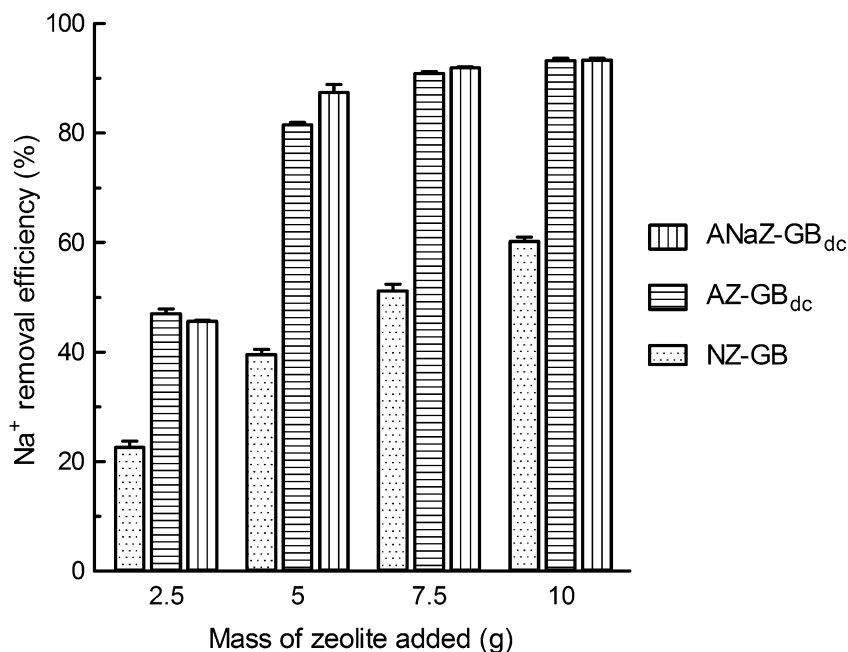


**Figure 5.8:**  $\text{Na}^+$  removal efficiency for different amounts of NZ-GB, AZ- $\text{GB}_{\text{dc}}$ , and ANaZ- $\text{GB}_{\text{dc}}$  ( $V = 30 \text{ mL}$ ).

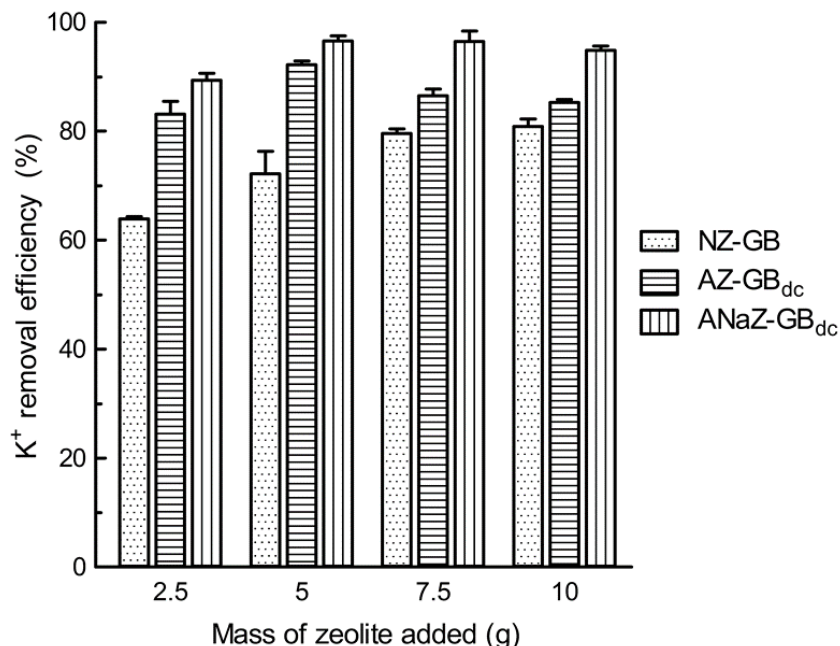


**Figure 5.9:**  $K^+$  removal efficiency for different amounts of NZ-GB, AZ-GB<sub>dc</sub>, and ANaZ-GB<sub>dc</sub> ( $V = 30$  mL).

The removal efficiencies for  $Na^+$  and  $K^+$  were slightly higher with ANaZ than with AZ. Because  $H^+$  can ion exchange with exceptional ease, this may be attributable to ANaZ being in a more homoionic H-form relative to AZ. The exchangeable cations (i.e.,  $H^+$  or native cations) were determined through several analyses. First, during adsorption the AZ sample released much more  $Ca^{2+}$  and  $Mg^{2+}$  than ANaZ (Figure 5.10). For instance, at an adsorbent mass of 10 g, the  $Ca^{2+}$  and  $Mg^{2+}$  concentrations ( $14.4 \pm 7.4$  mg/L in the GB<sub>dc</sub> feed solution) were  $28.5 \pm 10.3$  mg/L for ANaZ compared to  $106 \pm 12.3$  mg/L for AZ. This is direct evidence that the AZ sample had significant  $Ca^{2+}$  and  $Mg^{2+}$  remaining as exchangeable cations. The chemical composition analysis (Table 5.5) also confirmed that AZ had more exchangeable cations than ANaZ (4.80% in ANaZ compared to 5.69% in AZ). Finally, the ANaZ sample was much more acidic than AZ (Figure 5.11), indicating it is in a more homoionic H-form. Starting at an initial pH of 12.80, the minimum pH achieved with 10 g of AZ was 8.59. In contrast, a neutral pH (7.72) was achieved using a mass of 7.5 g ANaZ.

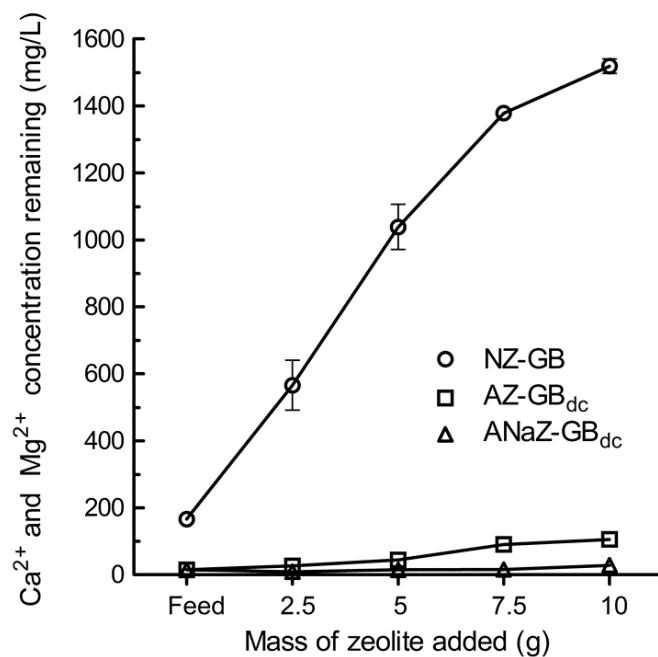


**Figure 5.10:**  $\text{Ca}^{2+}$  and  $\text{Mg}^{2+}$  concentration remaining for varying masses of ANaZ-GB<sub>dc</sub>, AZ-GB<sub>dc</sub>, and NZ-GB ( $V = 30$  mL).

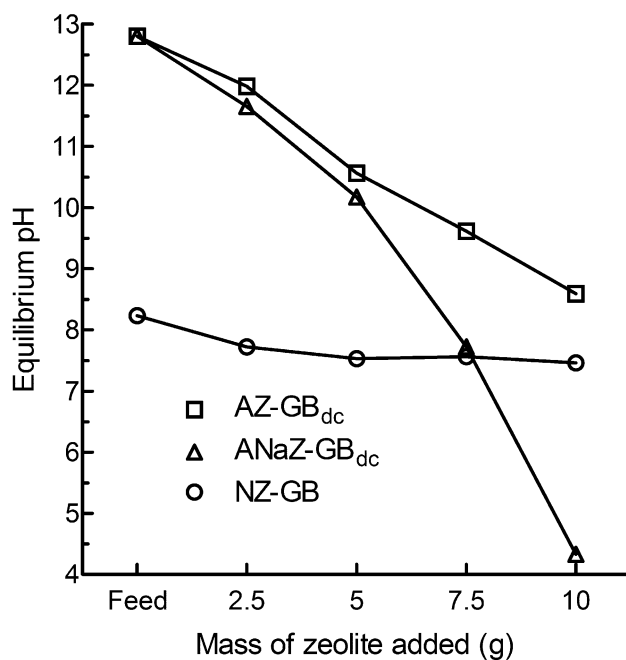


**Figure 5.11:** Equilibrium pH for varying masses of AZ-GB<sub>dc</sub>, ANaZ-GB<sub>dc</sub>, and NZ-GB ( $V = 30$  mL).

The SAR of the GB solution was 36.5. The ANaZ and AZ were able to reduce this value to as low as 6.6 and 3.6, respectively, which are acceptable values for agricultural irrigation (Figure 5.12).<sup>48</sup> This was accomplished almost entirely through the aforementioned 93% reduction in  $\text{Na}^+$  (ion exchange with protons); it was not caused by  $\text{Ca}^{2+}$  and  $\text{Mg}^{2+}$  release, which was negligible (Figure 5.10). In contrast, because natural zeolite exchanged  $\text{Ca}^{2+}$  and  $\text{Mg}^{2+}$  for  $\text{Na}^+$ , the SAR was also reduced (e.g., to 5.5 at a mass of 10 g NZ), but very hard water was generated. At the highest adsorbent mass (10 g), the hardness was  $3950 \pm 62$  mg/L as  $\text{CaCO}_3$  for NZ-GB compared to  $344 \pm 40$  and 105.5 mg/L as  $\text{CaCO}_3$  for AZ-GB<sub>dc</sub> and ANaZ-GB<sub>dc</sub>, respectively.

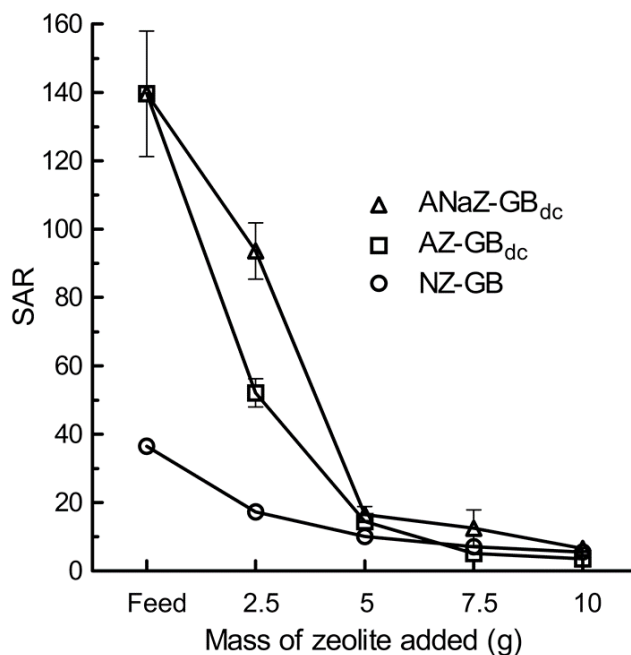


**Figure 5.12:** SAR values for varying masses of ANaZ-GB<sub>dc</sub>, AZ-GB<sub>dc</sub>, and NZ-GB ( $V = 30$  mL).

Overall, combined application of CLDH and NaCl/HCl-treated zeolite efficiently removes cations and anions (i.e.,  $\text{Na}^+$ ,  $\text{K}^+$ ,  $\text{Ca}^{2+}$ ,  $\text{Mg}^{2+}$ , and  $\text{Cl}^-$ ) and produces a neutral effluent pH. The chemical composition of the GB solution initially, after CLDH treatment (2.5 g/30 mL), and after the dual adsorbent treatment (CLDH 2.5 g/30 mL; ANaZ 7.5 g/30 mL) is summarized in Table 5.2.

#### 5.4.5. Zeolite Regeneration

The regeneration potential was evaluated over four adsorption–desorption cycles using ANaZ, which was the best-performing zeolite sample in the adsorption experiments. For each cycle, the Na<sup>+</sup>/K<sup>+</sup> removal efficiency is given in Figure 5.13; the Na<sup>+</sup>/K<sup>+</sup> net uptake is given in Figure 5.14; and the zeolite mass, equilibrium pH, and Na<sup>+</sup>/K<sup>+</sup> desorption efficiency is given in Table 5.7. Originally, 7.5 g of ANaZ was used with 30 mL of GB<sub>dc</sub> solution. With each regeneration cycle the zeolite mass decreased due to minor dissolution in the acidic solution and fine particle loss during filtration. Despite this mass loss, the K<sup>+</sup> removal efficiency remained greater than 90% over the four regeneration cycles. However, the adsorbed K<sup>+</sup> did not substantially desorb meaning that, with each cycle, fewer ion-exchange sites were occupied by protons and more with K<sup>+</sup> (i.e., transition to K-form zeolite). Because K<sup>+</sup> does not readily ion exchange with Na<sup>+</sup>, the Na<sup>+</sup> removal efficiency declined from 91.9 to 54.1%. The Na<sup>+</sup> was also efficiently desorbed with acid treatment. In the third and fourth cycles, the Na<sup>+</sup> desorption efficiency exceeded 100%, meaning that more Na<sup>+</sup> was desorbed than was adsorbed for that cycle. Due to the reduced Na<sup>+</sup>/H<sup>+</sup> exchange, the pH after adsorption increased (7.72 in cycle one to 11.24 in cycle four). By the fourth cycle, the zeolite sample had a net K<sup>+</sup> loading of 21.2 mg/g compared with 8.7 mg/g for Na<sup>+</sup>. The K<sub>2</sub>O content was determined to be 5.34% in KZ relative to 3.38 and 4.09% in the precursor ANaZ and NZ, respectfully (Table 5.5). Thus, simultaneous desalination and K-form zeolite production was feasible. Further research is necessary to determine the effectiveness of this K-form zeolite as a slow-release K<sup>+</sup> fertilizer or soil amendment (e.g., vegetation for abandoned mines).

**Table 5.7:** Adsorbent mass, equilibrium pH, and desorption efficiencies over four consecutive adsorption–desorption cycles using ANaZ-GB<sub>dc</sub>.

Cycle	Mass (g)	pH <sub>eq</sub>	Na <sup>+</sup> Desorption (%)	K <sup>+</sup> Desorption (%)
1	7.50 ± 0.00	7.72 ± 0.14	58.2 ± 3.9	13.1 ± 1.3
2	7.14 ± 0.10	10.48 ± 0.05	84.2 ± 5.1	13.0 ± 0.2
3	6.82 ± 0.07	11.02 ± 0.00	128.6 ± 4.9	16.0 ± 0.4
4	6.59 ± 0.04	11.24 ± 0.01	119.7 ± 12.6	22.2 ± 0.6

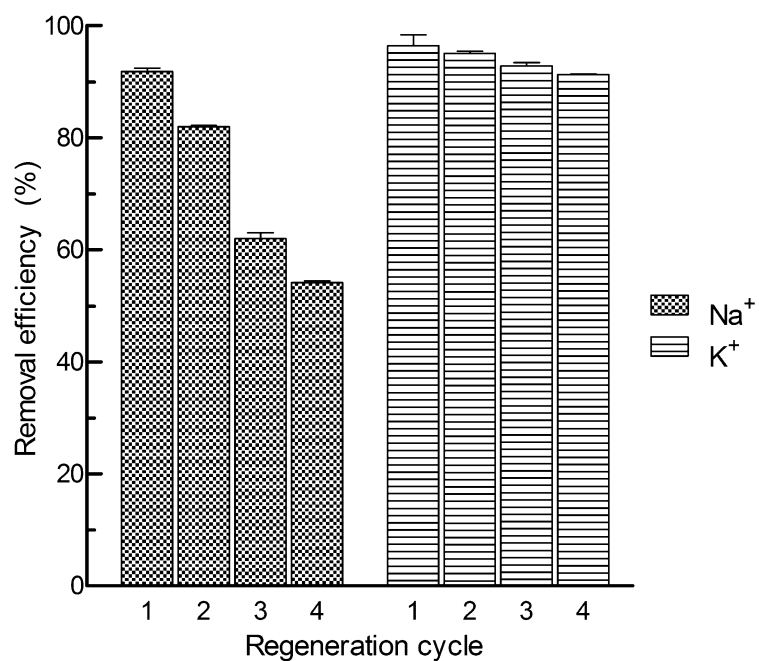


**Figure 5.13:**  $\text{Na}^+$  and  $\text{K}^+$  removal efficiency over four consecutive cycles with ANaZ-GB<sub>dc</sub>.

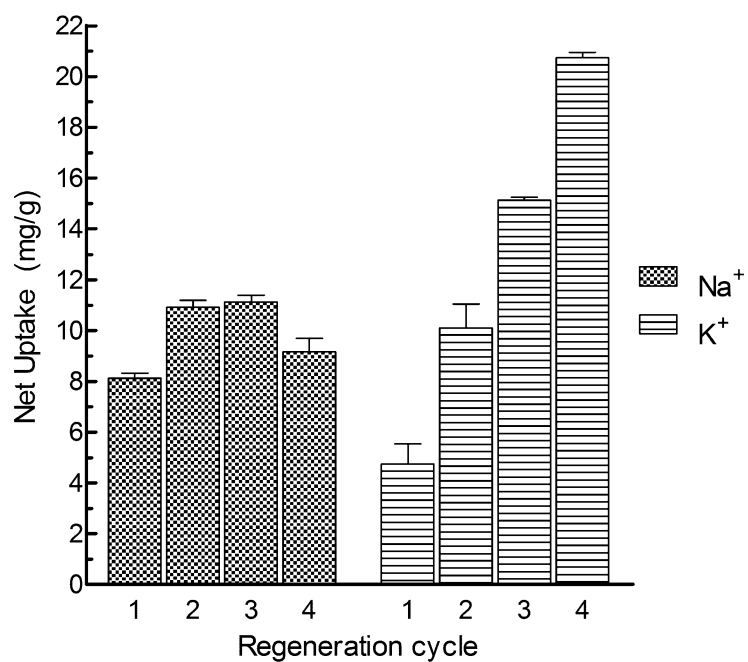


**Figure 5.14:** Net uptake of  $\text{Na}^+$  and  $\text{K}^+$  over four consecutive cycles with ANaZ-GB<sub>dc</sub>.

## 5.5. Conclusion

In this study, pre-conditioning clinoptilolite zeolite with  $\text{Na}^+$  (prior to acid treatment) enhanced its adsorption capacity and crystallinity. Using combined CLDH and ANaZ adsorbent treatment, 90–96% removal efficiencies were attainable for  $\text{Cl}^-$ ,  $\text{Na}^+$ ,  $\text{K}^+$ ,  $\text{Ca}^{2+}$ , and  $\text{Mg}^{2+}$ , resulting in significant reductions in SAR and hardness in potash-brine-spiked groundwater. In the zeolite regeneration experiments (four adsorption–desorption cycles),  $\text{Na}^+$  efficiently desorbed but  $\text{K}^+$  loading greatly increased from 4.8 to 21.2 mg/g, and thus K-rich zeolites are formed. This K-form zeolite could potentially be used as a slow-release fertilizer. Zeolite-based adsorbents for desalination have been thoroughly pursued as a potential treatment. The desalination, regeneration, and recycling of K-form zeolites improves the potential applicability, cost-effectiveness, and sustainability of this dual adsorbent treatment for salinized groundwater.

## 5.6. Acknowledgements

We acknowledge technical advice and assistance provided by Jeff Meadows, Kathlene Jacobson, Richard Weighaupt, and Al Shpyth through the International Minerals Innovation Institute (IMII). Thanks also to Blain Paul for assistance with XRD analysis and Kyowa Chemical Industry for providing the LDH sample. This research was funded by PotashCorp, Agrium, The Mosaic Company, the IMII, a Mathematics of Information Technology and Complex Systems (Mitacs) Accelerate Cluster Grant (IT04529), and the Natural Sciences and Engineering Research Council of Canada (CRDPJ 487008-15).

# Chapter Six

## Conclusions and Recommendations

### 6.1. Conclusions

A dual-adsorbent was developed to desalinate potash brine-impacted groundwater. Using synthetic NaCl solution, the maximum adsorption capacity for  $\text{Cl}^-$  onto CLDH was 116.3 mg/g. This adsorption capacity was high and in agreement with previous studies on CLDHs.<sup>57, 75, 77</sup> Based on XRD analysis, the  $\text{Cl}^-$  adsorption mechanism was determined to be structural reconstruction, which was also consistent with previous research.<sup>73, 75</sup> When a groundwater–brine solution was used,  $\text{SO}_4^{2-}$ ,  $\text{Ca}^{2+}$ , and  $\text{Mg}^{2+}$  were also efficiently removed by the CLDH. The mechanisms of divalent cation sorption onto CLDH were not investigated, but have been reviewed by Liang.<sup>123</sup>

Following CLDH application, acid-treated zeolite was needed to neutralize the pH and adsorb monovalent cations (i.e.,  $\text{Na}^+$  and  $\text{K}^+$ ). Acid-treated zeolites have been previously evaluated for  $\text{Na}^+$  adsorption,<sup>20</sup> but invariably the acid treatment is weak (e.g., 0.1 M  $\text{H}_2\text{SO}_4$ ). Stronger acid treatments are likely uncommon because of the severe pH reductions. For example, when AZ(1-HCl) was equilibrated with synthetic NaCl solution, the pH was around 2.0, which would preclude most environmental remediation applications. However, in this study the acid-treated zeolite was equilibrated with a highly basic solution (after CLDH), and thus the pH reduction was desirable. In terms of  $\text{Na}^+$  adsorption, zeolite treated with 1.0 M  $\text{H}_2\text{SO}_4$  was equal to 2 M  $\text{H}_2\text{SO}_4$  and superior to 0.1 M  $\text{H}_2\text{SO}_4$  and untreated zeolite. The type of acid ( $\text{HNO}_3$ ,  $\text{HCl}$ , or  $\text{H}_2\text{SO}_4$ ) did not have an effect.

Adsorption isotherms were obtained for NZ- $\text{NaCl}$ , AZ(1-HCl)- $\text{NaCl}$ , NZ- $\text{Na}_{\text{dc}}$ , and AZ(1-HCl)- $\text{Na}_{\text{dc}}$ . Modelled by the Langmuir equation, the maximum uptake of  $\text{Na}^+$  was 16.7 mg/g for AZ(1-HCl)- $\text{Na}_{\text{dc}}$ , 19.5 mg/g for NZ- $\text{Na}_{\text{dc}}$ , and 28.4 mg/g for AZ(1-HCl)- $\text{Na}_{\text{dc}}$ . The Langmuir model did not apply for the NZ- $\text{NaCl}$  sample, but its highest  $\text{Na}^+$  loading obtained experimentally



was only 8.0 mg/g. The maximum  $\text{Na}^+$  adsorption capacity of the AZ(1-HCl)- $\text{Na}_{\text{dc}}$  sample, 28.4 mg/g, was more than twice as high as all other reported values in the literature (among zeolites). This exceptional performance was attributed to (1) zeolite acid treatment and (2) solution pre-treatment (dechlorination) using CLDH. These factors were investigated in detail through XRD, XRF, porosimetry, and STXM.

A  $\text{Na}^+$  pre-conditioning step prior to acid treatment proved beneficial, as was hypothesized based on previous studies.<sup>96, 127</sup> With this pre-conditioning,  $\text{Na}^+$  ions substituted for zeolite's native cations, such as  $\text{Ca}^{2+}$  and  $\text{Mg}^{2+}$ . Then, upon acid treatment, the  $\text{Na}^+$  was easily swapped for protons. This resulted in a complete conversion of the zeolite to its homoionic H-form. Without  $\text{Na}^+$  pre-conditioning, acid-treatment did not fully convert the zeolite to its homoionic H-form, as evidenced by the ion concentrations in the leachate, and the equilibrium pH, and the  $\text{Ca}^{2+}$  and  $\text{Mg}^{2+}$  concentrations after adsorption. Due to the greater abundance of adsorbed  $\text{H}^+$  and the ease of  $\text{Na}^+/\text{H}^+$  and  $\text{K}^+/\text{H}^+$  ion-exchange, the ANaZ sample showed the highest adsorption capacity.

It was confirmed through XRF, XRD, and leachate chemical analysis that the acid treatment of natural zeolite caused substantial dealumination and a change in crystallinity. The Na-form zeolite, however, showed enhanced resistance to acid treatment (i.e., less dealumination and higher crystallinity). It can be concluded that the zeolite's exchangeable ions affect its resistance to acid treatment. Because  $\text{Na}^+/\text{H}^+$  exchange is more favourable than  $\text{Ca}^{2+}/\text{H}^+$ , the framework lattice of the natural zeolite (having  $\text{Ca}^{2+}$  as the predominant counterion) was more vulnerable to proton attack.

Using brine-impacted groundwater, the dual-adsorbent reduced the concentration of  $\text{Cl}^-$  by 95.8%,  $\text{Ca}^{2+}$  by 89.8%,  $\text{Mg}^{2+}$  by 92.3%,  $\text{Na}^+$  by 91.9%,  $\text{K}^+$  by 96.5%, neutralized the pH (7.72), and lowered the sodium adsorption ratio (36.5 to 12.5) and the hardness (574 to 56.3 mg/L as  $\text{CaCO}_3$ ). In contrast, natural zeolite alone only removed 51.2% of the  $\text{Na}^+$  and 79.6% of the  $\text{K}^+$ , and also generated extremely hard water (3620 mg/L as  $\text{CaCO}_3$ ) due to  $\text{Ca}^{2+}$  and  $\text{Mg}^{2+}$  desorption.

In zeolite regeneration studies (using 0.1 M HCl), the  $\text{Na}^+$  efficiently desorbed, but  $\text{K}^+$  remained. Over four consecutive adsorption–desorption cycles, the net  $\text{K}^+$  loading increased from 4.8 (cycle one) to 21.2 mg/g (cycle four). Thus,  $\text{K}^+$  was selectively extracted from brine and

concentrated on the zeolite. This K-form zeolite could potentially be applied as a slow-release fertilizer, thereby transforming a potash mine waste material into a valuable resource.

## **6.2. Recommendations**

Further research and development is needed to advance this area of study and address specific knowledge gaps and technical issues associated with the dual-adsorbent. Several ideas and considerations are discussed below.

### **6.2.1. Dual-Adsorbent Implementation and Scale Up**

Scaling up this dual-adsorbent process is a major area of future research. Substantial modifications may be needed to contend with new phenomena not present at the laboratory-scale. For example, the low hydraulic conductivity of CLDH may be problematic.

Potential industrial applications for the dual-adsorbent include pump and treat systems (column or batch reactors), permeable reactive barriers, containment systems, and leachate collection systems. The feasibility of these options largely depends on site-specific needs. Pilot-scale studies are warranted.

### **6.2.2. Investigation of Other Zeolites and LDHs**

There are over 40 different types of natural zeolites, each occurring with varying quantities of impurities.<sup>138</sup> The effectiveness of these other zeolites remains to be determined. For cost-savings, it would be prudent to evaluate a locally sourced zeolite, such as Canadian Mining Zeolite (Princeton, BC).

Similarly, it would be informative to evaluate other LDHs with different constituent cations and variable divalent/trivalent cation molar ratios. It would also be valuable to assess a OH-intercalated LDH, such as meixnerite, in which case calcination would not be necessary.<sup>69</sup>

It is preferable to synthesize the LDH in the laboratory, rather than obtaining commercially. This allows for greater configuration and control over the different variables and synthesis techniques. It also ensures full scientific transparency.

### 6.2.3. Adsorbent Re-use

Disposal of the spent CLDH and zeolite is not an economically viable option. Instead, the Na- and Cl-saturated adsorbents can be reused for other environmental remediation applications. Because LDH has relatively low selectivity for  $\text{Cl}^-$ , Cl-LDH can be used to remove a range of hazardous anionic species through anion-exchange (e.g., dyes,  $\text{PO}_4^{3-}$ , As(5), Cr(VI),  $\text{F}^-$ ,  $\text{SO}_4^{2-}$ ).<sup>56</sup> There have been comprehensive investigations on using Cl-LDH to remove  $\text{PO}_4^{3-}$  and  $\text{SO}_4^{2-}$ .<sup>139</sup><sup>140</sup> In Saskatchewan, Cl-LDH could potentially be reused to remove U and As oxyanions from uranium mining wastewater.<sup>60, 97</sup> Similarly, given that zeolite has a relatively low affinity for  $\text{Na}^+$ , Na-form zeolites can be used for the adsorption of other contaminants, including heavy metals,  $\text{NH}_4^+$ , and radioactive ions. For instance, the Na-form can be used to remove metals from mining wastewater.<sup>141</sup> The Na-form zeolite could also be re-used as a water softener.

### 6.2.4. CLDH Regeneration

Regeneration of CLDH was outside of the research scope, but worth evaluating. Typically, LDHs are regenerated using either  $\text{NaHCO}_3$  or  $\text{Na}_2\text{CO}_3$ . The  $\text{CO}_3^{2-}$  intercalates with ease, resulting in  $\text{MgAl-CO}_3$  LDH which can be calcined and re-used for adsorption. Although this approach is effective, the inputs are costly and NaCl and  $\text{CO}_2$  waste is generated (from the repeated calcination of the LDH). Instead, a potentially superior technique is thermal treatment of Cl-LDH under streaming water vapour. With this technique, over 90% of the interlayer  $\text{Cl}^-$  can be liberated, leaving CLDH, which can be used again for  $\text{Cl}^-$  adsorption. Concentrated HCl (greater than 20%) is obtained as a by-product.<sup>142</sup> The presence of water vapour is essential for removing the interlayer  $\text{Cl}^-$  as gaseous HCl.<sup>58</sup>

### 6.2.5. Economic Feasibility Study

In a feasibility study from 2006, the estimated cost of using St. Cloud zeolite to treat saline-sodic mine wastewater was \$3/barrel (159 L), compared with 0.75-\$4/barrel for deep well injection.<sup>40</sup> The St. Cloud zeolite had a maximum  $\text{Na}^+$  adsorption capacity of 2.8 mg/g. For the zeolite treatment to be competitive with deep well injection, the authors state that the  $\text{Na}^+$  adsorption capacity would have to be augmented 10-fold. In the present research, the  $\text{Na}^+$  uptake for the AZ(1-HCl)- $\text{Na}_{\text{dc}}$  was 28.4 mg/g, the requisite 10-fold increase. Although the cost of the CLDH adsorbent must also be factored in, this implies that the dual-adsorbent could potentially

be competitive with deep well injection. An economic feasibility study for the dual-adsorbent process is warranted.

## References

- (1) McEachern, R.; Wist, W.; Lehr, J. H. *Water softening with potassium chloride: process, health, and environmental benefits*. John Wiley & Sons: 2009.
- (2) Holter, M. E. *The Middle Devonian Prairie Evaporite of Saskatchewan*; Regina, 1969. Available at <http://www.economy.gov.sk.ca/Potash>
- (3) Saskatchewan Geological Survey *Mineral and Energy Resources of Saskatchewan: Potash*; Government of Saskatchewan: 2015. <http://www.economy.gov.sk.ca/Potash>
- (4) Stothart, P. *Facts and Figures of the Canadian Mining Industry*; The Mining Association of Canada: 2013.
- (5) Berenyi, J. *Saskatchewan Economy - Minerals Industry*; Regina, SK, 2016.
- (6) Reid, K. W.; Getzlaf, M. N. Decommissioning planning for Saskatchewan's potash mines. 2004. Available from <https://open.library.ubc.ca/media/download/pdf/59367/1.0042463/1>.
- (7) Tallin, J.; Pufahl, D.; Barbour, S. Waste Management Schemes of Potash Mines in Saskatchewan. *Can. J. Civ. Eng.* **1990**, *17*, (4), 528-542.
- (8) Vonhof, J. Waste disposal problems near potash mines in Saskatchewan, Canada. *Inland Waters Directorate, Environment Canada, Scientific Series* **1975**.
- (9) Barbour, S.; Yang, N. A review of the influence of clay-brine interactions on the geotechnical properties of Ca-montmorillonitic clayey soils from western Canada. *Can. Geotech. J.* **1993**, *30*, (6), 920-934.
- (10) Gabbasova, I.; Suleymanov, R.; Garipov, T. Degradation and remediation of soils polluted with oil-field wastewater. *Eurasian Soil Sci.* **2013**, *46*, (2), 204-211.
- (11) Keren, R., Saline and Boron-Affected Soils. In *Handbook of Soil Science*, Sumner, M., Ed. CRC Press: Boca Raton, FL, 2012; pp 17.1-17.20.
- (12) Xu, G.; Magen, H.; Tarchitzky, J.; Kafkafi, U. Advances in Chloride Nutrition of Plants. *Adv. Agron.* **1999**, *68*, 97-150.
- (13) White, P. J.; Broadley, M. R. Chloride in Soils and its Uptake and Movement Within the Plant: a Review. *Ann. Bot.* **2001**, *88*, (6), 967-988.
- (14) World Health Organization. *Guidelines for drinking-water quality: recommendations*. World Health Organization: 2004; Vol. 1.

- (15) Health Canada, Guidelines for Canadian Drinking Water Quality Summary Table. Water and Air Quality Bureau, Healthy Environments and Consumer Safety Branch, Health Canada, Ottawa, Ontario: 2014.
- (16) Findlay, S. E. G.; Kelly, V. R. Emerging indirect and long-term road salt effects on ecosystems. *Ann. N. Y. Acad. Sci.* **2011**, *1223*, (1), 58-68.
- (17) Adsorption. In *Merriam-Webster*, 2016.
- (18) Goh, K.-H.; Lim, T.-T.; Dong, Z. Application of layered double hydroxides for removal of oxyanions: a review. *Water Res.* **2008**, *42*, (6), 1343-1368.
- (19) Misaelides, P. Application of natural zeolites in environmental remediation: A short review. *Micropor. Mesopor. Mat.* **2011**, *144*, (1-3), 15-18.
- (20) Wang, X.; Ozdemir, O.; Hampton, M. A.; Nguyen, A. V.; Do, D. D. The effect of zeolite treatment by acids on sodium adsorption ratio of coal seam gas water. *Water Res.* **2012**, *46*, (16), 5247-5254.
- (21) Maathuis, H.; Van der Kamp, G. Comprehensive evaluation of groundwater resources in the Regina area. **1988**.
- (22) Golder *Yancoal Southey Project Environmental Impact Statement*; 2016. Available from <http://publications.gov.sk.ca/deplist.cfm?d=66&c=4433#2>.
- (23) MDH Engineered Solutions *PotashCorp Rocanville West Expansion*; 2008.
- (24) BHP Canada Inc *Jansen Project Environmental Impact Statement*; 2010.
- (25) The Mosaic Company and MDH Engineered Solutions Corp. *Mosaic Potash Esterhazy K2 Phase IV TMA Expansion*; 2009. Available from <http://environment.gov.sk.ca/2008-078EISK2PhaseIVEISMainDocument>.
- (26) Ferguson, G. Deep injection of waste water in the western Canada sedimentary basin. *Groundwater* **2015**, *53*, (2), 187-194.
- (27) Gendzwill, D.; Horner, R.; Hasegawa, H. Induced earthquakes at a potash mine near Saskatoon, Canada. *Can. J. Earth Sci.* **1982**, *19*, (3), 466-475.
- (28) Zhao, H.; Vance, G. F.; Urynowicz, M. A.; Gregory, R. W. Integrated treatment process using a natural Wyoming clinoptilolite for remediating produced waters from coalbed natural gas operations. *Appl. Clay Sci.* **2009**, *42*, (3), 379-385.
- (29) Xu, R.; Pang, W.; Yu, J.; Huo, Q.; Chen, J. *Chemistry of zeolites and related porous materials: synthesis and structure*. John Wiley & Sons: 2009.

- (30) Zhao, M.; Tang, Z.; Liu, P. Removal of methylene blue from aqueous solution with silica nano-sheets derived from vermiculite. *J. Hazard. Mater.* **2008**, *158*, (1), 43-51.
- (31) Ćurković, L.; Cerjan-Stefanović, Š.; Filipan, T. Metal ion exchange by natural and modified zeolites. *Water Res.* **1997**, *31*, (6), 1379-1382.
- (32) Zhao, H.; Vance, G. F.; Ganjegunte, G. K.; Urynowicz, M. A. Use of zeolites for treating natural gas Co-produced waters in Wyoming, USA. *Desalination* **2008**, *228*, (1), 263-276.
- (33) Inglezakis, V. J. The concept of “capacity” in zeolite ion-exchange systems. *J. Colloid Interface Sci.* **2005**, *281*, (1), 68-79.
- (34) Shimzu, T.; Wajima, T.; Ikegami, Y. Ion exchange properties of natural zeolite in the preparation of an agricultural cultivation solution from seawater. *Jap. Ion Exch. J.* **2007**, *18*, (4), 540-543.
- (35) Thomas, T.; Thomas, K.; Sadrieh, N.; Savage, N.; Adair, P.; Bronaugh, R. Research strategies for safety evaluation of nanomaterials, part VII: evaluating consumer exposure to nanoscale materials. *Toxicol. Sci.* **2006**, *91*, (1), 14-19.
- (36) Bish, D. L.; Boak, J. M. Clinoptilolite-heulandite nomenclature. *Reviews in mineralogy and geochemistry* **2001**, *45*, (1), 207-216.
- (37) Babel, S.; Kurniawan, T. A. Low-cost adsorbents for heavy metals uptake from contaminated water: a review. *J. Hazard. Mater.* **2003**, *97*, (1), 219-243.
- (38) Bhattacharyya, K. G.; Gupta, S. S. Influence of acid activation on adsorption of Ni(II) and Cu(II) on kaolinite and montmorillonite: Kinetic and thermodynamic study. *Chem. Eng. J.* **2008**, *136*, (1), 1-13.
- (39) Mumpton, F. A. La roca magica: uses of natural zeolites in agriculture and industry. *Proc. Natl. Acad. Sci. USA* **1999**, *96*, (7), 3463-3470.
- (40) Huang, F. Y.; Natrajan, P. Feasibility of using natural zeolites to remove sodium from coal bed methane-produced water. *J. Environ. Eng.* **2006**, *132*, (12), 1644-1650.
- (41) Ganjegunte, G. K.; Vance, G. F.; Gregory, R. W.; Urynowicz, M. A.; Surdam, R. C. Improving saline–sodic coalbed natural gas water quality using natural zeolites. *J. Environ. Qual.* **2011**, *40*, (1), 57-66.

- (42) Millar, G. J.; Couperthwaite, S. J.; Alyuz, K. Behaviour of natural zeolites used for the treatment of simulated and actual coal seam gas water. *J. Environ. Chem. Eng.* **2016**, *4*, (2), 1918-1928.
- (43) Splettstoesser, T. The microporous molecular structure of a zeolite. Available at <http://commons.wikimedia.org/wiki/File:Zeolite-ZSM-5-3D-vdW.png#file>
- (44) Wang, X. Investigation of the potential application of natural and acid activated zeolites for treating CSG Co-produced saline water. The University of Queensland, 2014.
- (45) Wang, X.; Nguyen, A. V. Characterisation of electrokinetic properties of clinoptilolite Before and After activation by sulphuric acid for treating CSG water. *Micropor. Mesopor. Mat.* **2016**, *220*, 175-182.
- (46) Santiago, O.; Walsh, K.; Kele, B.; Gardner, E.; Chapman, J. Novel pre-treatment of zeolite materials for the removal of sodium ions: potential materials for coal seam gas Co-produced wastewater. *SpringerPlus* **2016**, *5*, 571.
- (47) Inglezakis, V. J.; Loizidou, M. M.; Grigoropoulou, H. P. Ion exchange studies on natural and modified zeolites and the concept of exchange site accessibility. *J. Colloid Interface Sci.* **2004**, *275*, (2), 570-576.
- (48) Canadian Council of Ministers of the Environment (CCME). *Canadian Water Quality Guidelines*. Winnipeg, Manitoba, Canada, 1987.
- (49) Argun, M. E. Use of clinoptilolite for the removal of nickel ions from water: kinetics and thermodynamics. *J. Hazard. Mater.* **2008**, *150*, (3), 587-595.
- (50) Mills, S.; Christy, A.; Génin, J.-M.; Kameda, T.; Colombo, F. Nomenclature of the hydrotalcite supergroup: natural layered double hydroxides. *Mineralogical Magazine* **2012**, *76*, (5), 1289-1336.
- (51) Zaneva, S.; Stanimirova, T. Crystal chemistry, classification position and nomenclature of layered double hydroxydes. *Proceedings of Bulgarian Geological Society* **2004**, 1-3.
- (52) Miyata, S. O., Akira Synthesis of Hydrotalcite-like Compounds. *Clays Clay Miner.* **1976**, *25*, 14-18.
- (53) Cavani, F.; Trifirò, F.; Vaccari, A. Hydrotalcite-type anionic clays: Preparation, properties and applications. *Catal. Today* **1991**, *11*, (2), 173-301.
- (54) Rives, V. *Layered double hydroxides: present and future*. Nova Publishers: 2001.



- (55) Auerbach, S. M.; Carrado, K. A.; Dutta, P. K. *Handbook of layered materials*. CRC Press: 2004.
- (56) Miyata, S. Anion-exchange properties of hydrotalcite-like compounds. *Clays Clay Miner.* **1983**, *31*, (4), 305-311.
- (57) Lv, L.; Sun, P.; Gu, Z.; Du, H.; Pang, X.; Tao, X.; Xu, R.; Xu, L. Removal of chloride ion from aqueous solution by ZnAl-NO<sub>3</sub> layered double hydroxides as anion-exchanger. *J. Hazard. Mater.* **2009**, *161*, (2–3), 1444-1449.
- (58) Pless, J. D.; Philips, M. L.; Voigt, J. A.; Moore, D.; Axness, M.; Krumhansl, J. L.; Nenoff, T. M. Desalination of brackish waters using ion-exchange media. *Ind. Eng. Chem. Res.* **2006**, *45*, (13), 4752-4756.
- (59) Ulibarri, M. A.; Pavlovic, I.; Barriga, C.; Hermosín, M. C.; Cornejo, J. Adsorption of anionic species on hydrotalcite-like compounds: effect of interlayer anion and crystallinity. *Appl. Clay Sci.* **2001**, *18*, (1–2), 17-27.
- (60) Goh, K.-H.; Lim, T.-T.; Dong, Z. Application of layered double hydroxides for removal of oxyanions: A review. *Water Res.* **2008**, *42*, (6–7), 1343-1368.
- (61) Nowack, B.; Bucheli, T. D. Occurrence, behavior and effects of nanoparticles in the environment. *Environ. Pollut.* **2007**, *150*, (1), 5-22.
- (62) Salomao, R.; Milena, L.; Wakamatsu, M.; Pandolfelli, V. C. Hydrotalcite synthesis via co-precipitation reactions using MgO and Al(OH)<sub>3</sub> precursors. *Ceram. Int.* **2011**, *37*, (8), 3063-3070.
- (63) Xu, Z. P.; Lu, G. Q. Hydrothermal synthesis of layered double hydroxides (LDHs) from mixed MgO and Al<sub>2</sub>O<sub>3</sub>: LDH formation mechanism. *Chem. Mater.* **2005**, *17*, (5), 1055-1062.
- (64) Mitchell, S.; Biswick, T.; Jones, W.; Williams, G.; O'Hare, D. A synchrotron radiation study of the hydrothermal synthesis of layered double hydroxides from MgO and Al<sub>2</sub>O<sub>3</sub> slurries. *Green Chemistry* **2007**, *9*, (4), 373-378.
- (65) Salomão, R.; Dias, I. M.; Arruda, C. C. Hydrotalcite: A Potentially Useful Raw Material for Refractories. Proceedings of the Unified International Technical Conference on Refractories. Wiley Online Library: 2013; pp 1151-1156.

- (66) Ferencz, Z.; Kukovecz, Á.; Kónya, Z.; Sipos, P.; Pálinkó, I. Optimisation of the synthesis parameters of mechanochemically prepared CaAl-layered double hydroxide. *Applied Clay Science* **2015**, *112–113*, (0), 94-99.
- (67) Tongamp, W.; Zhang, Q.; Saito, F. Preparation of meixnerite (Mg–Al–OH) type layered double hydroxide by a mechanochemical route. *J. Mat. Sci* **2007**, *42*, (22), 9210-9215.
- (68) Zhang, X.; Qi, F.; Li, S.; Wei, S.; Zhou, J. A mechanochemical approach to get stunningly uniform particles of magnesium–aluminum-layered double hydroxides. *Appl. Surf. Sci.* **2012**, *259*, 245-251.
- (69) Guo, Q.; Reardon, E. J. Fluoride removal from water by meixnerite and its calcination product. *Appl. Clay Sci.* **2012**, *56*, (0), 7-15.
- (70) Zhang, F.; Du, N.; Li, H.; Liu, J.; Hou, W. Synthesis of Mg–Al–Fe–NO<sub>3</sub> layered double hydroxides via a mechano-hydrothermal route. *Solid State Sci.* **2014**, *32*, (0), 41-47.
- (71) Zhang, F.; Du, N.; Song, S.; Liu, J.; Hou, W. Mechano-hydrothermal synthesis of Mg<sub>2</sub>Al–NO<sub>3</sub> layered double hydroxides. *J. Solid State Chem.* **2013**, *206*, (0), 45-50.
- (72) Zhang, F.; Du, N.; Song, S.; Hou, W. Mechano-hydrothermal synthesis of SDS intercalated LDH nanohybrids and their removal efficiency for 2, 4-dichlorophenoxyacetic acid from aqueous solution. *Mater. Chem. Phys.* **2015**, *152*, 95-103.
- (73) Zhao, Y.; Hu, W.; Chen, J.; Lv, L. Factors influencing the chloride removal of aqueous solution by calcined layered double hydroxides. *Desal. Water Treat.* **2011**, *36*, (1-3), 50-56.
- (74) Jiang, J.-Q.; Ashekuzzaman, S. M. Development of novel inorganic adsorbent for water treatment. *Curr. Opin. Chem. Eng.* **2012**, *1*, (2), 191-199.
- (75) Lv, L.; He, J.; Wei, M.; Evans, D.; Duan, X. Uptake of chloride ion from aqueous solution by calcined layered double hydroxides: equilibrium and kinetic studies. *Water Res.* **2006**, *40*, (4), 735-743.
- (76) *Canada's Potash Industry* Natural Resources Canada: 2012.  
<http://www.nrcan.gc.ca/media-room/backgrounders/2012/3275>
- (77) Kameda, T.; Yoshioka, T.; Uchida, M.; Miyano, Y.; Okuwaki, A. New Treatment Method for Dilute Hydrochloric Acid Using Magnesium-Aluminum Oxide. *Bull. Chem. Soc. Jpn.* **2002**, *75*, (3), 595-599.

- (78) Li, Y.; Yang, M.; Zhang, X.; Wu, T.; Cao, N.; Wei, N.; Bi, Y.; Wang, J. Adsorption removal of thiocyanate from aqueous solution by calcined hydrotalcite. *J. Environ. Sci. (China)* **2005**, *18*, (1), 23-28.
- (79) Yang, Y.; Gao, N.; Deng, Y.; Zhou, S. Adsorption of perchlorate from water using calcined iron-based layered double hydroxides. *Applied Clay Science* **2012**, *65*, 80-86.
- (80) Wajima, T. Ion exchange properties of Japanese natural zeolites in seawater. *Anal. Sci.* **2013**, *29*, (1), 139-141.
- (81) Wajima, T. Desalination Behavior of Calcined Hydrotalcite From Seawater for Preparation of Agricultural Cultivation Solution Using Natural Zeolite. *Energy Environ. Res.* **2014**, *4*, (2), p3.
- (82) Wajima, T.; Shimizu, T.; Yamato, T.; Ikegami, Y. Removal of NaCl from seawater using natural zeolite. *Toxicological & Environmental Chemistry* **2010**, *92*, (1), 21-26.
- (83) Wajima, T.; Shimizu, T.; Ikegami, Y. New simple process of making agricultural cultivation solution from seawater. *J. Jpn. Soc. Seawater* **2006**, *60*, (3), 201-202.
- (84) Kaushal, S. S.; Groffman, P. M.; Likens, G. E.; Belt, K. T.; Stack, W. P.; Kelly, V. R.; Band, L. E.; Fisher, G. T. Increased Salinization of Fresh Water in the Northeastern United States. *Proc. Natl. Acad. Sci. USA* **2005**, *102*, (38), 13517-13520.
- (85) Kelly, V. R.; Lovett, G. M.; Weathers, K. C.; Findlay, S. E.; Strayer, D. L.; Burns, D. J.; Likens, G. E. Long-term Sodium Chloride Retention in a Rural Watershed: Legacy Effects of Road Salt on Streamwater Concentration. *Environ. Sci. Technol.* **2007**, *42*, (2), 410-415.
- (86) Kaushal, S. S. Increased Salinization Decreases Safe Drinking Water. *Environ. Sci. Technol.* **2016**, *55*, (6), 2765-2766.
- (87) Kaushal, S. S.; Likens, G. E.; Utz, R. M.; Pace, M. L.; Grese, M.; Yepsen, M. Increased River Alkalinization in the Eastern US. *Environ. Sci. Technol.* **2013**, *47*, (18), 10302-10311.
- (88) Lauer, N. E.; Harkness, J. S.; Vengosh, A. Brine Spills Associated with Unconventional Oil Development in North Dakota. *Environ. Sci. Technol.* **2016**, *50*, (10), 5389-5397.
- (89) Levy, G., Sodcity. In *Handbook of Soil Science*, Sumner, M., Ed. CRC Press: Boca Raton, FL, 2012; pp 18.1-18.28.

- (90) Revie, R. W.; Uhlig, H. H. *Uhlig's corrosion handbook*. John Wiley & Sons: 2011; Vol. 51.
- (91) Belbase, S.; Urynowicz, M. A.; Vance, G. F.; Dangi, M. B. Passive remediation of coalbed natural gas Co-produced water using zeolite. *J. Environ. Manage.* **2013**, *131*, 318-324.
- (92) Vance, G. F.; Zhao, H.; Urynowicz, M. A.; Ganjegunte, G. K.; Gregory, R. W. Potential utilization of natural zeolites for treating coalbed natural gas (CBNG) produced waters studies. 2007. Available from <http://citeseerx.ist.psu.edu/viewdoc/summary?doi=10.1.1.182.9213>.
- (93) Shaffer, D. L.; Arias Chavez, L. H.; Ben-Sasson, M.; Romero-Vargas Castrillón, S.; Yip, N. Y.; Elimelech, M. Desalination and reuse of high-salinity shale gas produced water: drivers, technologies, and future directions. *Environ. Sci. Technol.* **2013**, *47*, (17), 9569-9583.
- (94) Nghiem, L. D.; Ren, T.; Aziz, N.; Porter, I.; Regmi, G. Treatment of coal seam gas produced water for beneficial use in Australia: a review of best practices. *Desal. Water Treat.* **2011**, *32*, (1-3), 316-323.
- (95) Wang, X.; Wang, K.; Plackowski, C. A.; Nguyen, A. V. Sulfuric acid dissolution of 4A and Na-Y synthetic zeolites and effects on Na-Y surface and particle properties. *Appl. Surf. Sci.* **2016**.
- (96) Rivera, A.; Farías, T.; de Ménorval, L. C.; Autié-Pérez, M.; Lam, A. Natural and sodium clinoptilolites submitted to acid treatments: Experimental and theoretical studies. *J. Phys. Chem. C* **2013**, *117*, (8), 4079-4088.
- (97) Theiss, F. L.; Couperthwaite, S. J.; Ayoko, G. A.; Frost, R. L. A review of the removal of anions and oxyanions of the halogen elements from aqueous solution by layered double hydroxides. *J. Colloid Interface Sci.* **2014**, *417*, 356-368.
- (98) Cejka, J.; Van Bekkum, H.; Corma, A.; Schueth, F. *Introduction to Zeolite Molecular Sieves*. Elsevier: 2007; Vol. 168.
- (99) Carter, M. R. *Soil sampling and methods of analysis*. CRC Press: 1993.
- (100) Moir, D. Electrodeposition of actinides from saline groundwaters for alpha-spectrometric determination. *J. Radioanal. Nucl. Chem.* **1994**, *180*, (2), 201-208.

- (101) Isa, N. M.; Aris, A. Z. Identification of saltwater intrusion/assessment scheme in groundwater using the role of empirical knowledge. *Procedia Environmental Sciences* **2015**, *30*, 291-296.
- (102) Li, L. Y.; Tazaki, K.; Lai, R.; Shiraki, K.; Asada, R.; Watanabe, H.; Chen, M. Treatment of acid rock drainage by clinoptilolite—adsorptivity and structural stability for different pH environments. *Appl. Clay Sci.* **2008**, *39*, (1), 1-9.
- (103) Langmuir, I. The Adsorption of Gases on Plane Surfaces of Glass, Mica and Platinum. *J. Am. Chem. Soc.* **1918**, *40*, (9), 1361-1403.
- (104) Freundlich, H. Over the adsorption in solution. *J. Phys. Chem* **1906**, *57*, (385471), 1100-1107.
- (105) American Public Health Association and American Water Works Association. *Standard methods for the examination of water and wastewater: selected analytical methods approved and cited by the United States Environmental Protection Agency*. American Public Health Association: 1981.
- (106) Dynes, J. J.; Lawrence, J. R.; Korber, D. R.; Swerhone, G. D.; Leppard, G. G.; Hitchcock, A. P. Quantitative Mapping of Chlorhexidine in Natural River Biofilms. *Sci. Total Environ.* **2006**, *369*, (1), 369-383.
- (107) Hitchcock, A. aXis2000. <http://unicorn.mcmaster.ca/aXis2000.html>
- (108) Rasband, W. ImageJ Plugin. <http://wwwfacilities.uhnresearch.ca/wcif/imagej/index.htm>
- (109) Radha, A.; Kamath, P. V.; Shivakumara, C. Order and Disorder Among the Layered Double Hydroxides: Combined Rietveld and DIFFaX Approach. *Acta Crystallogr. Sect. B: Struct. Sci.* **2007**, *63*, (2), 243-250.
- (110) Pigna, M.; Dynes, J. J.; Violante, A.; Sommella, A.; Caporale, A. G. Sorption of Arsenite on Cu-Al, Mg-Al, Mg-Fe, and Zn-Al Layered Double Hydroxides in the Presence of Inorganic Anions Commonly Found in Aquatic Environments. *Environ. Eng. Sci.* **2016**, *33*, (2), 98-104.
- (111) Kameda, T.; Yoshioka, T.; Watanabe, K.; Uchida, M.; Okuwaki, A. Dehydrochlorination behavior of a chloride ion-intercalated hydrotalcite-like compound during thermal decomposition. *Appl. Clay Sci.* **2007**, *35*, (3–4), 173-179.

- (112) Kameda, T.; Yoshioka, T.; Watanabe, K.; Uchida, M.; Okuwaki, A. Dehydrochlorination and recovery of hydrochloric acid by thermal treatment of a chloride ion-intercalated hydrotalcite-like compound. *Appl. Clay Sci.* **2007**, *37*, (1), 215-219.
- (113) Vasylechko, V.; Gryshchouk, G.; Kuz'ma, Y. B.; Zakordonskiy, V.; Vasylechko, L.; Lebedynets, L.; Kalytavs'ka, M. Adsorption of cadmium on acid-modified Transcarpathian clinoptilolite. *Micropor. Mesopor. Mat.* **2003**, *60*, (1), 183-196.
- (114) Lv, L. Defluoridation of drinking water by calcined MgAl-CO<sub>3</sub> layered double hydroxides. *Desalination* **2007**, *208*, (1), 125-133.
- (115) Yamamoto, S.; Sugiyama, S.; Matsuoka, O.; Kohmura, K.; Honda, T.; Banno, Y.; Nozoye, H. Dissolution of zeolite in acidic and alkaline aqueous solutions as revealed by AFM imaging. *J. Phys. Chem.* **1996**, *100*, (47), 18474-18482.
- (116) Lin, H.; Liu, Q.-L.; Dong, Y.-B.; He, Y.-H.; Wang, L. Physicochemical properties and mechanism study of clinoptilolite modified by NaOH. *Micropor. Mesopor. Mat.* **2015**, *218*, 174-179.
- (117) Che, M.; Védrine, J. C., Chapter 19: Surface area/porosity, adsorption, diffusion. In *Characterization of solid materials and heterogeneous catalysts: from structure to surface reactivity*, John Wiley & Sons: 2012; Vol. 1 and 2.
- (118) Alberti, A. The Crystal Structure of Two Clinoptilolites. *Tschermaks Petr. Mitt.* **1975**, *22*, (1), 25-37.
- (119) Groen, J.; Peffer, L. A.; Moulijn, J.; Pérez-Ramí, J. On the introduction of intracrystalline mesoporosity in zeolites upon desilication in alkaline medium. *Micropor. Mesopor. Mat.* **2004**, *69*, (1), 29-34.
- (120) Ören, A. H.; Kaya, A. Factors affecting adsorption characteristics of Zn<sup>2+</sup> on two natural zeolites. *J. Hazard. Mater.* **2006**, *131*, (1), 59-65.
- (121) Cabrera, C.; Gabaldón, C.; Marzal, P. Sorption characteristics of heavy metal ions by a natural zeolite. *J. Chem. Technol. Biotechnol.* **2005**, *80*, (4), 477-481.
- (122) Taffarel, S. R.; Rubio, J. On the removal of Mn<sup>2+</sup> ions by adsorption onto natural and activated Chilean zeolites. *Miner. Eng.* **2009**, *22*, (4), 336-343.
- (123) Liang, X.; Zang, Y.; Xu, Y.; Tan, X.; Hou, W.; Wang, L.; Sun, Y. Sorption of metal cations on layered double hydroxides. *Colloids Surf. Physicochem. Eng. Aspects* **2013**, *433*, 122-131.

- (124) Bernstein, L. Effects of salinity and sodicity on plant growth. *Annu. Rev. Phytopathol.* **1975**, *13*, (1), 295-312.
- (125) Wang, S.; Peng, Y. Natural zeolites as effective adsorbents in water and wastewater treatment. *Chemical Engineering Journal* **2010**, *156*, (1), 11-24.
- (126) Zhao, H.; Vance, G. F.; Ganjegunte, G. K.; Urynowicz, M. A. Use of zeolites for treating natural gas Co-produced waters in Wyoming, USA. *Desalination* **2008**, *228*, (1–3), 263-276.
- (127) Rožić, M.; Cerjan-Stefanović, Š.; Kurajica, S.; Mačefat, M. R.; Margeta, K.; Farkaš, A. Decationization and dealumination of clinoptilolite tuff and ammonium exchange on acid-modified tuff. *J. Colloid Interface Sci.* **2005**, *284*, (1), 48-56.
- (128) Wang, X. Y.; Ozdemir, O.; Hampton, M. A.; Nguyen, A. V.; Do, D. D. The effect of zeolite treatment by acids on sodium adsorption ratio of coal seam gas water. *Water Res.* **2012**, *46*, (16), 5247-5254.
- (129) Evans, D. G.; Slade, R. C., Structural aspects of layered double hydroxides. In *Layered double hydroxides*, Springer: 2006; pp 1-87.
- (130) Li, J.; Wee, C.; Sohn, B. Effect of ammonium-and potassium-loaded zeolite on kale (*Brassica alboglabra*) growth and soil property. *Am. J. Plant Sci.* **2013**, *4*, (10), 1976.
- (131) Hershey, D.; Paul, J.; Carlson, R. Evaluation of potassium-enriched clinoptilolite as a potassium source for potting media. *HortScience (USA)* **1980**, *15*, (1), 87-89.
- (132) Ming, D. W.; Allen, E. R. Use of natural zeolites in agronomy, horticulture and environmental soil remediation. *Rev. Min. Geochem.* **2001**, *45*, (1), 619-654.
- (133) Williams, K. A.; Nelson, P. V. Using precharged zeolite as a source of potassium and phosphate in a soilless container medium during potted chrysanthemum production. *J. Am. Soc. Hort. Sci.* **1997**, *122*, (5), 703-708.
- (134) Milosevic, T.; Milosevic, N. The effect of zeolite, organic and inorganic fertilizers on soil chemical properties, growth and biomass yield of apple trees. *Plant Soil Environ.* **2009**, *55*, 528-535.
- (135) Ahmed, O. H.; Azrumi, N. A. B.; Jalloh, M. B.; Jol, H., Using Clinoptilolite Zeolite for Enhancing Potassium Retention in Tropical Peat Soil. In *Advances in Tropical Soil Science*, Universiti Putra Malaysia Press: 2015; Vol. 3.

- (136) Chubar, N.; Samanidou, V.; Kouts, V.; Gallios, G.; Kanibolotsky, V.; Strelko, V.; Zhuravlev, I. Adsorption of fluoride, chloride, bromide, and bromate ions on a novel ion exchanger. *J. Colloid Interface Sci.* **2005**, *291*, (1), 67-74.
- (137) Koul, V.; Gupta, A. Uptake of sodium chloride by mixture of weakly acidic and weakly basic ion exchange resins: equilibrium and kinetic studies. *Chem. Eng. Sci.* **2004**, *59*, (7), 1423-1435.
- (138) International Zeolite Association Database of Zeolite Structures. Available from <http://www.iza-structure.org/databases/>.
- (139) Tsujimura, A.; Uchida, M.; Okuwaki, A. Synthesis and sulfate ion-exchange properties of a hydrotalcite-like compound intercalated by chloride ions. *J. Hazard. Mater.* **2007**, *143*, (1-2), 582-586.
- (140) Jia, Y.; Wang, H.; Zhao, X.; Liu, X.; Wang, Y.; Fan, Q.; Zhou, J. Kinetics, isotherms and multiple mechanisms of the removal for phosphate by Cl-hydrocalumite. *Appl. Clay Sci.* **2016**, *129*, 116-121.
- (141) Mier, M. V.; Callejas, R. L.; Gehr, R.; Cisneros, B. E. J.; Alvarez, P. J. Heavy metal removal with mexican clinoptilolite:: multi-component ionic exchange. *Water Res.* **2001**, *35*, (2), 373-378.
- (142) Kameda, T.; Yoshioka, T.; Watanabe, K.; Uchida, M.; Okuwaki, A. Dehydrochlorination and recovery of hydrochloric acid by thermal treatment of a chloride ion-intercalated hydrotalcite-like compound. *Appl. Clay Sci.* **2007**, *37*, (1-2), 215-219.



# Appendix

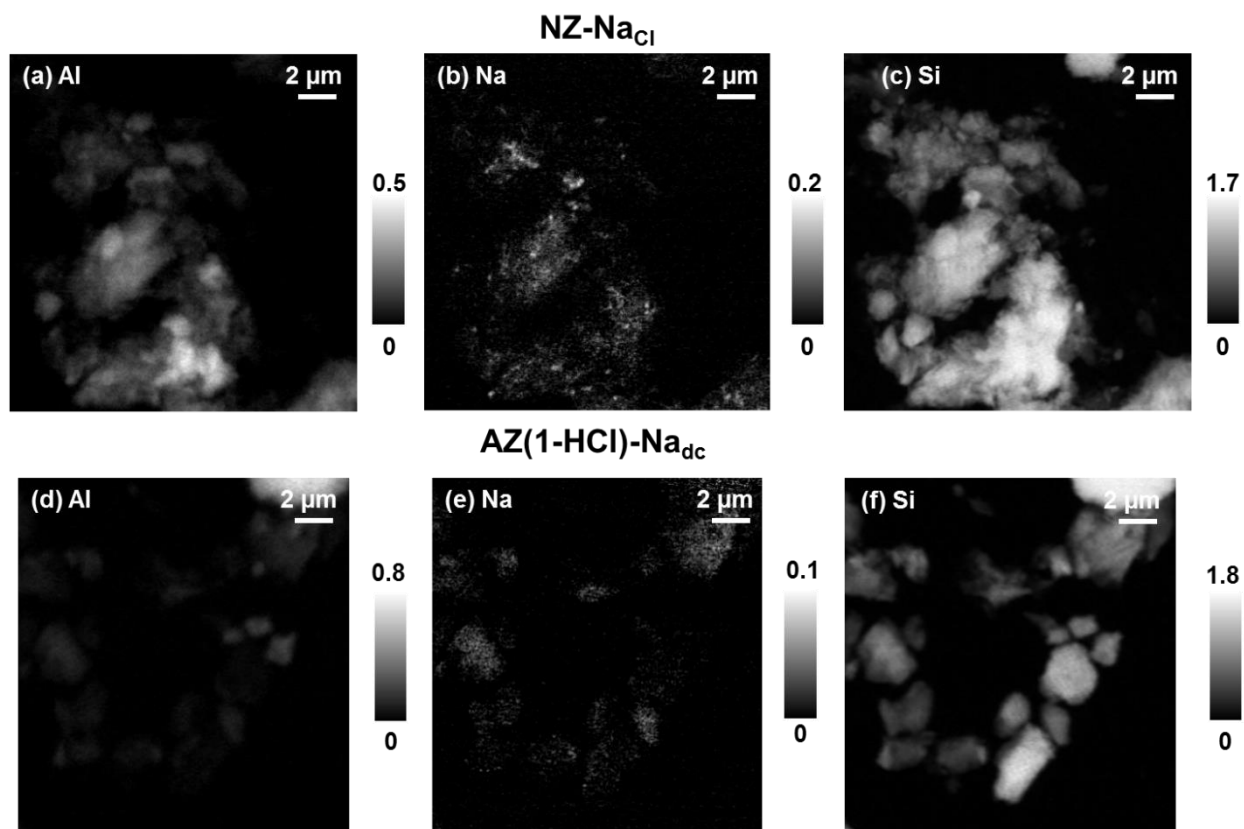


**Figure A1:** Image difference maps for (a) Al, (b) Na and (c) Si for the NZ- $\text{NaCl}$  system; (d) Al, (e) Na, and (f) Si for the AZ(1-HCl)- $\text{Na}_{dc}$  system. The gray scales indicate optical density.